5-1996

Thermodynamics and Kinetics of Small Molecule Binding to [Cyclopentadienyl-Ru-NO] and [Rh-CO] Electrophilic Centers

Anna Svetlanova
Utah State University

THERMODYNAMICS AND KINETICS OF SMALL MOLECULE BINDING TO [CYCLOPENTADIENYL-Ru-NO] AND [Rh-CO] ELECTROPHILIC CENTERS

by

Anna Svetlanova

A dissertation submitted in partial fulfillment
of the requirements for the degree

of

DOCTOR OF PHILOSOPHY

in

Chemistry

UTAH STATE UNIVERSITY
Logan, Utah

1996

ABSTRACT

Thermodynamics and Kinetics of Small Molecule Binding to

[Cyclopentadienyl-Ru-NO] and [Rh-CO]

Electrophilic Centers

by

Anna Svetlanova, Doctor of Philosophy

Utah State University, 1996

Major Professor: John L. Hubbard
Department: Chemistry and Biochemistry

This work is concentrated on the thermodynamic and kinetic aspects of water, alcohols, alkyl halides, ethers, and lactones bound and activated by the electrophilic $[Cp'Ru(NO)]^{+2}$ and $[Cp'Ru(NO)(CH_3)]^{+}$ centers (Cp' = cyclopentadienyl group). Counterions in these systems include $OSO_2CF_3^-$ (OTf^-) and $[(3,5\text{-}(CF_3)_2C_6H_3)_4B]^-$ ($[BAr_4']^-$). The displacement of OTf^- in $Cp'Ru(NO)(OTf)_2$ by H_2O in dichloromethane is exothermic but entropically unfavorable due to the required reorganization of the solvent cage around released triflate ions. Thermodynamic parameters are also determined for OTf^- displacement by chloride and tetrahydrofuran (THF) using the ^{19}F nuclear magnetic resonance (NMR) spectroscopy. The conversion of the $[Cp'Ru(NO)(OH_2)_2]^{+2}$ to $[Cp'Ru(NO)(\mu\text{-}OH)]_2^{+2}$ in aqueous solutions is characterized thermodynamically and kinetically by potentiometric and NMR methods.

The results of the study of rhodium triflato complex *trans*-$[Rh(CO)(PPh_3)_2(OTf)]$ show that OTf^- coordinates to the metal center in wet dichloromethane solutions, but the compound crystallizes as a water-coordinated triflate salt *trans*-$[Rh(CO)(PPh_3)_2(OH_2)][OTf]$. Thermodynamic parameters for alcohol (methanol, ethanol, isopropanol) binding to the $Cp^*Ru(NO)(OTf)_2$ are determined from the ^{19}F NMR spectroscopic data. The kinetics of the oxidation of alcohols to aldehydes or ketones via

Ru(II) $\longrightarrow$ Ru(0) redox process is studied by NMR methods. The results of the study support β-hydrogen elimination mechanism, comprising one of the very few mechanistic investigations on reactions of this kind. Alkyl iodides are found to bind to the $[Cp^*Ru(NO)(CH_3)]^+$ fragment via displacement of a THF ligand in the presence of a $BAr_4'^-$ counterion, forming alkyl halide complexes that convert to $[Cp'Ru(NO)(\mu\text{-}I)]_2^{+2}$. The mixed ruthenium-chromium complex $[CpCr(NO)_2(\mu\text{-}I)(Ru(Cp')(NO)]^+$ is characterized as primarily a [Ru-I $\rightarrow$ Cr] system as opposed to a [Ru$\leftarrow$I-Cr] model. The complex $[Cp^*Ru(NO)(CH_3)(THF)]^+$ is found to catalyze aerobic oxidation of THF to γ-butyrolactone. The new γ-butyrolactone ruthenium complex is isolated and characterized by X-ray methods in the solid state. The mechanism of catalytic oxidation is studied by ^{18}O-labeled infrared spectroscopic methods. Radical decomposition of the intermediate hydroperoxy-tetrahydrofuran gives 1,6-diol-diformate $[CH(O)\text{-}(CH_2)_6\text{-}CH(O)]$. The radical mechanism for the catalytic oxidation of THF is proposed.

(152 pages)

ACKNOWLEDGMENTS

The support of the National Science Foundation (Grant CHE-9215872) is gratefully acknowledged. Also acknowledged are the Utah State University Research Office and the National Science Foundation (CHE-9002379) for funding the purchase of the X-ray diffractometer. For the X-ray structure determinations, the training and help from Dr. John L. Hubbard are greatly appreciated.

Anna Svetlanova-Larsen

CONTENTS

LIST OF TABLES

LIST OF FIGURES

CHAPTER 1

INTRODUCTION

Electrophilic transition metal complexes are an important part of modern catalysis.[1] Soluble transition-metal complexes, which can be tuned electronically and sterically by varying the metal and/or ligands, provide broad opportunities for such transformations.[2] With such variations in reactivity, success with transition-metal catalysts seems to depend on serendipity to a large extent, due to a lack of background knowledge necessary for the invention of new catalytic processes.[3] Therefore, mechanistic studies of procatalytic reactions of transition-metal complexes constitute an important contribution to the development of the research field of catalysis.

The $[Cp^*Ru(NO)]^{+2}$ and $[Cp^*Ru(NO)(R)]^{+}$ organometallic fragments in the presence of labile (OTf^-) and non-coordinating ($BAr_4'^-$) counterions possess valuable features ($OTf = OSO_2CF_3$, $[BAr_4'] = [[(3,5\text{-}(CF_3)_2C_6H_3)_4B]^-$). Both systems are electrophilic and reactive with a wide host of donors like THF, H_2O, NR_3, ROH, etc. The triflate ruthenium complexes are water-soluble and, thus, related to the important area of study of "benign" chemistry. Aqueous organometallic chemistry is especially attractive because of the environmentally and financially benevolent properties of water-based processes.[4-6]

Chapter 2 of this dissertation describes aqueous organometallic chemistry of the $[Cp^*Ru(NO)]^{+2}$ electrophilic fragment. This study is focused on the thermodynamic and kinetic aspects of binding and activation of an H_2O ligand by the ruthenium center under various conditions. The organometallic system under consideration offers a simple format for the evaluation of water and OTf^- as competing ligands for the electrophilic ruthenium center. Although water is viewed as a common ligand in coordination chemistry,[7] there is still considerable interest in the nature of water and hydroxo ligands in organometallic systems, especially with regard to their ability to displace coordinating counterions and reactive substrates.[8] We show the ancillary NO ligand to be particularly valuable because the ν_{NO} and $\angle$ Ru-N-O values provide insight about the donor ability of the H_2O ligand.[9]

In Chapter 3, the issue of behavior of rhodium triflate aqua complexes in solution and the

solid state relates to the determination of the nature of the OTf^- ligand in the presence of competing H_2O ligands. The nature of weakly coordinating ions is important in the discussion of coordination unsaturation and catalytic reactivity.[10,11] There is a continuing interest in the equilibria of OTf^- displacement by coordinating solvents and weak ligands. In concert with the work on $Cp^*Ru(NO)(OTf)_2$ (Chapter 2), some previous work has shown OTf^- to be a "moderately strong" ligand.[12,13] For example, a kinetic study of the $M(CO)_5(OTf)$ complexes (M = Mn, Re) showed substitution of OTf^- by oxygen donor solvents in CH_2Cl_2 to occur for M = Mn but not for M = Re.[13] If one considers OTf^- to be a fairly good ligand, the report that *trans*-$[Rh(CO)(PPh_3)_2(OH_2)][OTf]$ persists in solution with no detectable traces of the parent complex *trans*-$[Rh(CO)(PPh_3)_2(OTf)]$ would be counterintuitive[14] even though the dissociation of OTf^- in the "basic" d^8 Rh complexes might be expected to be more favorable than in electrophilic d^6 complexes like $Cp^*Ru(NO)(OTf)_2$.[14,15] Prompted by the rather sketchy analytical details reported for *trans*-$[Rh(CO)(PPh_3)_2(OH_2)][OTf]\cdot H_2O$[16] and the importance of square planar rhodium complexes in catalytic reactions,[17] this study constitutes a reinvestigation of this case to see if H_2O actually displaces the OTf^- ligand in CH_2Cl_2. The results of this study show that OTf^- is a better ligand than H_2O in CH_2Cl_2.

The work presented in Chapter 4 is concerned with the binding and oxidation of alcohols by ruthenium triflate complexes.[18] The study concentrates on the thermodynamic characterization of the triflate-alcohol coordination equilibrium and the kinetic aspects of the subsequent oxidation of alcohols. The available mechanistic characterization of the catalytic and stoichiometric oxidation of alcohols is rather scarce.[19] Thus, the kinetic study reported here is one of the very few mechanistic studies performed on reactions of this kind. Isolation and crystallographic characterization of a new chelate-stabilized diol complex is also reported.

The study of alkyl halide, metal halide, and metal(halomethyl) complex ligation to the $[Cp^*Ru(NO)(CH_3)]^+$ fragment is presented in Chapter 5. The oxidative addition of an alkyl halide to a coordinatively unsaturated metal complex is a key step in a variety of important catalytic and stoichiometric processes.[20] Although several mechanisms of oxidative addition have been

documented, a prior alkyl halide coordination step is possible in nearly all cases.[20] Thus, characterization of new complexes containing a direct M-XR linkage should improve our mechanistic understanding of these reactions. Another important aspect of these complexes is that they are expected to offer a rich coordination chemistry, since halocarbons have ligand strengths far weaker than other main group alkyls such as amines, phosphines, ethers, and sulfides.[21] Indeed, a very recent report describes a new iridium(III) CH_2Cl_2-coordinated complex with a BAr_4' counterion that carries out exceptionally selective C-H activation under very mild conditions.[22] The present study reports the generation and characterization of alkyl halide complexes utilizing the Lewis acidity of the cationic fragment arising from the dissociation of THF from the complex salt $[Cp^*Ru(NO)(CH_3)(THF)][BAr_4']$. [23]

Chapter 6 comprises the study of catalytic aerobic oxidation of THF to γ-butyrolactone in the presence of $[Cp^*Ru(NO)(CH_3)(THF)][BAr_4']$ complex. Several instances of catalytically assisted conversion of primary ethers to esters (or lactones) have been reported in recent years.[24-28] In spite of these reports, information leading to the mechanistic understanding of the catalytic oxidation of THF with molecular oxygen is rather limited.[26-29] The present work utilizes a synthetic approach to the ruthenium lactone complex, which combines the Lewis acidity of the $[Cp^*Ru(NO)(CH_3)]^+$ fragment with the ability of the ruthenium center to catalyze THF conversion to γ-butyrolactone in the presence of O_2. Some details of the mechanism of the catalytic oxidation reaction are revealed as a result of this study.

References

(1) (a) Hlatky, G. G.; Turner, H. W.; Eckman, R. R. *J. Am. Chem. Soc.*, **1989**, *111*, 2728. (b) Hlatky, G. G.; Eckman, R. R.; Turner, H. W. *Organometallics* **1992**, *11*, 1413. (c) Sishta, C.; Hawthorn, R. M.; Marks, T. J. *J. Am. Chem. Soc.*, **1992**, *114*, 1112. (d) Marks, T. J. *Acct. Chem. Res.*, **1992**, *23*, 57. (e) Yang, X.; Stern, C. L.; Marks, T. J. *J. Am. Chem. Soc.*, **1991**, *113*, 3623. (f) Yang, X.; Stern, C. L.; Marks, T. J.

Organometallics **1991**, *10*, 840. (g) Lin, Z.; Le Marechal, J.-F.; Sabat, M.; Marks, T. J. *J. Am. Chem. Soc.* **1987**, *109*, 4127. (h) Dalton, D. M.; Gladysz, J. A. *J. Organomet. Chem.* **1989**, *370*, C17. (i) Saura-Llamas, I.; Gladysz, J. A. *J. Am. Chem. Soc.*, **1992**, *114*, 2136. (j) Klein, D. P.; Gladysz, J. A.; *J. Am. Chem. Soc.* **1992**, *114*, 8710. (k) Winter, C. H.; Zhou, X.-X.; Heeg, M. J. *Inorg. Chem.* **1992**, *31*, 1808.

(2) Collman, J. P.; Hegedus, L. S.; Norton, J. R.; Finke, R. G. *Principles of Organotransition Metal Chemistry*; University Science Books: Mill Valley, CA, 1987; Chapter 1 .

(3) Rouhi, A.M. *Chem. & Eng. News,* **1995,** *6*, 32.

(4) (a) Wang, L.; Flood, T. C. *J. Am. Chem. Soc.*, **1992**, *114*, 3169. (b) Wang, C.; Ziller, J. W.; Flood, T. C. *J. Am. Chem. Soc.*, **1995**, *117*, 1647. (c) Wang, L.; Lu, R. S.; Bau, R.; Flood, T. C. *J. Am. Chem. Soc.*, **1993**, *115*, 6999.

(5) (a) Haggin , J. *Chem. & Eng. News,* **1994,** *10,* 28. (b) Fish, R. H.; Baralt, E.; Kim, H.-S.; *Organometallics*, **1991**, *10*, 1965. (c) Baralt, E.; Smith, S. J.; Hurwitz, J.; Horvath, I. T.; Fish, R. H. *J. Am. Chem. Soc.*, **1992**, *114*, 5187. (d) Smith, D. P.; Baralt, E.; Moreles, B.; Olmstead, M. M.; Maestre, M. F.; Fish, R. H. *J. Am. Chem. Soc.*, **1992**, *114*, 10647. (e) Smith, D. P.; Olmstead, M. M.; Noll, B. C.; Maestre, M. F.; Fish, R. F. *Organometallics*, **1993**, *12*, 593. (f) Smith, D. P.; Griffin, M. T.; Olmstead, M. M.; Maestre, M. F.; Fish, R. H. *Inorg. Chem.* **1993**, *32*, 4677. (g) Chen, H.; Maestre, M. F.; Fish, R. H. *J. Am. Chem. Soc.*, **1995**, *117*, 3631. (h) Eisen, M. S.; Haskel, A.; Chen, H.; Olmstead, M. M.; Smith, D. P.; Maestre, M. F.; Fish, R. H. *Organometallics*, **1995**, *14*, 2806. (i) McGrath, D. V.; Grubbs, R. H. *Organometallics*, **1994**, *13*, 224. (j) Dadci, L.; Elias, H.; Frey, U.; Hörnig, A.; Koelle, U.; Merbach, A.C.; Paulus, H.; Schneider, J.S. *Inorg. Chem.* **1995**, *34*, 306-315. (k) Darensbourg, D. J.; Joo, F.; Kannisto, M.; Katho, A.; Reibenspies, J. H.; Daigle, D. J. *Inorg. Chem.* **1994**, *33*, 200. (l) Barton, M.; Atwood, J. D. *J. Coord. Chem.* **1991**, *24*, 43-67. (m) Rauscher, D. J.; Thaler, E. G.; Huffman, J. C.; Caulton, K. G. *Organometallics*, **1991**, *10*, 2209. (n) Labinger, J. A.; Herring, A. M.; Lyon, D. K.;

Luinstra, G. A.; Bercaw, J. E.; Horvath, I. T.; Eller, K. *Organometallics*, **1993**, *12*, 895. (o) Agbossou, S. K.; Roger, C.; Igau, A.; Gladysz, J. A. *Inorg. Chem.*, **1992**, *31*, 419. (p) Le, T. X.; Merola, J. S. *Organometallics*, **1993**, *12*, 3798. (q) Dobbs, D. A.; Bergman, R. G. *Organometallics*, **1994**, *13*, 4594.

(6) (a) Kang, J.W.; Maitlis, P.M. *J. Organomet. Chem.* **1971**, *30(1)*, 127. (b) Nutton, A.; Bailey, P.; Maitlis, P.M.; *J. Chem. Soc., Dalton Trans.*, **1981**, 1997. (c) Hirai, K.; Nutton, A.; Maitlis, P.M. *J. Mol. Cat.* **1981**, *203-211*, 203. (d) Nutton, A.; Maitlis, P.M. *J. Chem. Soc., Dalton Trans.*, **1981**, 2335. (e) Miguel-Garcia, J.A.; Adams, H.; Bailey, N.A.; Maitlis, P.M. *J. Organomet. Chem.* **1991**, *413*, 427. (f) Gusev, O.V.; Rubezhov, A.Z.; Miguel-Garcia, J.A.; Maitlis, P.M. *Mendeleev. Commun.*, **1991**, 21. (g) Wei, C.; Aigbirhio, F.; Adams, H.; Bailey, N.A.; Hempstead, P.D.; Maitlis, P.M. *J. Chem. Soc. Chem. Commun.*, **1991**, 883. (h) Miguel-Garcia, J.A.; Adams, H.; Bailey, N.A.; Maitlis, P.M. *J. Chem. Soc., Dalton Trans.*, **1992**, 131. (i) Gusev, O.; Sergeev, S.; Saez, I.M.; Maitlis, P.M.; *Organometallics*, **1994**, *13*, 2059.(j) Fan, Li; Turner, M.L.; Hursthouse, M.B.; Abdul Malik, K.M.; Gusev, O.V.; Maitlis, P.M. *J. Am. Chem. Soc.*, **1994**, *116*, 385.

(7) (a) Grover, N.; Gupta, N.; Thorp, H. H. *J. Am. Chem. Soc.*, **1992**, *114*, 3390. (b) Call, J. T.; Hughes, K. A.; Harman, W. D.; Finn, M. G. *Inorg. Chem.* **1993**, *32*, 2123. (c) Banyai, I. Glaser, J.; Read, M. C.; Sandstrom, M. *Inorg. Chem.* **1995**, *34*, 2423. (d) Dimitrou, K.; Folting, K.; Streib, W. E.; Christou, G. *J. Am. Chem. Soc.*, **1993**, *115*, 6432.

(8) (a) Lou, X.-L.; Schulte, G. K.; Crabtree, R. H. *Inorg. Chem.* **1990**, *29*, 682. (b) Kubas, G. J.; Burns, C. J.; Khalsa, G. R. K.; Van Der Sluys, L. S.; Kiss, G.; Hoff, C. D. *Organometallics*, **1992**, *11*, 3390.

(9) (a) Rothfuss, H.; Huffman, J. C.; Caulton, K. G. *J. Am. Chem. Soc.*, **1994**, *116*, 187. (b) Gusev, D. G.; Kulhman, R.; Rambo, J. R.; Berke, H.; Eisenstein, O.; Caulton, K. G. *J. Am. Chem. Soc.*, **1995**, *117*, 281. (c) Johnson, T. J.; Folting, K.; Streib, W. E.; Martin, J. D.; Huffman, J. C.; Jackson, S. A.; Eisenstein, O.; Caulton, K. G. *Inorg. Chem.* **1995**, *34*,

488. (d) Caulton, K. G. *New J. Chem.* **1994**, *18*, 25.

(10) (a) Lawrance, G. A. *Chem. Rev.* **1986**, *86*, 17 and references therein. (b) Beck, W.; Sünkel, K.; *Chem. Rev.* **1988**, *88*, 1405 and references therein. (c) Blosser, P. W.; Gallucci, J. C.; Wojcicki, A. *Inorg. Chem.* **1992**, *31*, 2376.

(11) Humphrey, R. B.; Lamanna, W. M.; Brookhart, M.; Husk, G. R. *Inorg. Chem.* **1983**, *22*, 3355.

(12) (a) Hollis, T. K.; Robinson, N. P.; Bosnich, B. *Organometallics*, **1992**, *11*, 2645. (b) Hollis, T. K.; Robinson, N. P.; Bosnich, B. *J. Am. Chem. Soc.*, **1992**, *114*, 5464. (c) Bonnesen, P. V.; Puckett, C. L.; Honeychuck, R. V.; Hersh, W. H.; *J. Am. Chem. Soc.* **1989**, *111*, 6070. (d) Honeychuck, R. V.; Bonnesen, P.V.; Farahi, J.; Hersh, W. H.; *J. Org. Chem.* **1987**, *52*, 5293. (e) Odenkirk, W.; Rheingold, A. L.; Bosnich, B. *J. Am. Chem. Soc.*, **1992**, *114*, 6392. (f) Haggin, J. *Chem. & Eng. News,* **1994,** *10*, 28. (g) Wang, L.; Flood, T. C. *J. Am. Chem. Soc.*, **1992**, *114*, 3169. (h) Wang, C.; Ziller, J. W.; Flood, T. C. *J. Am. Chem. Soc.*, **1995**, *117*, 1647. (i) Wang, L.; Lu, R. S.; Bau, R.; Flood, T. C. *J. Am. Chem. Soc.*, **1993**, *115*, 6999. (j) Darensbourg, D. J.; Stafford, N. W.; Joo, F.; Reibenspies, J. H. *J. Organomet. Chem.* **1995**, *488*, 99. (k) McGrath, D. V.; Grubbs, R. H. *Organometallics*, **1994**, *13*, 224.

(13) (a) Nitschke, J.; Schmidt, S. P.; Trogler, W. C. *Inorg. Chem.* **1985**, *24*, 1972. (b) Trogler, W. C. *J. Am. Chem. Soc.*, **1979**, *101*, 6459.

(14) Branan, N.M.; Hoffman, N.W.; McElroy, E.A.; Prokopuk, N.; Salazar, A.B.; Robbins, M.J.; Hill, W.E.; Webb, T.R. *Inorg. Chem.* **1991**, *30*, 1200.

(15) (a) Werner, H. *Pure Appl. Chem.* **1982**, *54*, 177. (b) Werner, H. *Angew. Chem., Int. Ed. Engl.* **1983**, *22*, 927.

(16) (a) Neither the work in ref. 15 or references therein reported the combustion analysis, mp, and solid-state IR ν_{CO} data for the Rh-OTf complex. (b) Branan, D.M.; Hoffman, N.W.; McElroy, E.A.; Ramage, D.L.; Robbins, M.J; Eyler, J.R.; Watson, C.H.; deFur, P.;

and solid-state IR ν_{CO} data for the Rh-OTf complex. (b) Branan, D.M.; Hoffman, N.W.; McElroy, E.A.; Ramage, D.L.; Robbins, M.J; Eyler, J.R.; Watson, C.H.; deFur, P.; Leary, J.A. *Inorg. Chem.* **1990**, *29*, 1915.

(17) Reference 2, chapters 10-12 and references therein.

(18) Zoch, C. R. Dissertation, Utah State University, 1993.

(19) (a) Blum, O.; Milstein, D. *J. Am. Chem. Soc.*, **1995**, *117*, 4582. (b) Hoffman, D.M.; Lappas, D.; Wierda, D.A. *J. Am. Chem. Soc.*, **1989**, *111*, 1531. (c) Bryndza, H.E.; Calabrese, J.C.; Marsi, M.; Roe, D.C.; Tam, W.; Bercaw, J.E.; *J. Am. Chem. Soc.*, **1986**, *108*, 4805

(20) Reference 2, Part III, p. 306-310 and references therein.

(21) Colsman, M. R.; Noirot, M. D.; Miller, M. M.; Anderson, O. P.; Strauss, S. H. *J. Am. Chem. Soc.*, **1988**, *110*, 1988.

(22) Arndtsen, B. A.; Bergman, R. G. *Science*, **1995**, *270*, 1970.

(23) Yi, G.-B. Dissertation, Utah State University, 1995.

(24) Hata, E.; Takai, T.; Mukaiyama, T. *Chem.Lett.* **1993**, *53*, 1513.

(25) Fazlur-Rahman, A. K., Tsai, J. -C., Nicholas, K. M. *J. Chem. Soc, Chem.Com.* **1992**, *78*, 1335.

(26) Aresta, M., Fragale, C., Quaranta, E., Tommasi, I. *J. Chem. Soc., Chem. Comm.*. **1992**, *33*, 315.

(27) Carlsen, H. J., Katsuki, T., Martin. V., Sharpless, B. *J. Org. Chem.* **1981**, *46*, 3936.

(28) Bressan, M., Morvillo, A., Romanello., G *Inorg. Chem.* **1990**, *29*, 2976.

(29) (a) Braunstein, P., Matt, D., Nobel, D. *J. Am. Chem. Soc.* **1988**, *110*, 3207. (b) Hirai, K.; Nutton, A.; Maitlis, P. M. *J. Mol. Cat.* **1981**, *10*, 203.

CHAPTER 2

AQUEOUS ORGANOMETALLIC CHEMISTRY OF THE ELECTROPHILIC $[(\eta\text{-}C_5(CH_3)_5)Ru(NO)]^{2+}$ FRAGMENT

Abstract

The ditriflate complexes Cp'Ru(NO)$(OTf)_2$ (**1a,b**) exist in equilibria

$$\mathbf{1a} \overset{K_1}{\rightleftarrows} \underset{\mathbf{2a^+}}{[Cp^*Ru(NO)(OTf)(H_2O)]^+} + OTf^- \overset{K_2}{\rightleftarrows} \underset{\mathbf{3a^{+2}}}{[Cp^*Ru(NO)(OH_2)_2]^{+2}} + 2\ OTf^-$$

in 0.1 **M** H_2O/CH_2Cl_2 solution with **1a** being the predominant complex and ΔH_1 = -15 (3) kcal/mol and ΔS_1 = -60 (30) eu (for K_1) and ΔH_2 = -9 (1) kcal/mol and ΔS_2 = -40 (25) eu (for K_2) (Cp' = η-$C_5(CH_3)_5$, Cp*, **1a**; η-$C_5(CH_3)_4(CH_2CH_3)$, Cp^, **1b**). The complex salts $[Cp^\wedge Ru(NO)(OTf)(OH_2)][OTf]$ (**2b**) and $[Cp^\wedge Ru(NO)(OH_2)_2][OTf]_2$ (**3b**) can be isolated from the hydration of **1b**. X-ray structural data (223 K) for **3b**, ($C_{13}H_{21}NO_9S_2F_6Ru$): monoclinic space group *C*2/m, a = 21.380 (6) Å, b = 8.907 (2) Å, c = 13.481 (3) Å, β = 115.70 (2)°, Z = 4, R_1 = 0.0569 (on F^2). The equilibria

$$\mathbf{1a} \overset{K_1}{\rightleftarrows} [Cp^*Ru(NO)(OTf)(THF)]^+ + OTf^- \overset{K_2}{\rightleftarrows} [Cp^*Ru(NO)(THF)_2]^{+2} + 2\ OTf^-$$

exist in neat tetrahydrofurane (THF) with ΔH_1 = -4.5 (3) kcal/mol and ΔS_1 = -30 (10) eu for K_1 and ΔH_2 = -4.1 (1) kcal/mol and ΔS_2 = -20 (10) eu for K_2. The anion exchange equilibria in CH_2Cl_2

$$\mathbf{1a} + 2\ Cl^- \overset{\mathbf{K_1}}{\rightleftarrows} [Cp^*Ru(NO)(OTf)(Cl) + OTf^- + Cl^- \overset{\mathbf{K_2}}{\rightleftarrows} [Cp^*Ru(NO)Cl_2] + 2\ OTf^-$$

has ΔH_1 = -9 (1) kcal/mol and ΔS_1 = -30 (10) eu for K_1 and ΔH_2 = -11 (1) kcal/mol and ΔS_2 = -30 (10) eu for K_2. While loss of the OTf$^-$ ligands is exothermic, the displacement of OTf$^-$ from the coordination sphere carries a significant entropy cost due to the formation of ions in a more-ordered solvent cage. Complex salts **1a,b** dissolve in water to give acidic red-orange solutions containing an equilibrium mixture of the diaqua complex cations $[Cp'Ru(NO)(OH_2)_2]^{+2}$ ($\mathbf{3a}^{+2}$, pK_a = 2.7; $\mathbf{3b}^{+2}$) and the dinuclear cations $[Cp'Ru(NO)(\mu\text{-}OH)]_2^{+2}$ ($\mathbf{4a}^{+2}$, pK_a = 5.5; $\mathbf{4b}^{+2}$). The cations $\mathbf{4a}^{+2}$ and $\mathbf{4b}^{+2}$ exist as a mixture of *cis* (major) and *trans* (minor) isomers. X-ray data (173 K) for *cis*- **4b**, ($C_{24}H_{36}N_2O_{10}S_2F_6Ru_2$): orthorhombic space group *Pbcn*, a = 15.148 (3) Å, b = 14.809 (3) Å, c = 15.214 (6) Å, Z = 4 , R/R_w = 0.0309/0.0432. Crossover between $\mathbf{4a}^{+2}$ and $\mathbf{4b}^{+2}$ to give the mixed Cp*/Cp^ dimer $\mathbf{4c}^{+2}$ occurs readily under acidic conditions but not under basic conditions. The pH dependence together with kinetic and van't Hoff analyses support the process: 2 $\mathbf{3a}^{+2} \rightleftarrows \mathbf{4a}^{+2} + 2\ H_3O^+$. The ∠ Ru-N-O values of ca. 160°, correspondingly low ν_{NO} values in the Nujol mull IR spectra, and relatively short Ru-O bonds show the H_2O and OH^- ligands to be significant π-donors to the electrophilic Ru center. Dissolution of **4a,b** in basic D_2O causes complete deuteration of the ring CH_3 groups but no deuteration of the Cp^-CH_2CH_3 group; the CD_3 groups are easily exchanged to CH_3 by exposure to basic H_2O conditions. Chloride substitution by H_2O occurs when $Cp'Ru(NO)Cl_2$ is dissolved in water, giving an equilibrium mixture of undissociated $[Cp'Ru(NO)Cl_2]_{aq}$ together with the $[Cp'Ru(NO)(Cl)(OH_2)]^+$ and $[Cp'Ru(NO)(\mu\text{-}OH)]_2^{+2}$ ions. H/D exchange on the Cp' ring CH_3 groups also occurs slowly when $Cp'Ru(NO)Cl_2$ is dissolved in D_2O but not when dissolved in a D_2O/DCl mixture. The present work suggests that Cp'-ring slippage and the reversible release of H^+/D^+ is facilitated by the π-donor ability of the H_2O and OH^- ligands.

Introduction

Electrophilic transition metal complexes are an important part of modern catalysis.[1] Especially important in this area is the subject of metal-triflate (M-OTf) complexes that have seen

increasing application as precursors to unsaturated electrophilic metal centers (OTf = OSO_2CF_3).[2] Such catalysts have been shown to accelerate Diels-Alder reactions by as much as 10^5 as compared to uncatalyzed reactions.[3] Dissociation of OTf$^-$ from chiral precursors leads to stereoselective electrophilic metal catalysts.[4,5] There are several recent reports on the generation and reactivity of late-metal systems where triflate dissociation leads to catalysts that copolymerize CO and olefins.[6] Triflate dissociation from (η^3-1,4,7-trimethyl-1,4,7-triazacyclononane)Rh(CH_3)($OTf)_2$ and related species have been shown to initiate ethylene polymerization even in the presence of water.[7] The study of aqueous organometallic chemistry has a long history dating back into the 1800s and has reemerged as an important area of study because of the environmentally and financially benevolent properties of water-based processes.[8] Synthetic reactions performed in aqueous media can actually exhibit higher activity and better selectivity than in organic solvents.[7,9,10] Furthermore, there is an increasing demand to study catalysis that is more closely related to the chemistry in naturally occurring biocatalytic systems.

Continuing from our interest in complexes containing the versatile [Cp'Ru(NO)]$^{+2}$ fragment,[11,12] we present here the characterization of the Lewis acid nature of the [Cp´Ru(NO)]$^{+2}$ fragment (Cp' = η-$C_5(CH_3)_5$, Cp*; η-$C_5(CH_3)_4(CH_2CH_3)$, Cp^). Previous work from Brookhart and from our laboratory shows that the [Cp*Ru(NO)(R)]$^+$ fragment, generated by H_2O dissociation from [Cp*Ru(NO)(CH_3)(H_2O)]$^+$ or by OTf$^-$ dissociation from Cp*Ru(NO)(CH_3)(OTf), can bind and activate olefins[13] and alkynes.[11] While some kinetic aspects of OTf$^-$ substitution have been described,[14] a comprehensive characterization of the equilibrium between bound and free OTf$^-$ in the presence of coordinating solvents has yet to be reported.[15] In particular, it is important to distinguish between the materials that crystallize from a solution and the actual species *present* in solution.

The systems we present here offer a simple format for the evaluation of H_2O and OTf$^-$ as competing ligands in the presence of an electrophilic metal center. Although water is considered a common ligand in coordination chemistry,[16] there is still considerable interest in the nature of water and hydroxo ligands in organometallic systems, especially in regard to their ability to displace

coordinating counterions and reactive substrates.[17] We show the ancillary NO ligand to be especially valuable because the ν_{NO} and $\angle$ Ru-N-O values provide insight about the π-donor ability of the H_2O ligand.[18] The work here employs a combination of traditional techniques like pH, conductivity measurements, and structural methods coupled with a direct assessment of chemical equilibria and kinetics by nuclear magnetic resonance (NMR) spectroscopy in H_2O.

Results

Substitution of OTf⁻ in Organic Solvents. Complexes Cp'Ru(NO)$(OTf)_2$ **1a,b** (Cp' = Cp*, **1a**; Cp', **1b**) are synthesized according to literature procedures.[12c] Dissolution of **1a** in 0.1 **M** H_2O/CH_2Cl_2 gives a purple solution that displays three signals in the ^{19}F NMR spectrum. The major resonance at δ -77.0 is identified as Cp*Ru(NO)$(OTf)_2$ and two minor broad resonances at δ -76.7 and δ -78.6 are assigned as the mono-aqua $[Cp^*Ru(NO)(OTf)(OH_2)]^+$ cation ($\mathbf{2a}^{+2}$) and free OTf⁻, respectively. The intensity due to free OTf⁻ is greater than the intensity of the signal from $\mathbf{2a}^+$ implying the presence of a third (and ^{19}F NMR silent) cationic complex $[Cp^*Ru(NO)(OH_2)_2]^{+2}$ ($\mathbf{3a}^{+2}$). The amount of $\mathbf{3a}^{+2}$ is readily determined from the initial concentration of **1a** and the measured integrals of $\mathbf{2a}^+$ and free OTf⁻ versus an internal standard (see Experimental Section). The ^{19}F NMR signal intensities are temperature dependent and the results of a van't Hoff analysis for the two-step equilibrium process of eq 1 are shown in Fig. 2-1 (Table 2-1), giving ΔH_1 = -15 (3) kcal/mol and ΔS_1 = -60 (30) eu for K_1 and ΔH_2 = -8 (1) kcal/mol and ΔS_2 = -40 (20) eu for K_2. At 298 K, the solution contains a ca. 20:5:1 mixture of **1a**, $\mathbf{2a}^+$, and $\mathbf{3a}^{+2}$, respectively. The errors in ΔS are large due to the restriction of the analysis to a relatively small temperature range (between +10 °C and +35 °C) to avoid the separation of an aqueous phase at lower temperatures. If 10 equiv of HOTf is added to the solution, OTf⁻ dissociation from **1a** is completely suppressed.

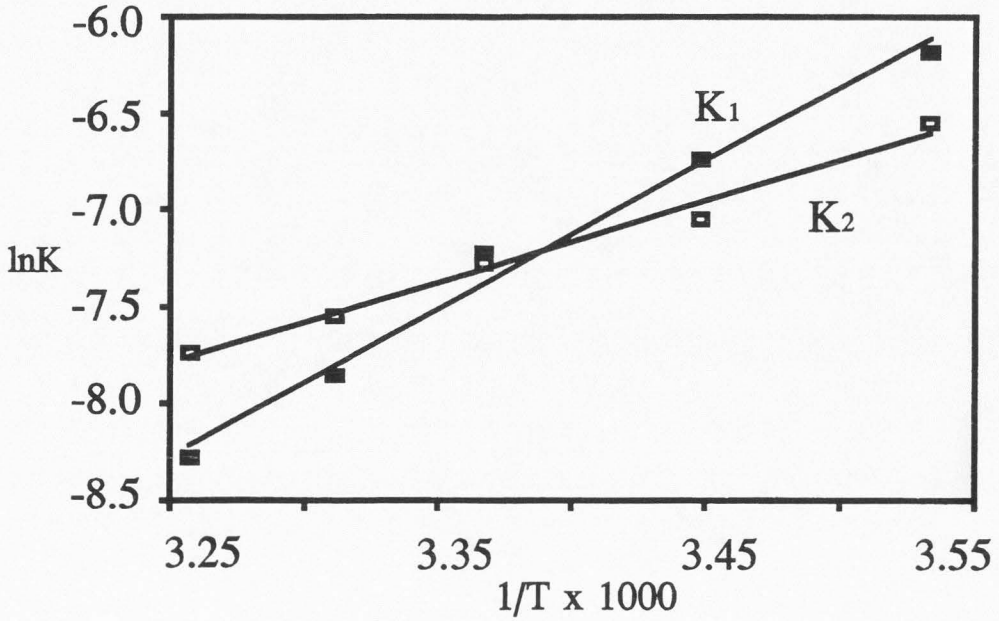

Figure 2-1. The van't Hoff plots for the equilibrium of complex **1a** with H_2O in CH_2Cl_2.

Table 2-1. Temperature dependence of the equilibrium constants K_1 and K_2 for the equilibrium **1a** ⇄ $[Cp^*Ru(NO)(OTf)(OH_2)]^+ + OTf^- \rightleftarrows [Cp^*Ru(NO)(OH_2)_2]^{+2} + OTf^-$ in water-saturated dichloromethane.

Temperature, K	$K_1 \times 10^3$	$K_2 \times 10^3$
283	2.1	1.4
290	1.2	0.9
297	0.7	0.7
302	0.4	0.5
307	0.2	0.4

Change in the concentration of free water due to the reaction is negligible (< 1%) and is not included in the calculations.

$$\underset{0.1\ \mathbf{M}\ H_2O/CH_2Cl_2}{\overset{K_1}{\rightleftarrows}} \qquad \underset{0.1\ \mathbf{M}\ H_2O/CH_2Cl_2}{\overset{K_2}{\rightleftarrows}} \qquad \text{(eq 1)}$$

$$\mathbf{1a} \rightleftarrows \underset{\mathbf{2a^+}}{[Cp^*Ru(NO)(OTf)(OH_2)]^+} + OTf^- \rightleftarrows \underset{\mathbf{3a^{+2}}}{[Cp^*Ru(NO)(OH_2)_2]^{+2}} + 2\ OTf^-$$

As monitored by ^{19}F NMR spectroscopy, the addition of two equiv of $[Ph_3PNPPh_3]Cl$ to **1a** dissolved in dry CH_2Cl_2 results in the decrease of the original δ -77.0 signal and the appearance of new signals at δ -77.2 assigned as Cp*Ru(NO)(OTf)(Cl) and free OTf^- at δ -78.6. The intensity due to free OTf^- is greater than the intensity of the signal from Cp*Ru(NO)(OTf)(Cl), implying the presence of a third (and ^{19}F NMR silent) complex $Cp^*Ru(NO)Cl_2$. The ^1H NMR spectrum of this mixture indeed shows a signal for $Cp^*Ru(NO)Cl_2$ at δ 1.84 and a signal at δ 1.82 assigned to Cp*Ru(NO)(OTf)(Cl) in addition to the original δ 1.88 signal of $Cp^*Ru(NO)(OTf)_2$. Quantitation of $Cp^*Ru(NO)Cl_2$ by ^{19}F NMR spectroscopy is based on the initial concentration of **1a** and measuring the integral intensities of Cp*Ru(NO)(OTf)Cl and free OTf^- versus an internal standard (see Experimental Section). The NMR spectra are temperature dependent and the results of a van't Hoff analysis for the two-step equilibrium process (eq 2) gives ΔH_1 = -9(1) kcal/mol and ΔS_1 = -30(10) eu for K_1 and ΔH_2 = -11(1) kcal/mol and ΔS_2 = -30(10) eu for K_2 (Fig. 2-2, Table 2-2). At 298 K, the solution contains a ca. 1:2:7 mixture of **1a**, Cp*Ru(NO(OTf)(Cl), and $Cp^*Ru(NO)Cl_2$, respectively.

$$\underset{}{\overset{K_1}{\rightleftarrows}} \qquad \underset{}{\overset{K_2}{\rightleftarrows}} \qquad \text{(eq 2)}$$

$$\mathbf{1a} + 2\ Cl^- \rightleftarrows [Cp^*Ru(NO)(OTf)Cl] + OTf^- + Cl^- \rightleftarrows Cp^*Ru(NO)Cl_2 + 2\ OTf^-$$

Dissolution of **1a** in neat THF gives red solutions (λ_{max} = 536 nm) with a ^{19}F NMR signal of free OTf^- at δ -78.7 and two other signals at δ -77.4 and δ -77.0 assigned as the $Cp^*Ru(NO)(OTf)_2$ and $[Cp^*Ru(NO)(OTf)(THF)]^+$ complexes, respectively, on the basis of their relative intensities to

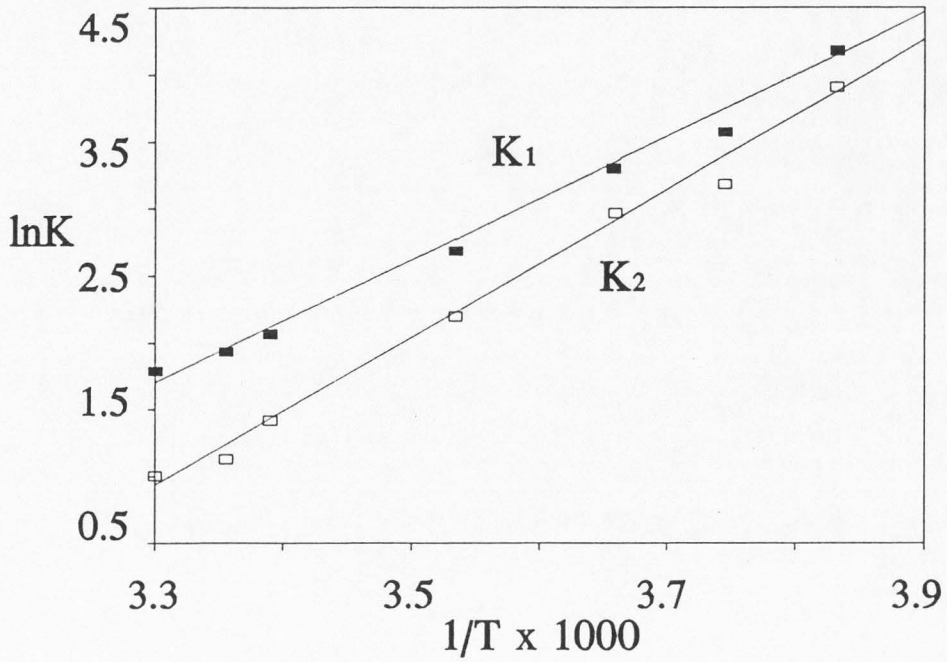

Figure 2-2. The van't Hoff plots for the equilibrium of **1a** with Cl^- in CH_2Cl_2.

Table 2-2. Equilibrium constants for the equilibrium of **1a** with 2 equiv of PPNCl in dichloromethane.

T	K1	K2
261	65.0	49.7
267	35.4	24.1
273	23.8	15.8
283	14.6	9.0
295	7.9	4.1
298	6.9	3.1
303	6.0	2.7

that of free OTf. The quantity of the ^{19}F NMR-silent species$[Cp^*Ru(NO)(THF)_2]^{+2}$ is deduced from the amount of free OTf not accounted to the formation of $[Cp^*Ru(NO)(OTf)(THF)]^+$ (see Experimental Section). The ^1H NMR spectrum of this mixture does not show well-resolved signals for the individual complexes. The ^{19}F NMR signal intensities are temperature dependent and the results of a van't Hoff analysis for the two-step equilibrium process (eq 3)

$$\mathbf{1a} \overset{K_1}{\rightleftarrows} [Cp^*Ru(NO)(OTf)(THF)]^+ + OTf^- \overset{K_2}{\rightleftarrows} [Cp^*Ru(NO)(THF)_2]^{+2} + OTf^- \qquad \text{(eq 3)}$$

gives ΔH_1 = -4.5(3) kcal/mol and ΔS_1 = -30(10) eu for K_1 and ΔH_2 = -4.1(1) kcal/mol and ΔS_2 = -20(10) eu for K_2 (Fig. 2-3, Table 2-3). At 293 K, the solution contains a ca. 3:6:1 mixture of **1a**, $[Cp^*Ru(NO)(OTf)(THF)]^+$, and $[Cp^*Ru(NO)(THF)_2]^{+2}$, respectively. The addition of 10 equiv of LiOTf to the THF solution of **1a** completely suppresses the ionization shown in eq 3. The IR spectra of **1a** or **1b** in THF show a single ν_{NO} absorption at 1850 cm^{-1} for both cases. Removal of solvent from these samples *in vacuo* and redissolution in CH_2Cl_2 cleanly regenerates **1a** or **1b** as shown by a single ^{19}F NMR resonance at δ -77.0.

Isolation of Diaqua Complex Salt 3b. Red, single-crystals of diaqua complex salt **3b** precipitate from H_2O-saturated (homogeneous) $CDCl_3$ solutions of **1b** at 25°C. These crystals display a strong ν_{NO} absorption at 1815 cm^{-1} when ground in a Nujol mull. Redissolving crystalline **3b** in CH_2Cl_2 results in a purple solution containing an equilibrium mixture of **1b** (major), $\mathbf{2b}^+$, and $\mathbf{3b}^{+2}$ as monitored by ^{19}F NMR spectroscopy.

The X-ray parameters for **3b** are summarized in Tables 2-4 and 2-5 and the structure is presented in Fig. 2-4. The complex cation adopts a piano-stool geometry with a crystallographically imposed mirror plane containing the [Ru-N-O] moiety. The Ru-O(2) bond length is 2.135 (5) Å and the ∠Ru-N-O of 160.6 (9)°. The H-atoms were not clearly located in the electron density difference map. Nevertheless, the O(2)-O(4) distance of 2.62 Å shows one unique OTf ion (with S(2)) to

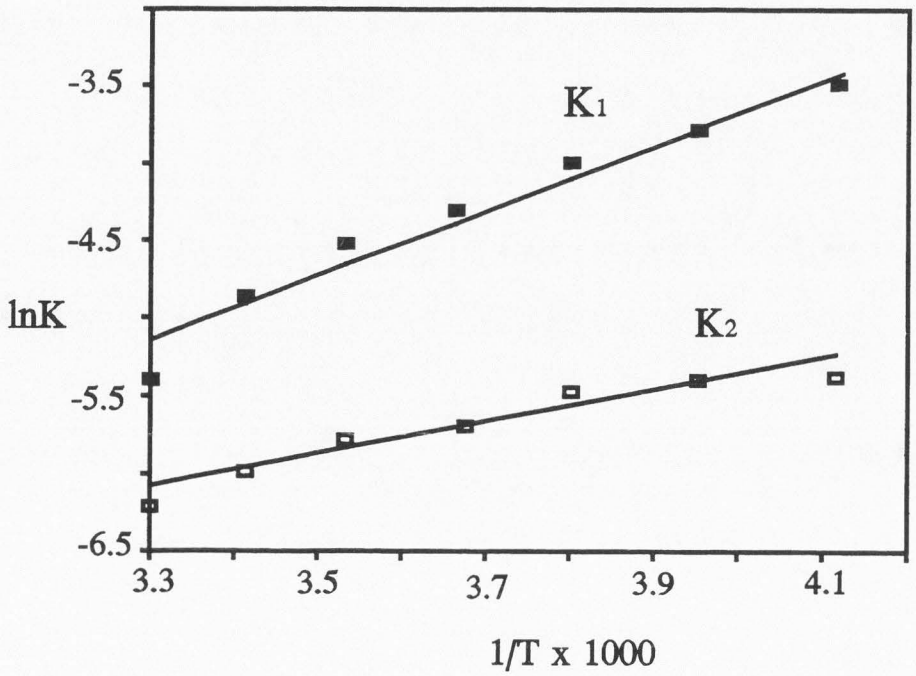

Figure 2-3. The van't Hoff plots for the equilibrium of complex **1a** in THF.

Table 2-3. Equilibrium constants for **1a** in THF determined from ^{19}F NMR data.

T, (K)	$K_1 \times 10^3$	$K_2 \times 10^3$
303	4.5	2.0
293	7.7	2.5
283	10.8	3.1
273	14.3	3.9
263	18.4	4.2
253	22.7	4.0
243	26.8	4.6

Table 2-4. Summary of crystallographic data for complexes **3b** and **4b**.

	3b	**4b**
Formula	$C_{13}H_{21}NO_9F_6S_2Ru$	$C_{24}H_{36}N_2O_{10}F_6S_2Ru_2$
Formula Wt, amu	614.5	446.1
Crystal system	Monoclinic	Orthorhombic
Space group	*C*2/m (No.12)	*P*bcn (No.60)
a (Å)	21.380 (4)	15.148 (4)
b (Å)	8.907 (2)	14.809 (3)
c (Å)	13.481 (3)	15.214 (6)
α (°)	90	90
β (°)	115.70 (3)	90
γ (°)	90	90
V (Å^3)	2113.2 (8)	3410.0 (6)
Z	4	4
T,K	223	173
μ (Mo Kα) (mm^{-1})	0.95	1.09
ρ_{calc} (g/cm^3)	1.76	1.74
final R, R_w	0.0569[a] wR_2 = 0.1536[c]	0.0309[a] 0.0432[b]

[a] $R = \Sigma \mid \mid Fo \mid - \mid F_c \mid \mid / \Sigma \mid F_o \mid$ [b] $R_w = [\Sigma w(\mid F_o \mid - \mid F_c \mid)^2 / \Sigma w \mid F_o \mid ^2]^{1/2}$; $w = 1/\sigma^2(\mid F_o \mid)$ [c] $wR2 = \mid \Sigma[w(F_o^2-F_c^2)]^2]/\Sigma[w(F_o^2)^2]]^{1/2}$

Table 2-5. Selected geometric data for **3b**.

Bond distances, Å		Bond angles (°)	
Ru-N	1.783 (9)	Ru-N-O(1)	160.6 (9)
Ru-O(2)	2.135 (5)	O(2)-Ru-O(2a)	82.9 (7)
Ru-C(1)	2.186 (9)	N-Ru-O(2)	103.1 (8)
Ru-C(2)	2.220 (6)	N-Ru-O(3)	100.9 (9)
Ru-C(3)	2.221 (6)		
N-O(1)	1.125 (12)	$Cp^{\wedge}_{cent}$ = centroid of	
S(1)-O(4)	1.303 (10)	η-$C_5(CH_3)_4(CH_2CH_3)$ ligand	
S(1)-O(3)	1.359 (13)		
S(1)-C20)	1.76 (2)		
S(2)-O(5)	1.348 (10)		
S(2)-O(6)	1.429 (8)		
S(2)-C(30)	1.795 (13)		
C-F_{ave}	1.25 (3)		
O(2)---O(6)	2.63		
O(2)---O(3)	3.13		
O(2)---O(4)	3.26		
O(4)---C(13)	3.74		
$Cp^{\wedge}_{cent}$-Ru	1.85		

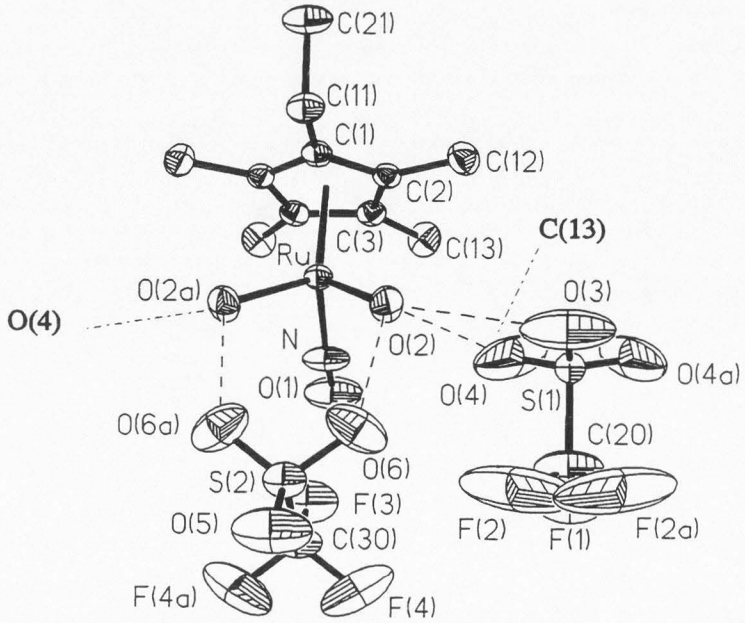

Figure 2-4. Thermal elipsoid plot and atom numbering scheme for complex **3b**.

strongly H-bond to the *cis*-diaqua ligands. The other unique OTf^- ion links the $[Cp^*Ru(NO)]^{+2}$ cations in a one-dimensional chain with the O(3)-O(2) separation being 3.15 Å. The O(4) position of this OTf^- ion is located 3.74 Å from the C(13) methyl group of a $[Cp^*Ru(NO)]^{+2}$ cation in an adjacent chain.

Reactivity of 1a with Water. Complex **1a** readily dissolves in water to form an acidic red-orange solution (λ_{max} = 377 nm) that displays a single ^{19}F NMR resonance at δ -78.0 that is coincident with free OTf^-. The molar conductance of a formally 7.0 x 10^{-3} **M** aqueous solution of **1a** is 286 $\Omega^{-1}cm^{-1}mol^{-1}$ and does not change upon dilution. The potentiometric titration of **1a** in H_2O with standardized aqueous NaOH leads to a curve typical for a weak acid/strong base process and shows a pK_a = 2.7 for **1a**. A freshly prepared sample of **1a** in H_2O displays Cp* signals at δ 1.84 (labeled as species $\mathbf{3a}^{+2}$) and δ 1.76 (labeled as species $\mathbf{4a}^{+2}$) in the ^1H NMR spectrum. Over time the initial intensity of $\mathbf{3a}^{+2}$ decreases with a corresponding increase in the intensity of $\mathbf{4a}^{+2}$ until equilibrium is reached in ca. 2 h at 25 °C (λ_{max} shifted slightly to 382 nm). A representative kinetic profile for the equilibration of species $\mathbf{3a}^{+2}$ and $\mathbf{4a}^{+2}$ (eq 4) as monitored by ^1H NMR spectroscopy in H_2O solvent is presented in Fig. 2-5. In this case the starting solution is formally 1.5 x 10^{-2} **M** solution of **1a** in H_2O and trials with initial **1a** concentrations of 1.0 x 10^{-2} **M** and 2.0 x 10^{-2} **M** give similar profiles. The results of a kinetic simulation (KINSIM) analysis are also plotted.[19] The parameters for this simulation are the initial concentration of $\mathbf{3a}^{+2}$, the stoichiometry in eq 4, and initial estimates for k_f and k_r. The best fit of the experimental data gives k_f = 0.04 $M^{-1}s^{-1}$ and k_r = 1.0 $M^{-2}s^{-1}$ after an iterative process. The rate constants at the higher and lower initial concentrations of **1a** are the same within 20%.

$$2\ \mathbf{3a}^{2+} \underset{k_r}{\overset{k_f}{\rightleftarrows}} \mathbf{4a}^{2+} + 2\ H_3O^+ \qquad \text{(eq 4)}$$

After equilibration at 298 K, a formally 0.005 **M** solution of **1a** in water contains a ca. 5:2 ratio of $\mathbf{4a}^{+2}$ to $\mathbf{3a}^{+2}$. Monitoring the ^1H NMR spectra of thermally equilibrated solutions of **1a** in

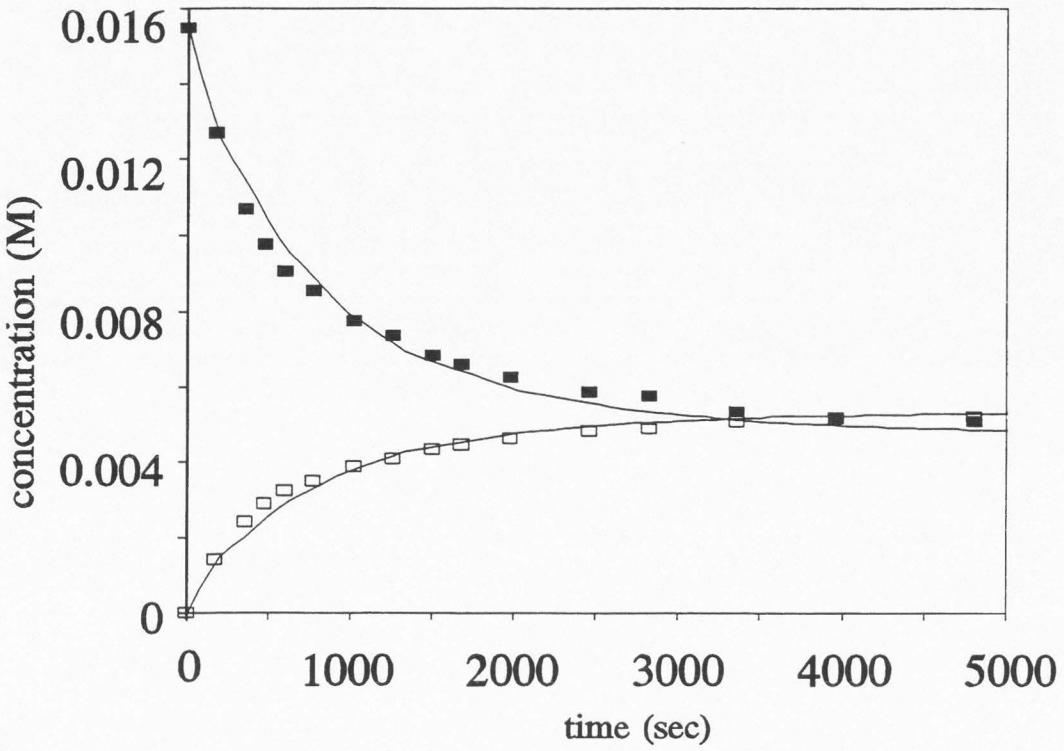

Figure 2-5. Kinetics of the equilibration of $\mathbf{3a}^{+2}$ and $\mathbf{4a}^{+2}$ in H_2O (solid line is simulation; ■ = [**3a**]; □ = [**4a**])

H_2O (eq 4) between 298 K and 358 K leads to good van't Hoff behavior, yielding the equilibrium thermodynamic values of ΔH = 5.0 (3) kcal/mol and ΔS = 11 (5) eu for eq 4 (Fig. 2-6, Table 2-6).

Addition of 0.5 equiv of NaCl to a 4.0 x 10^{-3} **M** solution of **1a** in H_2O produces signals at δ 1.84 (**3a**$^{+2}$), δ 1.81 ([Cp*Ru(NO)(OH_2)(Cl)]$^+$), δ 1.80 (Cp*Ru(NO)Cl_2), and δ 1.76 **4a**$^{+2}$ in a ca. 3:25:2:70 ratio, respectively, in the ^{1}H NMR spectrum. The ^{1}H NMR Cp* resonance of the **4a**$^{+2}$ ion is not affected by the change of OTf^- to Cl^-. Addition of 1.5 equiv of NaCl causes the δ 1.84 signal (**3a**$^{+2}$) to disappear completely and after the addition of 2.5 equiv of NaCl, the remaining resonances at δ 1.81 ([Cp*Ru(NO)(OH_2)Cl]$^+$), 1.80 (Cp*Ru(NO)Cl_2 and 1.76 (**4a**$^{+2}$) appear in a ca. 25:45:30 ratio. The solution at this point shows a λ_{max} of 560 nm.

X-ray Characterization of the μ-Hydroxy Complex Salt 4b. The complex salts [Cp'Ru(NO)(μ-OH)]$_2$[OTf]$_2$ (**4a,b**) can be preferentially extracted from aqueous solutions of **1a,b** by CH_2Cl_2 according to published procedures.[12c] Alternatively, **4a,b** precipitate directly from concentrated aqueous solutions of **1a** or **1b**. A single-crystal X-ray analysis of **4b** is repeated here, since the previous X-ray study was done for the crystals of **4b**·H_2O. The X-ray data for **4b** are summarized in Tables 2-4 and 2-7. Fig. 2-7 shows the molecule to be a C_2-symmetric *cis*-dinuclear complex situated about a two-fold crystal axis. The nonbonded Ru-Ru separation is 3.185 Å with the [Ru_2(μ-OH)$_2$] dihedral butterfly angle about the Ru-Ru vector being 129°. The NO ligands are located opposite to the butterfly angle. The plane containing the [H(2a)-O(2)-Ru] moiety forms an angle of 73° with the plane containing the [Ru-N-O1] linkage bent to 160°. The OTf^- ions are not disordered and are closely associated to the dinuclear cation to form an intramolecular bridge between the μ-OH^- ligand and a C(11) methyl group of the Cp^ ligand. The H-atoms were located and isotropically refined, showing the O(2)-H(2) distance to be 0.76 Å and the O(3) and O(5) atoms of the OTf^- ion to straddle H(2a) at 2.01 Å and 2.76 Å, respectively. The F(2) atom is 2.53 Å from the H(11a) atom on C(11) with the C(11)-F(2) distance being 3.33 Å. There are no significant intermolecular contacts between the [Cp^Ru(NO)(μ-OH)]$_2$[OTf]$_2$ units.

Dichloromethane solutions of **4a,b** display strong ν_{NO} IR absorptions at 1795 and 1799 cm^{-1},

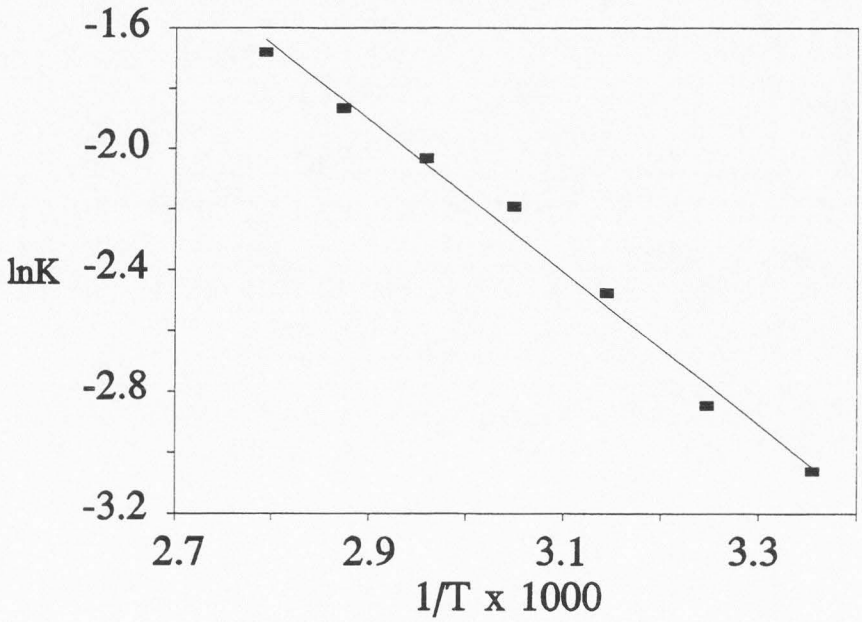

Figure 2-6. The van't Hoff plot for the equilibrium 2 **3a** ⇄ **4a** + $2H_3O^+$

Table 2-6. Equilibrium constants for complexes **3a** and **4a** in H_2O.

T (K)	K_{eq} x 10^2
298	4.7
308	5.8
318	8.4
328	11.2
338	13.1
348	15.5
358	18.6

Table 2-7. Selected geometric data for **4b**.

Bond distances, Å		Bond angles (°)	
Ru-N	1.788 (4)	Ru-N-O(1)	160.0 (3)
Ru-O(2)	2.069 (3)	N-Ru-O(2)	102.8 (1)
O(1)-N	1.147 (5)	O(2)-Ru-O(2A)	70.5 (1)
O(2)-H(2)	0.76 (2)	Ru-O(2)-RuA	100.6 (1)
S-O(3)	1.436 (4)	N-Ru-O(2A)	104.8 (1)
S-O(4)	1.416 (4)		
S-O(5)	1.454 (4)		
S-C(6)	1.810 (6)	$Cp^{\wedge}_{cent}$ = centroid of	
C(6)-F(1)	1.340 (7)	η-$C_5(CH_3)_4(CH_2CH_3)$ ligand	
C(6)-F(2)	1.287 (7)		
C(6)-F(3)	1.325 (7)		
Cp_{cent}-Ru	1.85		
Ru-Ru(a)	3.185		
O(2)---O(2a)	2.39		
O(2)---O(3)	2.01		
O(2)---O(5)	2.76		
F(2)---C(11)	3.44		
F(2)---H(11a)	2.53		
O(5)---H(2)	2.01		

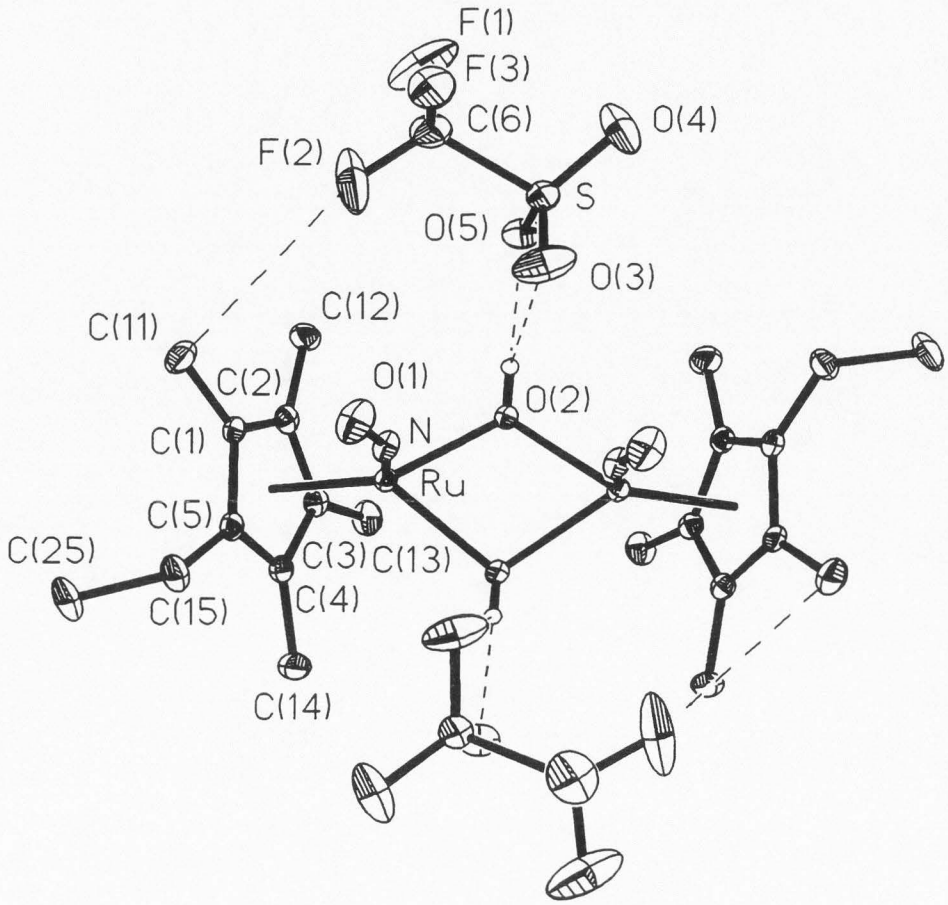

Figure 2-7. Thermal elipsoid plot and atom numbering scheme for complex **4b**.

respectively. The ^{1}H NMR spectra of these solutions show the presence of a major Cp' environment (95%) and a minor Cp' environment (5%). The relative intensity of the major and minor Cp' signals for **4b** are temperature dependent and a van't Hoff treatment of the ^{1}H NMR data for **4b** in 1,2-dichloroethane is linear over a 60°C range to give ΔH = 0.8(2) kcal/mol and ΔS = 1(5) eu (Fig. 2-8, Table 2-8). The relative area of the minor resonance increases to 10% when **4a** is dissolved in a 50/50 mixture of toluene/CH_2Cl_2. The hydroxyl ligands of **4a** and **4b** appear as singlets at δ 4.42 and δ 4.47, respectively, and the addition of 1 μL of D_2O to CH_2Cl_2 solutions of **4a,b** causes the hydroxyl proton signals to disappear immediately upon mixing. The addition of excess HOTf to **4a,b** in CH_2Cl_2 leads to the quantitative reformation of **1a,b** as monitored by ^{1}H NMR spectroscopy.

Reactivity of [Cp'Ru(NO)(μ-OH)]$_2$[OTf]$_2$ (4a,b). When equimolar amounts of **4a** and **4b** are dissolved together in H_2O, the residue after solvent removal contains a 1:1:2 mixture of **4a**, **4b,** and a new crossover species [(Cp*Ru(NO))(Cp^Ru(NO))(μ-OH)$_2$][OTf]$_2$ **4c** identifiable by a new ^{1}H NMR hydroxyl signal at δ 4.45 in CH_2Cl_2. No new Cp* or Cp^ ^{1}H NMR signals are resolvable from those seen for **4a**$^{+2}$ or **4b**$^{+2}$. The product **4c** is also obtained when equimolar amounts of **1a** and **1b** are mixed in H_2O. The rate of the formation of **4c** when equimolar amounts of **4a** and **4b** are allowed to stand in CH_2Cl_2 is dependent upon the amount of H_2O in the solvent. The observed kinetic data for the formation of **4c** from a mixture of **4a** and **4b** in 0.1 **M** H_2O/CH_2Cl_2 are shown in Fig. 2-9(A). The KINSIM simulation of the equilibration, starting from the initial concentrations of **4a** and **4b** and eq 5, is compared to the experimental data.[19] The iterative estimation of k_f and k_r shows a best fit with k_f = 3.2 x 10^{-4} **M**$^{-1}$s^{-1} and k_r = 8.0 x 10^{-5} **M**$^{-1}$s^{-1}. The rate of equilibration is ca. an order of magnitude slower in rigorously dried CH_2Cl_2, with k_f = 2.2 x 10^{-5} **M**$^{-1}$s^{-1} and k_r = 5.5 x 10^{-6} **M**$^{-1}$s^{-1} (Fig. 2-9[B]).

$$\mathbf{4a}^{+2} + \mathbf{4b}^{+2} \underset{k_r}{\overset{k_f}{\rightleftarrows}} 2\ \mathbf{4c}^{+2} \quad K_{eq} = 4 \qquad \text{(eq 5)}$$

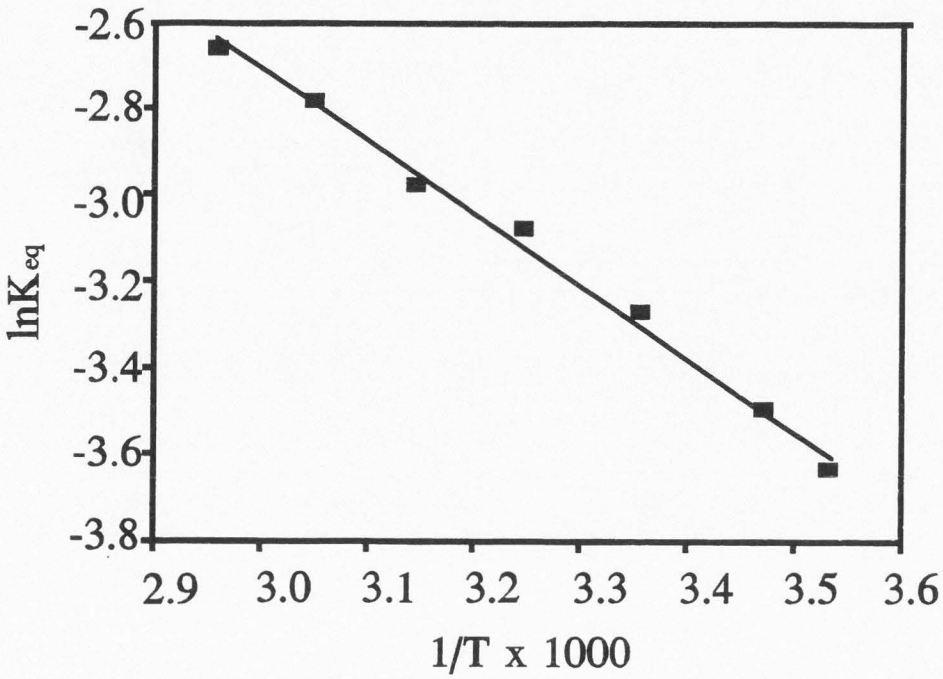

Figure 2-8. The van't Hoff plot for the isomerization of complex **4b** in 1,2-dichloroethane.

Table 2-8. Equilibrium constants for the *cis-trans* isomerization of **4b** in 1,2-dichloroethane.

T (K)	K_{eq} x 10^2 (*cis/trans*)
283	2.6
288	3.0
298	3.8
308	4.6
318	5.1
328	6.2
338	7.0

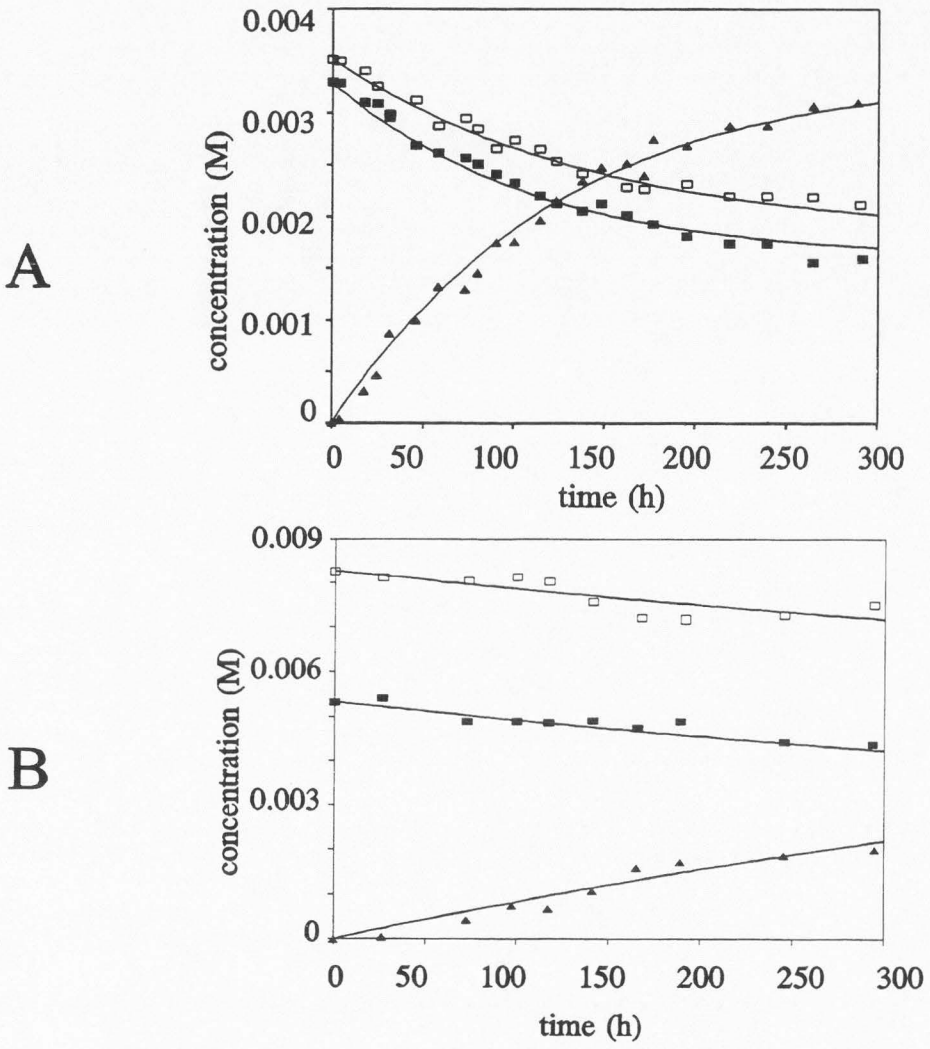

Figure 2-9. Kinetics of equilibration of $\mathbf{4a}^{+2}$ + $\mathbf{4b}^{+2}$ ⇄ $\mathbf{4c}^{+2}$ in CH_2Cl_2 (solid line is simulation; ■ = [**4a**]; □ = [**4b**]; ▲ = [**4c**

Aqueous solutions of **4a** are weakly acidic, leading to a determined pK_a of 5.5 by titration with standardized aqueous NaOH. Aqueous solutions of **4a** show only one Cp* environment by ^1H and ^{13}C NMR spectroscopy, with the major/minor isomer pair not being resolvable in H_2O. The putative conjugate base $[(Cp^*)_2Ru_2(NO)_2(\mu\text{-}OH)(\mu\text{-}O)]^+$ resulting from the deprotonation of $\mathbf{4a}^{+2}$ is not detected by NMR spectroscopy even at pH = 11.

Addition of NaOD to D_2O solutions of **4a** or **4b** results in the gradual decrease of the intensity of the methyl signals of the Cp* and Cp^ ligands with the corresponding development of broad, low intensity high-field shoulders adjacent to the CH_3 singlets over time. The signals from the ethyl group of the Cp^ ligand in $\mathbf{4b}^{+2}$ remain unaffected. The $t_{1/2}$ of the decrease in the methyl signal from 3.5 d at pD = 6 to 4 h at pD = 7 to 0.4 h at pD=11. Subsequent neutralization of the pD = 11 solutions with DCl after 24 h gives a green residue identified as the isotopically labeled d_{15}-$Cp^*Ru(NO)(Cl)_2$ and d_{12}-$Cp^\wedge Ru(NO)(Cl)_2$ complexes by ^2H NMR spectroscopy (eq 6-7). Treatment of the ^2H-labeled complexes with a large excess of H_2O at pH = 8 results in the quantitative regeneration of the ^1H-labeled complexes. The signals of $\mathbf{4a}^{+2}$ or $\mathbf{4b}^{+2}$ in H_2O at pH = 9 do not change measurably over a period of 3 d. Adjustment of the pH above 12 causes the gradual precipitation of a brown, intractable material that does not show any detectable ν_{NO} signal in the IR spectrum.

$$\mathbf{4a} \xrightarrow{D_2O} d_{15}\text{-}\mathbf{4a} \xrightarrow{D_2O/NaCl} d_{15}\text{-}Cp^*Ru(NO)Cl_2 \qquad \text{(eq 6)}$$

$$\mathbf{4b} \xrightarrow{D_2O} d_{12}\text{-}\mathbf{4b} \xrightarrow{D_2O/NaCl} d_{12}\text{-}Cp^\wedge Ru(NO)Cl_2 \qquad \text{(eq 7)}$$

Treatment of a 3.0×10^{-3} **M** aqueous solution of **4a** with 2 equiv of HCl causes a rapid color change from yellow to green (λ_{max} = 560 nm) and the ^1H NMR spectrum reveals three resonances in

a 10:50:40 ratio representing $[Cp^*Ru(NO)(OH_2)Cl]^+$ (δ 1.81), $Cp^*Ru(NO)Cl_2$ (δ 1.80), and $\mathbf{4a}^{+2}$ (δ 1.76), respectively. The treatment of a 3 x 10^{-3} **M** solution of **4a** with 2 equiv of NaCl results in no detectable reaction after 1 h, but the addition of 100 equiv of NaCl causes a color change to green within 5 min and the appearance of the single ^1H NMR resonance at δ 1.80 attributed to $Cp^*Ru(NO)Cl_2$.

Aqueous Chemistry of Cp´Ru(NO)Cl$_2$. At 25°C, $Cp^*Ru(NO)Cl_2$ dissolves in water to a formal concentration of 5.9 x 10^{-3} **M**. This saturated solution has a pH of 3.4 and the λ_{max} of 560 nm is only slightly lower than the value of 580 nm observed for $Cp^*Ru(NO)Cl_2$ dissolved in CH_2Cl_2. The molar conductance of this solution is 50 $\Omega^{-1}cm^{-1}mol^{-1}$ and increases significantly to 117 $\Omega^{-1}cm^{-1}mol^{-1}$ upon dilution to 1.8 x 10^{-4} **M**. The ^1H NMR spectrum of this solution shows three signals. Based upon the aqueous reactivity of **3a** and **4a** with Cl^- (vide supra), we can assign these signals to $[Cp^*Ru(OH_2)Cl]^+$ (δ 1.81), $Cp^*Ru(NO)Cl_2$ (δ 1.80), and $\mathbf{4a}^{+2}$ (δ 1.76), in a 10:10:1 ratio, respectively. Dilution to 3.6 x 10^{-4} **M** results in a corresponding 5:3:2 integral ratio for these signals and the λ_{max} of this solution is at 545 nm.

The addition of HCl to a formally 5.9 x 10^{-3} **M** solution of $Cp^*Ru(NO)Cl_2$ in H_2O causes the resonance due to $Cp^*Ru(NO)Cl_2$ (δ 1.80) to increase while the resonances due to $[Cp^*Ru(NO)(OH_2)Cl]$ (δ 1.81) and $\mathbf{4a}^{+2}$ (δ 1.76) decrease together in a fixed 10:1 ratio. After the addition of 10 equiv of HCl, only the signal of $Cp^*Ru(NO)Cl_2$ remains. When 8 equiv of NaCl is added to a 5.9 x 10^{-3} **M** aqueous solution of $Cp^*Ru(NO)Cl_2$, only the ^1H NMR signal of $Cp^*Ru(NO)Cl_2$ is detected. During the addition of HCl or NaCl, isosbestic points at 480 nm and 544 nm appear and the λ_{max} shifts to 573 nm. Over a period of 2-3 d at 25°C, solutions containing 10 or more equiv of HCl or NaCl eventually deposit green crystals of $Cp'Ru(NO)Cl_2$.

Addition of 1 equiv of NaOH to a formally 5.9 x 10^{-3} **M** aqueous solution of $Cp^*Ru(NO)Cl_2$ results in a color change to yellow (λ_{max} = 370 nm) and the appearance of ^1H NMR resonance of $\mathbf{4a}^{+2}$ (δ 1.76). The addition of 1 equiv of HCl restores the green color of the solution and results in the appearance of ^1H NMR signals from $[Cp^*Ru(NO)(OH_2)Cl]^+$ (δ 1.81), $Cp^*Ru(NO)Cl_2$ (δ 1.80),

and $\mathbf{4a}^{+2}$ (δ 1.76) in a 15:80:5 ratio, respectively. Addition of 10 equiv of HOTf to a formally 5.9 x 10^{-3} **M** aqueous solution of $Cp^*Ru(NO)Cl_2$ results in the disappearance of $\mathbf{4a}^{+2}$ in the ^1H NMR spectrum, leaving $[Cp^*Ru(NO)(OH_2)Cl]^+$ and $Cp^*Ru(NO)Cl_2$ in a ca. 2:1 ratio.

When $Cp'Ru(NO)Cl_2$ is dissolved in D_2O and monitored by ^1H NMR spectroscopy, the signals of the Cp' methyl groups gradually lose intensity with the simultaneous development of broad, high-field shoulders. This is most easily monitored in the case of $Cp^\wedge Ru(NO)Cl_2$, where the signals of the methyl singlets eventually disappear completely but the signals of the $Cp^\wedge$-ethyl group remain unaffected. A corresponding growth in the ^2H signals for the methyl groups is observed in the ^2H NMR spectrum. The $\mathbf{t_{1/2}}$ for the disappearance of the methyl signals is 42 h at 25°C (eq 8). When 1.5 equiv of NaOD is added to a fresh solution of $Cp'Ru(NO)Cl_2$ in D_2O, the $t_{1/2}$ for the loss of the methyl group signals decreases to 8 h. When a fresh D_2O solution of $Cp'Ru(NO)Cl_2$ is treated with 10 equiv of DCl, no changes in the ^1H NMR spectrum are observed over a period of 7 d (eq 9). The addition of 10 equiv of NaCl to $Cp^*Ru(NO)Cl_2$ in D_2O raises the pD by 0.6 units, but the rate of the loss of the methyl group signals in the ^1H NMR spectrum does not change significantly.

$$Cp^*Ru(NO)Cl_2 \xrightarrow{D_2O} d_{15}\text{-}Cp^*Ru(NO)Cl_2 \qquad \text{(eq 8)}$$

$$Cp^*Ru(NO)Cl_2 \xrightarrow{DCl/D_2O} \text{no reaction} \qquad \text{(eq 9)}$$

Discussion

Ligand Coordination to the $[Cp'Ru(NO)]^{+2}$ Fragment. A careful evaluation of the competition between species like OTf^-, Cl^-, H_2O, and OH^- ligands in organometallic complexes is especially important if the generation of a coordinatively unsaturated metal center is to be well understood. The combination of spectral and X-ray structural data available makes it possible to

closely assess the nature of ligand interactions with the $[Cp'Ru(NO)]^{+2}$ fragment. The NO ligand provides important information through its characteristic ν_{NO} values in nonaqueous conditions and the angle it forms when binding to the Ru center.

Previously reported results of X-ray structure studies for complexes **1b** and **2b** are discussed here in addition to the original investigation from the point of view of the OTf^- binding nature (Fig. 2-10, 2-11 and Tables 2-9, 2-10).[12c] While most previous studies have established the metal-OTf interaction to be primarily ionic in nature, the OTf^- ligands in **1b** and **2b** exhibit significant bond length changes upon binding to the electrophilic $[Cp'Ru(NO)]^{+2}$ center.[2b,14a] The structure of **1b** clearly shows the S(1)-O(2) bonds to be elongated from that seen in "free" OTf^- ions[20] and the S(1)-O(3) and S(2)-O(7) bond lengths of ca. 1.35 Å represent essentially localized S=O double bonds.[12c] The slightly longer S(1)-O(4) and S(2)-O6) bonds are consistent with the weak H-bonding interactions with these oxygen atoms in the crystal lattice. The X-ray structure of **2b** is particularly illustrative because both bound and "free" OTf^- ligands are present. Therein, the S(1)-O(3) bond distance is significantly elongated compared to the corresponding distances in the outer-sphere OTf^- ion. The relatively short (1.426 Å) S(1)-O(4) bond distance in the bound OTf^- shows somewhat less localization of S=O double bond character than seen in **1b**, perhaps due to the positive charge on the complex.[21] The short Ru-O bond lengths in complexes **1b** and **2b** are comparable to that found in Cp*Ru(NO)(Ph)(OTf) and are among the shortest reported Ru(II)-oxygen distances.[11]

The inspection of the ν_{NO} values for **1a,b** suggests that a OTf^- ligand possesses somewhat different donor properties from a chloride ligand. The ν_{NO} values for **1a,b** are ca. 56 cm^{-1} higher than in the corresponding $Cp'Ru(NO)Cl_2$ complexes.[12a] Following the work of Beck and others,[2g] the relatively high ν_{NO} values observed for **1a,b** might suggest weakly or nonbonded OTf^- ligands and a $[Cp'Ru(NO)(solvent)]^{+2}$ description with outersphere OTf^- ions. Without supporting evidence, this could be considered reasonable only if the π-donor ability of the Cl^- ligand is ignored.[18] The ability of Cl^- to π-donate can be expected to lower the ν_{NO} energy, whereas the strong π-withdrawing power anticipated for the $-SO_2CF_3$ moiety in the OTf^- case would be expected to

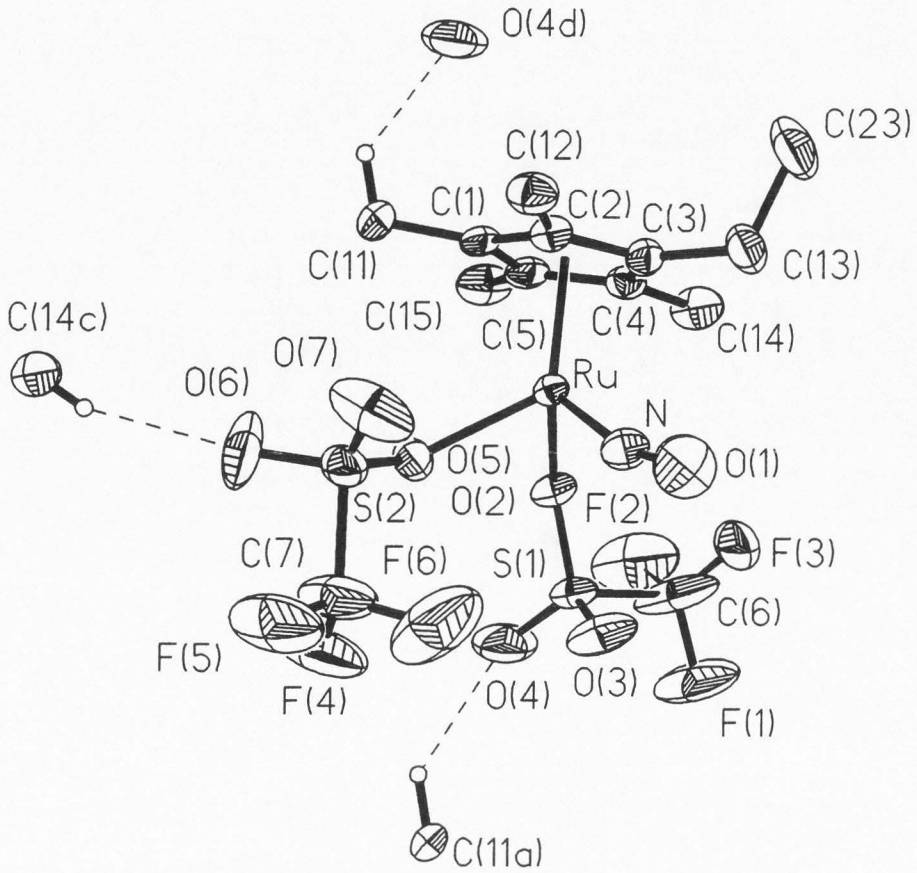

Figure 2-10. Thermal ellipsoid plot and numbering scheme for **1b** (Adapted from ref. 12c).

Table 2-9. Selected geometric data for **1b** (Adapted from ref. 12c).

Bond lengths (Å)		Bond angles (°)	
Ru-N	1.772 (8)	N-Ru-O(2)	102.9 (3)
Ru-O(2)	2.133 (5)	N-Ru-O(5)	102.0 (3)
Ru-O(5)	2.125 (5)	O(2)-Ru-O(5)	79.8 (2)
N-O(1)	1.136 (11)	Ru-N-O(1)	164.2 (7)
S(1)-C(6)	1.812 (19)	Ru-O(2)-S(1)	128.9 (3)
S(1)-O(2)	1.473 (5)	Ru-O(5)-S(2)	129.8 (3)
S(1)-O(3)	1.381 (7)	O(5)-Ru-O(2)	79.8 (2)
S(1)-O(4)	1.430 (9)	N-Ru-O2	102.9 (3)
S(2)-C(7)	1.745 (17)	N-Ru-O(5)	102.0 (3)
S(2)-O(5)	1.461 (6)		
S(2)-O(6)	1.456 (10)		
S(2)-O(7)	1.344 (9)	$Cp^{\wedge}_{cent}$ = centroid of	
C-F_{ave}	1.31 (2)	η-$C_5(CH_3)_4(CH_2CH_3)$ ligand	
$Cp^{\wedge}_{cent}$-Ru	1.85		
O(4)---C(11)	3.25		
O(6)---C(14)	3.26		

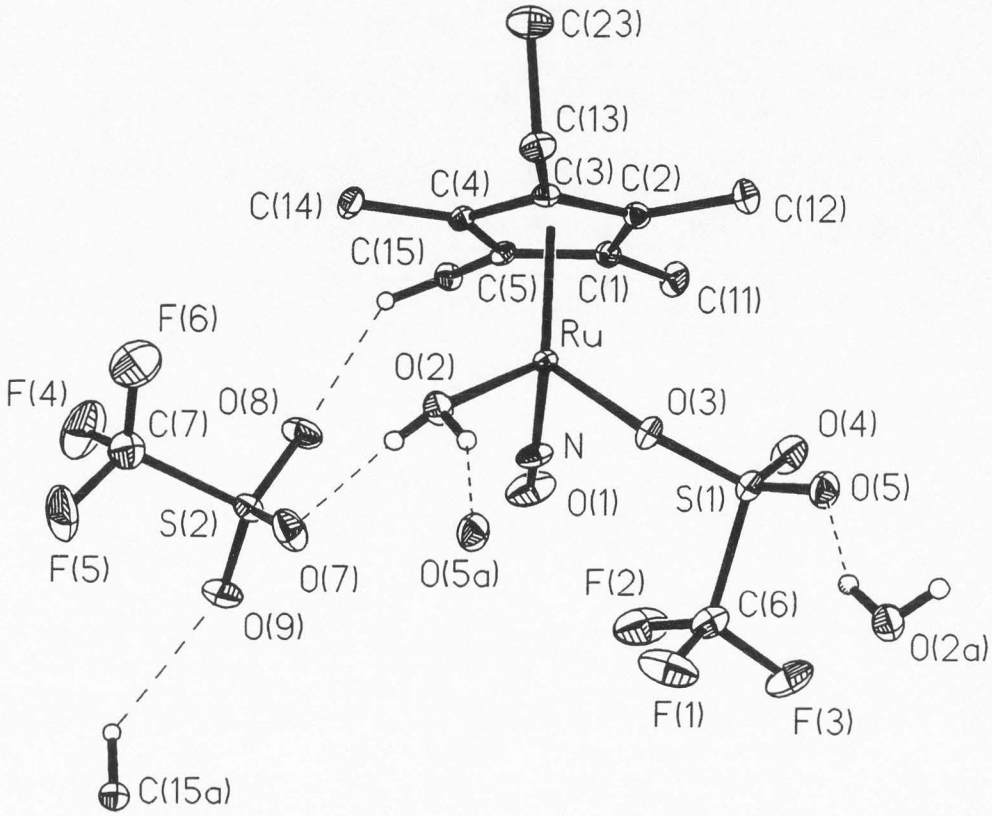

Figure 2-11. Thermal elipsoid plot and atom numbering scheme for complex **2b** (Adapted from ref. 12c).

Table 2-10. Selected geometric data for **2b** (Adapted from ref. 12c).

Bond distances, Å		Bond angles (°)	
Ru-N	1.782 (3)	N-Ru-O(2)	104.5 (1)
Ru-O(2)	2.128 (3)	N-Ru-O(3)	101.8 (1)
Ru-O(3)	2.141 (3)	O(2)-Ru-O(3)	77.9 (1)
N-O(1)	1.150 (5)	Ru-N-O(1)	159.5 (3)
S(1)-C(6)	1.826 (5)	O(5)-S(1)-C(6)	104.0 (2)
S(1)-O(3)	1.477 (3)	Ru-O(3)-S(1)	128.2 (2)
S(1)-O(4)	1.426 (3)	H(2a)-O(2)-H(2b)	107 (7)
S(1)-O(5)	1.432 (3)		
S(2)-C(7)	1.808 (5)		
S(2)-O(7)	1.449 (3)		
S(2)-O(8)	1.429 (3)		
S(2)-O(9)	1.428 (3)		
O(2)-H(2a)	0.90 (8)		
O(2)-H(2b)	0.71 (7)		
C-F_{ave}	1.32 (1)		
$Cp^{\wedge}_{cent}$-Ru	1.85		
O(7)-H(2b)	1.92		
O(7)-O(2)	2.63		
O(2)---O(5a)	2.79		
O(8)---C(15)	3.25		
O(8)---H(15a)	2.41		
O(9)---C(15a)	3.13		
Least squares planes (Å dev. from planarity):			
[Ru, O(2), H(2a), H(2b)]	0.0954 Å	angle to [Ru-N-O]	69.2°
Torsion angles (°)			
H(2a)-O(2)-Ru-N	101.4	$Cp^{\wedge}_{cent}$ = centroid of η-$C_5(CH_3)_4(CH_2CH_3)$ ligand	
H(2b)-O(2)-Ru-N	-26.4		

diminish the π-donor ability of the OTf donor O-atom, and cause the ν_{NO} energy to be relatively higher. Similar shifts are observed in the IR spectra for $Cp^*Fe(CO)_2Cl$ and $Cp^*Fe(CO)_2(OTf)$.[2b]

The $\angle$ Ru-N-O of ca. 160° in the structures of **2b** and **3b** and the corresponding decrease in the ν_{NO} energies from **1b** to **2b** to **3b** can be attributed to the presence of the H_2O ligands. The 21 cm^{-1} reduction n ν_{NO} from **1b** to **2b** and 15 cm^{-1} reduction from **2b** to **3b** suggests increasing the π-donation with an increasing number of aqua ligands. The H_2O ligand is poised for both σ-and π-donation to the Ru center. The structure of **2b** clearly shows a tightly bound H_2O ligand in a "planar" conformation, with the [Ru-OH_2] moiety deviating from planarity by only 0.1 Å. The NO ligand responds significantly, backing away from formal 3-electron (linear Ru-NO) donation toward a 1-electron (bent Ru-NO) configuration. The torsion angles about the Ru-O(2) bond further support that the NO ligand is backing away from the p-π-orbital perpendicular to the OH_2 plane. In the structure of **3b** the NO ligand is bent back in a symmetric disposition from the two H_2O ligands, lying in the mirror plane that bisects the [Cp^Ru(NO)] fragment.

The ca. 2.6 Å distance between the O atoms of the aqua ligands and the nearest non-coordinated triflate oxygen atoms in **2b** and **3b** clearly indicates the existence of moderately strong H-bonds in the solid state in comparison to other characterized H-bonding interactions.[22] Much weaker interactions are observed between the OTf ions and the CH_3 groups of the Cp' ligands, leading to an extended packing array in the crystal lattice.

Structural Aspects of the μ-Hydroxyl Complex 4b. The $\angle$ Ru-N-O in **4b** is 160°, indicating significant π-donation from the μ-hydroxyl ligands. The close association of the OTf counterions leads to the formation of discrete $[Cp^Ru(NO)(\mu\text{-}OH)]_2[OTf]_2$ units in the solid state. Two O-atoms of the SO_3 group effectively chelate the H-atom of the μ-OH ligand and a significant interaction occurs between an F-atom of the CF_3 group and an H-atom of a CH_3 group on the Cp^ ligand.

Substitution of Coordinated OTf in Nonaqueous Solvents. An important issue in the

study of reactive electrophilic metal centers is the generation of coordination unsaturation. With OTf^- ions being widely regarded as particularly weak ligands, our major concern has been to analytically characterize the competition between OTf^- binding and that of donor species like H_2O and THF. Without the use of spectral probes like those presented in this study, it is extremely difficult to discriminate between the species present in solution and those that crystallize from solution.

The equilibrium shown in eq 1 demonstrates that, even though H_2O in CH_2Cl_2 does displace the OTf^- ligand in a sequential process, the major species in solution is undissociated **1a**. This type of behavior is similar to that reported for $Re(CO)_5(OTf)$,[14] but is contradictory to the reported behavior of *trans*- $Rh(PPh_3)_2(CO)(OTf)$.[15,23] Interestingly, the equilibrium in eq 2 shows that, even though Cl^- is a stronger ligand than OTf^-, OTf^-/Cl^- exchange readily occurs. In neat THF, the equilibrium in eq 3 shows a relatively larger concentration of the $[Cp'Ru(NO)(OTf)(THF)]^+$ and $[Cp'Ru(NO)(THF)_2]^{+2}$ ions. It is clear from the van't Hoff analyses of eq 1-3 that substitution of OTf^- is consistently exothermic. Nevertheless, the negative ΔS values show there is a large entropic cost when OTf^- is released from the coordination sphere. In eq 1 and eq 3, this is consistent with the entropy decrease associated with the formation of a more-ordered solvent cage in connection with the newly formed ion-pair. The negative ΔS values for the equilibria shown in eq 2 would correlate with the solvation of the larger OTf^- ion as compared to the Cl^- ion.

The apparent coincidence of the ν_{NO} energies of the $Cp'Ru(NO)(OTf)_2$, $[Cp'Ru(NO)(OTf)(THF)]^+$, and $[Cp'Ru(NO)(THF)_2]^{+2}$ species when **1a,b** is dissolved in THF is similar to the situation when the $Cp^*Ru(NO)(R)(OTf)$ complexes are dissolved in THF ($R = CH_3$, C_6H_5).[9] As before, we ascribe this to the counterbalancing of two effects: the tendency for the ν_{NO} values to shift to higher energy in the cationic cases and the apparent ability of THF to be a significant π-donor (like H_2O) to the [Ru-NO] moiety.[24]

Aqueous Chemistry of the $[Cp'Ru(NO)]^{+2}$ Fragment. Complexes **1a,b** are strong electrolytes in H_2O, leading to the initial formation of $\mathbf{3a}^{+2}$ or $\mathbf{3b}^{+2}$ followed by the equilibration to $\mathbf{4a}^{+2}$ or $\mathbf{4b}^{+2}$ (eq 4). The rather electrophilic nature of the $[Cp'Ru(NO)]^{+2}$ moiety leads to a pK_a of

2.7 for $\mathbf{3a}^{+2}$. Similar to metals with low pK_a values (e.g., Al^{+3}, V^{+3} and Ga^{+3}), the formation of polynuclear complexes with μ-OH ligands is not unexpected.[25] Somewhat higher pK_a values are reported for a large variety of half-sandwich organometallic aqua complexes.[9k] The temperature dependence of the equilibrium between $\mathbf{3a}^{+2}$ and $\mathbf{4a}^{+2}$ (eq 4, Fig. 2-8) shows that monomer → dimer conversion is endothermic and that the bonding in the $[Ru_2(\mu\text{-}O)_2]$ core does not compensate for the liberation of the two H^+ ions required per dimer formed. The positive ΔS value reflects the fact that the number of solvated OTf^- ions does not change and the number of solute species increases by 50%. The conversion of $\mathbf{3a}^{+2}$ to $\mathbf{4a}^{+2}$ is slow enough to permit a kinetic analysis shown in Fig. 2-7. A simulation of the observed rate of equilibration agrees well with eq 4 being second-order in $\mathbf{3a}^{+2}$ and first-order in $\mathbf{4a}^{+2}$.

Potentiometric titration results in H_2O show the pK_a of **4a** to be 5.5. This is considerably less than the pK_a of $\mathbf{3a}^{+2}$ and indicative of the μ-OH proton being less acidic than bound H_2O. Attempts to generate spectroscopically detectable amounts of $[Cp'_2Ru_2(NO)_2(\mu\text{-}O)(\mu\text{-}OH)]^+$ have so far been unsuccessful (vide infra).

The conversion of monomeric $\mathbf{3a}^{+2}$ to dimeric $\mathbf{4a}^{+2}$ suggests the intermediacy of an undetected $[Cp^*Ru(NO)(OH_2)(OH)]^+$ complex. The observation of crossover between $\mathbf{4a}^{+2}$ and $\mathbf{4b}^{+2}$ in H_2O to give the mixed Cp*/Cp^ dimer $\mathbf{4c}^{+2}$ also requires a similar aqua(hydroxy) monomeric species. The fact that $\mathbf{4a}^{+2}/\mathbf{4b}^{+2}$ crossover is inhibited under basic conditions shows that the opening of the μ-OH linkage in $\mathbf{4a}^{+2}$ and $\mathbf{4b}^{+2}$ requires the addition of H_3O^+. In comparison to the reaction in 0.1 **M** H_2O in CH_2Cl_2, the crossover of **4a** and **4b** is extremely slow in "dry" CH_2Cl_2; the observation of any crossover in this case most likely reflects our inability to remove all adventitious H_2O from the reaction vessel. The extremely sluggish nature of these reactions has hampered our attempts to determine the exact order of H_2O.

It is apparent that the *cis*/*trans*-interconversion of the dimers $\mathbf{4b}^{+2}$ is not affected by pH or the presence of H_2O. We base our assignment of *cis*-$\mathbf{4b}^{+2}$ being the major isomer in CH_2Cl_2 and 1,2-dichloroethane by the increase in the minor ^1H NMR resonance when the solvent polarity is decreased

by the addition of toluene. The *trans*-structure would likely be less polar than the *cis*-isomer.

The immediate treatment of freshly prepared solutions of **1a** with less than 1 equiv of NaCl results in the observation of four species identified as $\mathbf{3a}^{+2}$, $\mathbf{4a}^{+2}$, $[Cp^*Ru(NO)(OH_2)(Cl)]^+$, and $Cp^*Ru(NO)Cl_2$ (eq 10). Cleavage of the dimer $\mathbf{4a}^{+2}$ to give $Cp^*Ru(NO)Cl_2$ occurs readily when **4a** is dissolved in aqueous HCl (eq 11) but much more slowly when **4a** is dissolved in aqueous NaCl (eq 12). As in the case of the crossover observed between $\mathbf{4a}^{+2}$ and $\mathbf{4b}^{+2}$ to give $\mathbf{4c}^{+2}$, opening of the dinuclear $[Ru_2(\mu\text{-}OH)_2]^{+2}$ core requires the addition of H_3O^+.

$$\mathbf{1a} \xrightarrow{\text{aq. NaCl}} \mathbf{3a} + \mathbf{4a} + [Cp^*Ru(NO)(OH_2)(Cl)]^+ + Cp^*Ru(NO)Cl_2 \qquad \text{(eq 10)}$$

$$\mathbf{4a} + \text{excess HCl} \rightarrow 2\ Cp^*Ru(NO)Cl_2 \quad \text{(fast)} \qquad \text{(eq 11)}$$

$$\mathbf{4a} + \text{excess NaCl} \rightarrow 2\ Cp^*Ru(NO)Cl_2 \quad \text{(slow)} \qquad \text{(eq 12)}$$

It is possible to approach an equilibrium of aqua(chloro) species by simply dissolving $Cp'Ru(NO)Cl_2$ in H_2O (eq 13). Conductivity, pH measurements, and electronic absorption data indicate that $Cp'Ru(NO)Cl_2$ is a weak electrolyte in H_2O and that a significant amount of undissociated $Cp'Ru(NO)Cl_2$ is present in solution. ^1H NMR spectroscopy measurements in H_2O show nearly equal concentrations of $Cp'Ru(NO)Cl_2$ and $[Cp'Ru(NO)(OH_2)(Cl)]^+$ with only a minor amount of the $\mathbf{4a}^{+2}$ or $\mathbf{4b}^{+2}$ ions being present. Under these conditions, the diaqua species $\mathbf{3a}^{+2}$ or $\mathbf{3b}^{+2}$ are not observed due to the relatively large amount of Cl^- present in solution.

$$Cp'Ru(NO)Cl_2 \overset{H_2O}{\rightleftarrows} [Cp'Ru(NO)(OH_2)(Cl)]^+ + Cl^- \overset{H_2O}{\rightleftarrows} 1/2\ [Cp'Ru(NO)(\mu\text{-}OH)]_2^{+2} + 2\ Cl^- + H^+ \qquad \text{(eq 13)}$$

Deuteration of the Cp'-Methyl Groups. Although we were initially surprised to see facile H/D exchange in the Cp'-methyl groups in our Ru complexes, a perusal of the literature shows that a similar phenomenon was reported over 20 years ago by Maitlis and coworkers for the $[(Cp^*M)_2(\mu\text{-}OH)_3]^+$ complexes (M = Rh, Ir).[10a] There continues to be considerable interest in this type of reactivity, especially with regard to slippage of the Cp'-ligand to an η^4-fulvene coordination mode.[10,26]

The present study offers new insight into the mechanism of reversible H/D exchange on a hydrocarbon ligand under aqueous conditions. The specificity of deuterium incorporation into only the Cp^-methyl groups suggests that the relative pK_a of the Cp' protons is the important parameter in the process. Since the pK_a of the methylene protons of the Cp^ ligand can be expected to be higher than the pK_a of the methyl substituents, we conclude that the H/D exchange involves an H^+ or D^+ transfer. The release of H^+ can be expected to be more facile upon Cp'-slippage. In order for the Cp' ligand to slip, ligands like O^{-2}, OH^{-1}, or H_2O that are capable of both σ and π-donation are required. The absence of H/D exchange when $Cp'Ru(NO)Cl_2$ is treated with D_2O/DCl (where no H_2O or OH^- ligation occurs) suggests that Cl^- ligands alone are not capable of causing the effect. In Scheme 2-1, we propose a tautomerization process from the unseen μ-oxo complex, where the Cp' ligand slips to an η^4-fulvene mode. Our experience with complexes like $\mathbf{4a}^+$ shows that exchange of H^+/D^+ could easily occur at the μ-hydroxyl positions. The decomposition at pH > 11 presumably arises from OH^- attack at the coordinated NO and greatly limits our ability to fully probe this reaction. The sluggishness of H/D exchange under acidic conditions is consistent with the need for a base to accept a proton from the Cp' ligand.

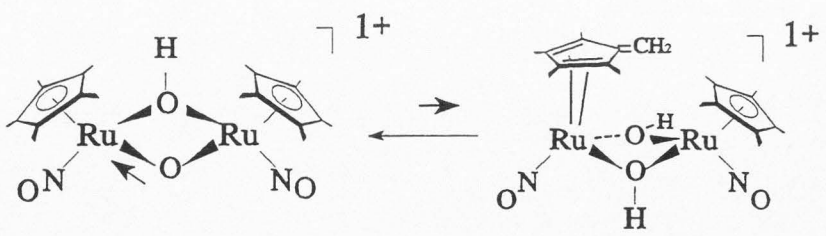

Scheme 2-1

Experimental

General. Standard Schlenk techniques were employed in all syntheses. The nitrogen reaction atmosphere was purified by passing through scavengers for water (Aquasorb, Mallinckrodt) and oxygen (Catalyst R3-11, Chemical Dynamics, So. Plainfield, NJ). Organic solvents were distilled under nitrogen over appropriate drying agents prior to use. The water used was purified and deionized (NANO-pure Ultrapure Water System) and saturated with N_2 gas prior to use. Concentration of H_2O in water-saturated CH_2Cl_2 at 298 K is 0.198 g H_2O/100 mL CH_2Cl_2 (ca. 0.1 **M**) as taken from the literature.[27] All chemical reagents were used as received from Aldrich unless stated otherwise. Cp*Ru(NO)Cl_2[12a] and Cp*Ru(NO)$(CH_3)_2$[28] were prepared as previously described. The preparation of Cp^Ru(NO)Cl_2 and Cp^Ru(NO)$(CH_3)_2$ followed similar procedures using $C_5(CH_3)_4(CH_2CH_3)H$ in place of $C_5(CH_3)_5H$; their characteristics are reported below. Infrared spectra were recorded on a Mattson Polaris-Icon FT-spectrometer.

The ^1H, ^2H, ^{13}C and ^{19}F NMR spectra were recorded on a Bruker ARX-400 NMR spectrometer operating at 400 MHz (^1H), 61.42 MHz (^2H), 100.62 Mhz (^{13}C), and 376.2 Mhz (^{19}F). The residual solvent peak of $CDCl_3$ was used as the internal NMR standard (^1H δ 7.24; ^{13}C δ 77.0 ppm), as well as residual peak of HDO (^1H δ 4.70). Routine spectra were recorded at 298 K. ^{19}F chemical shifts were referenced externally to $CFCl_3$ (δ 0.0) or internally to 3,5-bis(trifluoromethyl)benzene (δ -63.2); a relaxation delay of 12 s was used to optimize the integration. Free OTf^- appears at δ -78.6 in CH_2Cl_2 and δ -78.0 in H_2O, regardless of the counterions present. NMR spectra in CH_2Cl_2 and H_2O were measured using solvent presaturation techniques and were shimmed and referenced to the signals from $CDCl_3$ sealed inside a 1.5-mm capillary located concentrically inside the 5-mm NMR tube. When necessary, 5-mm NMR tubes with resealable Teflon valves were used (Brunfeld Co., Bartlesville, OK). The chemical shifts reported for the complexes in CH_2Cl_2 and H_2O are identical to those in the analogous deuterated solvents.

The equilibrium and kinetic studies utilized ^{19}F and ^1H NMR spectroscopy. The temperature inside the VT-NMR probe was calibrated according to literature procedures.[29] For van't Hoff

analyses, the samples were allowed to thermally equilibrate at the desired temperatures before spectra were recorded (15-120 min). The simulation of the kinetics for the equilibration of **3a** and **4a**, and the equilibration of **4a**, **4b**, and **4c** were performed on an IBM-compatible 486 personal computer using the program KINSIM.[19] Simulations started with initial concentrations, the stoichiometry specified in the corresponding equations, and estimated values for k_f and k_r. The values of k_f and k_r were systematically varied until a satisfactory fit to the experimental data was obtained.

Potentiometric titrations were performed with an Orion Research model 611 digital pH/millivolt meter and a glass pH electrode calibrated with standard buffer solutions at pH = 7.0 and pH = 10.0. The ca. 0.01 **M** NaOH solutions were standardized with KHP immediately before the measurements. The pK_a values were taken as the pH at the midpoint of the titration and were reproducible to within 0.1 pH units.

Conductivity measurements were performed on YSI Model 31A conductivity bridge. Solution series were prepared prior to the measurements in the purified water (solvent conductivity $\leq 10^{-6}\ \Omega^{-1}cm^{-1}$) by serial dilution (concentrations range from 6.0×10^{-3} **M** to 1.8×10^{-4} **M** of $Cp^*Ru(NO)Cl_2$ and from 7.0×10^{-3} **M** to 3.5×10^{-4} **M** of **1a**). The saturated $Cp'Ru(NO)Cl_2$ solution was prepared by saturating H_2O or D_2O for 30 min at the ambient temperatures over solid $Cp'Ru(NO)Cl_2$ and subsequent filtering the pale green supernatant through the pipette with a cotton plug.

Mass spectra were measured with an LKB 2091 mass spectrometer using electron impact ionization and a heated direct inlet probe. Melting points were measured with a Mel-Temp device (Laboratory Devices) in open capillaries and are uncorrected. UV-visible spectra were recorded on an HP 8452A Diode array spectrophotometer. Combustion analyses were performed by Atlantic Microlab, Inc., Norcross, GA.

K_{eq} Calculations for the Solvolysis of 1a. In the solvolysis of **1a** in either 0.1 **M** H_2O in CH_2Cl_2 or in neat THF, the concentration of the solvating ligand (H_2O or THF) is relatively large and constant. Thus, the two-step equilibria can be represented by eq 1 and eq 2, where the solvent

concentration is incorporated into the K_1 and K_2 values. A representative calculation for the solvolysis of **1a** by H_2O in CH_2Cl_2 is shown below.

A starting solution that was formally 0.0106 M **1a** and 0.1 **M** H_2O in CH_2Cl_2 was allowed to come to equilibrium at 290 K. The species **1a**, **2a**$^+$, and free OTf^- each have a corresponding ^{19}F NMR signal intensities represented as $\underline{a}$, $\underline{b}$, and $\underline{c}$, respectively. The sum $(\underline{a}+\underline{b}+\underline{c})$ represents the total ^{19}F signal that can be traced back to the initial concentration of **1a**, $[\mathbf{1a}]_i$ and referenced to an internal ^{19}F standard. Given that $\underline{a}$ = 129, $\underline{b}$ = 21, and $\underline{c}$ = 31,

$$[\mathbf{1a}] = (\underline{a}/(\underline{a}+\underline{b}+\underline{c}))\ ([\mathbf{1a}]_i) = [129/(129+21+31)](0.0106) = 0.00755\ \mathbf{M}$$

$$[\mathbf{2a}] = (\underline{b}/(\underline{a}+\underline{b}+\underline{c}))\ ([\mathbf{1a}]_i)(2) = [21/(129+21+31)](0.0106)(2) = 0.00246\ \mathbf{M}$$

$$[OTf^-] = (\underline{c}/(\underline{a}+\underline{b}+\underline{c}))\ ([\mathbf{1a}]_i)(2) = [31/(129+31+21)](0.0106)(2) = 0.00363\ \mathbf{M}$$

The concentration of **3a** was deduced according to the mass conservation considerations:

$$[\mathbf{1a}]_i = [\mathbf{1a}] + [\mathbf{2a}] + [\mathbf{3a}]$$

$$[\mathbf{3a}] = [\mathbf{1a}]_i - [\mathbf{1a}] - [\mathbf{2a}] = 0.0106 - 0.00755 - 0.00246 = 0.00059\ \mathbf{M}$$

From eq 1, K_1 and K_2 are expressed:

$K_1 = [\mathbf{2a}][OTf^-]/[\mathbf{1a}]$ $\qquad$ $K_2 = [\mathbf{3a}][OTf^-]/[\mathbf{2a}]$

Substitution of the values for [**1a**], [**2a**], [OTf^-], and [**3a**] gives:

$K_1 = [\mathbf{2a}][OTf^-] / [\mathbf{1a}] = (0.00246)(0.00363) / (0.00755) = 0.00118$

$K_2 = [\mathbf{3a}][OTf^-] / [\mathbf{2a}] = (0.00059)(0.00363) / (0.00246) = 0.00086$

A similar strategy was used for the calculation of K_1 and K_2 in neat THF (eq 3). For the case of triflate substitution by Cl^- (eq 2), the term [Cl^-] is included directly into the equilibrium expression.

Characterization of Cp^Ru(NO)Cl$_2$.[30] ^1H NMR ($CDCl_3$) δ 2.17 (q, 2H, $^3J_{HH}$=7.5 Hz, η^5-$C_5Me_4C\underline{H}_2CH_3$), δ 1.16 (t, 3H, $^3J_{HH}$=7.5 Hz, η^5-$C_5Me_4CH_2C\underline{H}_3$), δ 1.84 (s, 6H, (η^5-$C_5\underline{Me}_4CH_2CH_3$), 1.83 (s, 6H, ($\eta^5$-$C_5\underline{Me}_4CH_2CH_3$); ($C_6D_6$) δ 1.65 (q, 2H, $^3J_{HH}$=7.5 Hz, η^5-$C_5Me_4C\underline{H}_2CH_3$), δ 0.55 (t, 3H, $^3J_{HH}$= 7.8 Hz, η^5-$C_5Me_4CH_2C\underline{H}_3$), δ 1.20 (s, 6H, η^5-$C_5\underline{Me}_4CH_2CH_3$), 1.19 (s, 6H, η^5-$C_5\underline{Me}_4CH_2CH_3$); $^{13}C\{^1H\}$ ($CDCl_3$) δ 113.0, 111.8, 110.6 (η^5-$\underline{C}_5Me_4CH_2CH_3$), δ 17.6 (η^5-

$C_5Me_4\underline{C}H_2CH_3$), δ 13.0 ($\eta^5$-$C_5Me_4CH_2\underline{C}H_3$), δ 9.6, δ 9.4 ($\eta^5$-$C_5\underline{Me}_4CH_2CH_3$): IR (KBr) ν_{NO} 1769 cm^{-1} (vs); (CH_2Cl_2) ν_{NO} 1793 cm^{-1} (vs); Mass Spec (EI) [M^+] m/e 351 (33 %), [M-Cl] m/e 281 (11%), [M-Cl(NO)] m/e 285(82%). Anal. Calcd for $C_{11}H_{17}NOCl_2Ru$ (351.3): C, 37.64; H, 4.84; N, 3.99; Found: C, 37.57; H, 4.90; N, 3.93; mp 223 °C.

Characterization of Cp^Ru(NO)(CH_3)$_2$. ^1H NMR ($CDCl_3$) δ 2.15 (q, 2H, $^3J_{HH}$=7.5 Hz, η^5-$C_5Me_4C\underline{H}_2CH_3$), δ 1.06 (t, 3H, $^3J_{HH}$=7.5 Hz, η^5-$C_5Me_4CH_2C\underline{H}_3$), δ 1.76 (s, 6H, ($\eta^5$-$C_5\underline{Me}_4CH_2CH_3$), 1.64 (s, 6H, ($\eta^5$-$C_5\underline{Me}_4CH_2CH_3$), δ 0.47 (s, 3H, Ru-$C\underline{H}_3$); $^{13}C\{^1H\}$ ($CDCl_3$) δ 108.1, 101.5, 100.7 (η^5-$\underline{C}_5Me_4CH_2CH_3$), δ 17.9 ($\eta^5$-$C_5Me_4\underline{C}H_2CH_3$), δ 15.6 ($\eta^5$-$C_5Me_4CH_2\underline{C}H_3$), δ 9.3, δ 9.0 ($\eta^5$-$C_5\underline{Me}_4CH_2CH_3$), δ -1.6 (Ru-$\underline{C}H_3$): IR ($CH_2Cl_2$) ν_{NO} 1721 cm^{-1} (vs); mp 10°C (oil at 25°C).

Complexes **1a**, **1b** are obtained according to literature procedures.[12c]

X-ray Structural Analysis. Selected crystals were mounted in X-ray capillaries and examined on a Siemens P4 Autodiffractometer equipped with an LT-2a low-temperature device and a Mo Kα source. Unit cells were determined from the centering of a minimum of 25 randomly selected reflections with $15° \leq 2\theta \leq 30°$. Data were collected using the θ-2θ technique and solution of the structures was performed by Patterson methods (SHELXS program available from Siemens [Madison, WI]). The structures of **1b**, **2b**, and **4b** were refined to anisotropic convergence on a VAX 3100 workstation using F values (SHELXTL Plus program). The structure of **3b** was refined to anisotropic convergence on F^2 values using the PC-version of SHELXl-93 program available from Sheldrick.[31]

Isolation of Cp^Ru(NO)(H_2O)$_2$][OTf]$_2$ (3b). One mL of water-saturated $CDCl_3$ was treated with **1b** (0.010 g, 0.017 mmol) in a 5-mm NMR tube and allowed to stand at 25°C. Large red crystals of **3b** began to appear on the walls of the tube after 1 h. IR (nujol): ν_{NO} 1815 cm^{-1}; mp 86-88°C; Anal. Calcd for $C_{13}H_{21}NRuO_9S_2F_6$ (614.5): C, 25.40; H, 3.42; N, 2.28; Found: C, 25.47, H, 3.50; N, 2.17.

Isolation of Cp^Ru(NO)(H_2O)(OTf)][OTf] (3b). A crystalline mass of dark purple **1b** was allowed to stand in the air for 48 h giving **3b** as a red crystalline mass. IR (nujol): ν_{NO} 1830 cm^{-1}.

Preparation of Cp´Ru(NO)(μ-OH)]$_2$[OTf]$_2$·H$_2$O (4a,b).[12c] Stirring a solution of complex **1a** (0.046 g, 0.081 mmol) in 5 mL of H_2O produced a cloudy orange solution after 18 h at 25°C. The mixture was extracted with 4x15 mL portions CH_2Cl_2 until the organic fractions were colorless. The combined CH_2Cl_2 extracts were dried over anhydrous $MgSO_4$, filtered, and taken to dryness *in vacuo* to give 0.027 g (0.031 mmol, 77%) of orange crystalline **4a**. ^{1}H NMR (CH_2Cl_2): δ 1.81 (s) (15H, Cp* major isomer); δ 1.85 (s) (15H, Cp* minor isomer); δ 4.47 (s) (2H, O<u>H</u>); ^{13}C NMR ($CDCl_3$): δ 119.8 (q, $OSO_2\underline{C}F_3$, $J_{C\text{-}F}$ = 318.4 Hz); δ 110.2 ($\underline{C}_5Me_5$); δ 9.02 ($C_5\underline{Me}_5$) ; ^{19}F{^{1}H} NMR (CH_2Cl_2): δ -78.6; IR (KBr) ν_{NO} 1795 cm^{-1} (vs); ν_{OH} 3241 cm^{-1} (br); UV-vis (H_2O, λ_{max}, nm(ϵ,M^{-1}cm^{-1}), 326 (5400); 372 (2000); mp 197°C; Anal. Calcd for $C_{22}H_{32}N_2O_{10}Ru_2S_2F_6$ ·H_2O (864.8): C, 30.55; H, 3.73; N, 3.24; Found: C, 30.28; H, 3.67; N, 3.17.

The salt **4b** was prepared similarly starting from **1b**. ^{1}H NMR (CH_2Cl_2): δ 4.42 (s, 2H, μ-O<u>H</u>); δ 2.16 (q, 4H, $^3J_{HH}$= 7.7 Hz, η^5-$C_5(CH_3)_4\underline{CH_2}CH_3$); δ 1.81 (s, 12H, η^5-$C_5(\underline{CH_3})_4CH_2CH_3$); δ1.80 (s, 12H, η^5-$C_5(\underline{CH_3})_4CH_2CH_3$); δ 1.14 (t, 6H, $^3J_{HH}$= 7.7 Hz, η^5-$C_5(CH_3)_4CH_2\underline{CH_3}$); Cp^ signals of minor isomer: δ 2.20 (q, 4H, $^3J_{HH}$= 7.7 Hz, η^5-$C_5(CH_3)_4\underline{CH_2}CH_3$); δ 1.86 (s, 12H, η^5-$C_5(\underline{CH_3})_4CH_2CH_3$); δ1.85 (s, 12H, η^5-$C_5(\underline{CH_3})_4CH_2CH_3$); δ 1.17 (t, 6H, $^3J_{HH}$= 7.7 Hz, η^5-$C_5(CH_3)_4CH_2\underline{CH_3}$); ^{13}C{^{1}H} NMR ($CH_2Cl_2$): δ 119.8 (q, $OSO_2\underline{C}F_3$, $J_{C\text{-}F}$ = 318.4 Hz); δ 113.1, 111.0, 109.8 (η^5-$\underline{C}_5Me_4CH_2CH_3$); δ 16.90 (η^5-$C_5Me_4\underline{CH_2}CH_3$); δ 12.65 (η^5-$C_5Me_4CH_2\underline{CH_3}$); δ 9.05, 8.72 (η^5-$C_5\underline{Me}_4CH_2CH_3$); ^{19}F{^{1}H} NMR ($CH_2Cl_2$): δ -78.6;IR (thin film): ν_{NO} 1799 cm^{-1} (vs); ν_{OH} 3180 (br); mp 184°C; Anal. Calcd. for $C_{24}H_{36}N_2O_{10}S_2F_6Ru_2$ (892.8): C, 32.28; H, 4.06; N, 3.14; Found: C, 32.50; H, 4.12; N, 3.06.

Formation of $(C_5(CD_3)_4CH_2CH_3)Ru(NO)Cl_2$ and $(C_5(CD_3)_5)Ru(NO)Cl_2$. To a solution of 26 mg of **4b** in 3 mL of D_2O, 0.4 mL of 0.29 M NaOD was added. The resulting solution was kept for 2 h at ambient temperature and then 10 μL of concentrated DCl was added to the solution. The green precipitate immediately formed was collected and dried on the vacuum line. ^{1}H NMR (CH_2Cl_2): δ 2.17 (2H, quartet), 1.18 (3H, triplet). Small residual resonances appeared at δ 1.80 as a weak complex multiplet. ^{2}H NMR (CH_2Cl_2): δ 1.82 (s), δ 1.79 (s).

An analogous procedure was employed to obtain $(C_5(CD_3)_5)Ru(NO)Cl_2$ from aqueous solution of **4a**. ^2H NMR (CH_2Cl_2): δ 1.81 (s).

Treatment of **4a,b** under similar conditions using NaOH instead of NaOD resulted in no intensity changes in the ^1H NMR spectra. Subsequent treatment of these basic solutions with aqueous HCl produced green, crystalline $Cp^*Ru(NO)Cl_2$ and $Cp^{\wedge}Ru(NO)Cl_2$ upon a similar workup.

Formation of $[(Cp^*)(Cp^{\wedge})Ru_2(NO)_2(\mu\text{-}OH)_2][OTf]_2$ (4c) from 1a and 1b. A solution prepared from **1a** (0.006 g, 0.01 mmol) and **1b** (0.007 g, 0.01 mmol) in 10 mL H_2O was stirred at room temperature. Periodically, aliquots of the aqueous solutions were removed, extracted into CH_2Cl_2, dried over $MgSO_4$, and filtered. The ^1H NMR spectrum was then measured to observe formation of **4c**.

Crossover Reaction Between 4a and 4b. Method **A**: Compounds **4a** (1.8 mg) and **4b** (2.2 mg) were placed in 5 mL H_2O and allowed to stir at room temperature for 10 min. The solution was extracted with 4 x 10 mL of CH_2Cl_2 until the organic fraction was colorless and the combined extracts were concentrated to ca. 10 mL. The ^1H NMR spectrum of the sample was monitored to observe formation of $\mathbf{4c}^{+2}$. Method **B**: A solution prepared from 0.6 mL of dichloromethane, 2.1 mg of **4a**, and 1.7 mg of **4b** was placed in a 5-mm sealed NMR tube and held at 30°C for 2 weeks. ^1H NMR spectra were periodically measured at 30°C. Method **C**: Method **B** was repeated using H_2O-saturated CH_2Cl_2 (0.1 **M** H_2O/CH_2Cl_2).

References

(1) (a) Hlatky, G. G.; Turner, H. W.; Eckman, R. R. *J. Am. Chem. Soc.*, **1989**, *111*, 2728. (b) Hlatky, G. G.; Eckman, R. R.; Turner, H. W. *Organometallics* **1992**, *11*, 1413. (c) Sishta, C.; Hawthorn, R. M.; Marks, T. J. *J. Am. Chem. Soc.*, **1992**, *114*, 1112. (d) Marks, T. J. *Acct. Chem. Res.*, **1992**, *23*, 57. (e) Yang, X.; Stern, C. L.; Marks, T. J. *J. Am. Chem. Soc.*, **1991**, *113*, 3623. (f) Yang, X.; Stern, C. L.; Marks, T. J. *Organometallics* **1991**, *10*, 840. (g) Lin, Z.; Le Marechal, J.-F.; Sabat, M.; Marks, T. J.

J. Am. Chem. Soc. **1987**, *109*, 4127. (h) Dalton, D. M.; Gladysz, J. A. *J. Organomet. Chem.* **1989**, *370*, C17. (i) Saura-Llamas, I.; Gladysz, J. A. *J. Am. Chem. Soc.*, **1992**, *114*, 2136. (j) Klein, D. P.; Gladysz, J. A.; *J. Am. Chem. Soc.* **1992**, *114*, 8710. (k) Winter, C. H.; Zhou, X.-X.; Heeg, M. J. *Inorg. Chem.* **1992**, *31*, 1808.

(2) (a) Lawrance, G. A. *Chem. Rev.* **1986**, *86*, 17. (b) Humphrey, R. B.; Lamanna, W. M.; Brookhart, M.; Husk, G. R. *Inorg. Chem.* **1983**, *22*, 3355. (c) Stang, P. J.; Huang, Y. H.; Arif, A. M. *Organometallics* **1992**, *11*, 231. (d) Stang, P. J.; Cao, D. H.; Poulter, G. T.; Arif, A. M. *Organometallics*, **1995**, *14*, 1110. (e) Bennet, B. L.; Birnbaum, J.; Roddick, D. M. *Polyhedron*, **1995**, *14*, 187. (f) Blosser, P. W.; Gallucci, J. C.; Wojcicki, A. *Inorg. Chem.* **1992**, *31*, 2376. (g) Beck, W.; Sünkel, K.; *Chem. Rev.* **1988**, *88*, 1405.

(3) (a) Hollis, T. K.; Robinson, N. P.; Bosnich, B. *Organometallics*, **1992**, *11*, 2645. (b) Hollis, T. K.; Robinson, N. P.; Bosnich, B. *J. Am. Chem. Soc.*, **1992**, *114*, 5464. (c) Bonnesen, P. V.; Puckett, C. L.; Honeychuck, R. V.; Hersh, W. H.; *J. Am. Chem. Soc.* **1989**, *111*, 6070. (d) Honeychuck, R. V.; Bonnesen, P.V.; Farahi, J.; Hersh, W. H.; *J. Org. Chem.* **1987**, *52*, 5293; Odenkirk, W.; Rheingold, A. L.; Bosnich, B. *J. Am. Chem. Soc.*, **1992**, *114*, 6392.

(4) Jaquith, J. B.; Guan, J.; Wang, S.; Collins, S *Organometallics*, **1995**, *14*, 1079.

(5) Saura-Llamas, I.; Garner, C. M.; Gladysz, J. A. *Organometallics*, **1991**, *10*, 2533.

(6) (a) Rix, F. C.; Brookhart, M. *J. Am. Chem. Soc.*, **1995**, *117*, 1137. (b) Johnson, L. K.; Killian, C. M.; Brookhart, M. *J. Am. Chem. Soc.*, **1995**, *117*, 6414.

(7) (a) Wang, L.; Flood, T. C. *J. Am. Chem. Soc.*, **1992**, *114*, 3169. (b) Wang, C.; Ziller, J. W.; Flood, T. C. *J. Am. Chem. Soc.*, **1995**, *117*, 1647. (c) Wang, L.; Lu, R. S.; Bau, R.; Flood, T. C. *J. Am. Chem. Soc.*, **1993**, *115*, 6999.

(8) Collman, J. P.; Hegedus, L. S.; Norton, J. R.; Finke, R. G. *Principles of Organotransition Metal Chemistry*; University Science Books: Mill Valley, CA, 1987; chapter 1 and references therein.

(9) (a) Haggin, J. *Chem. & Eng. News,* **1994,** *10,* 28. (b) Fish, R. H.; Baralt, E.; Kim, H.-S.; *Organometallics*, **1991**, *10*, 1965. (c) Baralt, E.; Smith, S. J.; Hurwitz, J.; Horvath, I. T.; Fish, R. H. *J. Am. Chem. Soc.*, **1992**, *114*, 5187. (d) Smith, D. P.; Baralt, E.; Moreles, B.; Olmstead, M. M.; Maestre, M. F.; Fish, R. H. *J. Am. Chem. Soc.*, **1992**, *114*, 10647. (e) Smith, D. P.; Olmstead, M. M.; Noll, B. C.; Maestre, M. F.; Fish, R. F. *Organometallics*, **1993**, *12*, 593. (f) Smith, D. P.; Griffin, M. T.; Olmstead, M. M.; Maestre, M. F.; Fish, R. H. *Inorg. Chem.* **1993**, *32*, 4677. (g) Chen, H.; Maestre, M. F.; Fish, R. H. *J. Am. Chem. Soc.*, **1995**, *117*, 3631. (h) Eisen, M. S.; Haskel, A.; Chen, H.; Olmstead, M. M.; Smith, D. P.; Maestre, M. F.; Fish, R. H. *Organometallics*, **1995**, *14*, 2806. (i) Karlen, T.; Ludi, A. *J. Am. Chem. Soc.*, **1994**, *116*, 11375. (j) McGrath, D. V.; Grubbs, R. H. *Organometallics*, **1994**, *13*, 224. (k) Dadci, L.; Elias, H.; Frey, U.; Hörnig, A.; Koelle, U.; Merbach, A.C.; Paulus, H.; Schneider, J.S. *Inorg. Chem.* **1995**, *34*, 306-315. (l) Darensbourg, D. J.; Joo, F.; Kannisto, M.; Katho, A.; Reibenspies, J. H.; Daigle, D. J. *Inorg. Chem.* **1994**, *33*, 200. (m) Darensbourg, D. J.; Stafford, N. W.; Joo, F.; Reibenspies, J. H. *J. Organomet. Chem.* **1995**, *488*, 99. (n) Barton, M.; Atwood, J. D. *J. Coord. Chem.* **1991**, *24*, 43-67. (o) Rauscher, D. J.; Thaler, E. G.; Huffman, J. C.; Caulton, K. G. *Organometallics*, **1991**, *10*, 2209. (p) Labinger, J. A.; Herring, A. M.; Lyon, D. K.; Luinstra, G. A.; Bercaw, J. E.; Horvath, I. T.; Eller, K. *Organometallics*, **1993**, *12*, 895. (q) Agbossou, S. K.; Roger, C.; Igau, A.; Gladysz, J. A. *Inorg. Chem.*, **1992**, *31*, 419. (r) Le, T. X.; Merola, J. S. *Organometallics*, **1993**, *12*, 3798. (s) Herrmann, W. A.; Kohlpaintner, C. W. *Angew. Chem. Int. Ed. Engl.* **1993** *32*, 1524-1544. (t) Dobbs, D. A.; Bergman, R. G. *Organometallics*, **1994**, *13*, 4594. (u) Bartik, T.; Bartik, B.; Hanson, B. E.; Guo, I.; Toth, I. *Organometallics*, **1993**, *12*, 164. (v) Mandel, S. K.; Chakravarty, A. R. *Inorg. Chem.* **1993**, *32*, 3851. (w) Legzdins, P.; Lundmark, P. J.; Phillips, E. C.; Rettig, S. J.; Veltheer, J. E. *Organometallics*, **1992**, *11*, 2991. (x) Le, T. X.; Merola, J. S. *Organometallics*, **1993**, *12*, 3798.

(10) (a) Kang, J.W.; Maitlis, P.M. *J. Organomet. Chem.* **1971**, *30(1)*, 127. (b) Nutton, A.; Bailey, P.; Maitlis, P.M.; *J. Chem. Soc., Dalton Trans.*, **1981**, 1997. (c) Hirai, K.; Nutton, A.; Maitlis, P.M. *J. Mol. Cat.* **1981**, *211*, 203. (d) Nutton, A.; Maitlis, P.M. *J. Chem. Soc., Dalton Trans.*, **1981**, *197,* 2335. (e) Miguel-Garcia, J.A.; Adams, H.; Bailey, N.A.; Maitlis, P.M. *J. Organomet. Chem.* **1991**, *413*, 427. (f) Gusev, O.V.; Rubezhov, A.Z.; Miguel-Garcia, J.A.; Maitlis, P.M. *Mendeleev. Commun.*, **1991**, 21. (g) Wei, C.; Aigbirhio, F.; Adams, H.; Bailey, N.A.; Hempstead, P.D.; Maitlis, P.M. *J. Chem. Soc. Chem. Commun.*, **1991**, *144,* 883. (h) Miguel-Garcia, J.A.; Adams, H.; Bailey, N.A.; Maitlis, P.M. *J. Chem. Soc., Dalton Trans.*, **1992**, *198,* 131. (i) Gusev, O.; Sergeev, S.; Saez, I.M.; Maitlis, P.M.; *Organometallics*, **1994**, *13*, 2059. (j) Fan, Li; Turner, M.L.; Hursthouse, M.B.; Abdul Malik, K.M.; Gusev, O.V.; Maitlis, P.M. *J. Am. Chem. Soc.*, **1994**, *116*, 385.

(11) Hubbard, J.L.; Burns R.M. *J. Am. Chem. Soc.*, **1994**, *116*, 9514.

(12) (a) Hubbard, J. L.; Morneau, A.; Burns, R. M.; Zoch, C. R. *J. Am. Chem. Soc.*, **1991**, *113*, 9176. (b) Hubbard, J. L.; Morneau, A.; Burns, R. M.; Nadeau, O. W. *J. Am. Chem. Soc.*, **1991**, *113*, 9180. (c) Zoch, C. R. Dissertation, Utah State University, 1993.

(13) Hauptman, E.; Brookhart, M.; Fagan, P. J.; Calabrese, J. C. *Organometallics*, **1994**, *13*, 774.

(14) (a) Nitschke, J.; Schmidt, S. P.; Trogler, W. C. *Inorg. Chem.* **1985**, *24*, 1972. (b) Trogler, W. C. *J. Am. Chem. Soc.*, **1979**, *101*, 6459.

(15) Hoffman and coworkers have reported the ranges for the equilibrium constants for square planar Rh^{I} OTf^{-} complexes: (a) Branan, D. M.; Hoffman, N. W.; McElroy, E. A.; Prokopuk, N.; Salazar, A. B.; Robbins, M. J.; Hill, W. E.; Webb, T. R. *Inorg. Chem.* **1991**, *30*, 1200. (b) Branan, D.M.; Hoffman, N.W.; McElroy, E.A.; Ramage, D.L.; Robbins, M.J.; Eyler, J.R.; Watson, C.H.; deFur, P.; Leary, J.A *Inorg. Chem.* **1990**, *29*, 1915. (c) Araghizadeh, F.; Branan, D.M.; Hoffman, N.W.; Jones, J.H.; McElroy, E.A.;

Miller, N.C.; Ramage, D.L.; Salazar, A.B.;Young, S.H. *Inorg. Chem.* **1988**, *27*, 3752.

(16) (a) Grover, N.; Gupta, N.; Thorp, H. H. *J. Am. Chem. Soc.*, **1992**, *114*, 3390. (b) Call, J. T.; Hughes, K. A.; Harman, W. D.; Finn, M. G. *Inorg. Chem.* **1993**, *32*, 2123. (c) Banyai, I. Glaser, J.; Read, M. C.; Sandstrom, M. *Inorg. Chem.* **1995**, *34*, 2423. (d) Dimitrou, K.; Folting, K.; Streib, W. E.; Christou, G. *J. Am. Chem. Soc.*, **1993**, *115*, 6432.

(17) (a) Lou, X.-L.; Schulte, G. K.; Crabtree, R. H. *Inorg. Chem.* **1990**, *29*, 682. (b) Kubas, G. J.; Burns, C. J.; Khalsa, G. R. K.; Van Der Sluys, L. S.; Kiss, G.; Hoff, C. D. *Organometallics*, **1992**, *11*, 3390.

(18) For comparison, the π-donor abilities of halide ligands are now recognized as being very important for stabilizing coordinatively unsaturated metal centers: (a) Rothfuss, H.; Huffman, J. C.; Caulton, K. G. *J. Am. Chem. Soc.*, **1994**, *116*, 187. (b)Gusev, D. G.; Kulhman, R.; Rambo, J. R.; Berke, H.; Eisenstein, O.; Caulton, K. G. *J. Am. Chem. Soc.*, **1995**, *117*, 281. (c)Johnson, T. J.; Folting, K.; Streib, W. E.; Martin, J. D.; Huffman, J. C.; Jackson, S. A.; Eisenstein, O.; Caulton, K. G. *Inorg. Chem.* **1995**, *34*, 488. (d) Caulton, K. G. *New J. Chem.* **1994**, *18*, 25.

(19) Barshop, B. A.; Wrenn, R. F.; Frieden, C. *Anal. Biochem.* **1983** *130*, 134-145. The program is available via internet: anonymous login to WUARCHIVE.WUSTL.EDU, subdirectory: Package/KINSIM/DOS.

(20) Peng, S.-M.; Ibers, J. A.; Millar, M.; Holm, R. H. *J. Am. Chem. Soc.*, **1976**, *98*, 8037.

(21) A similar pattern of bond lengths is also reported (but not interpreted) in refs. 2d-e.

(22) (a) Seligson, A. L.; Cowan, R. L.; Trogler, W. C. *Inorg. Chem.* **1991**, *30*, 3371. (b) Koelle, U.; Flunkert, G.; Gorissen, R.; Schmidt, M. U.; Englert, U. *Angew. Chem., Int. Ed. Engl.*, **1992**, *31*, 440. (c) Kegley, S. E.; Schaverien, C. J.; Freudenberger, J. H.; Bergman, R. G. *J. Am. Chem. Soc.* **1987**, *109*, 6563. (d) Fawzi, R.; Hiller, W.; Lorenz, I.-P.; Mohyla, J.; Zeiher, C. *J. Organomet. Chem.* **1984**, *262*, C43. (e) Bertrand, J. A.; Black, T. D.; Eller, P. G.; Helm, F. T.; Mahmood, R. *Inorg. Chem.* **1976**, *12*, 2965. (f)

van Driel, G. J.; Driessen, W. L.; Reedijk, J. *Inorg. Chem.* **1985**, *24*, 2919. (g) Emsley, J. *J. Chem. Soc. Rev.*, **1980**, *133,* 91. (h) Olovsson, I.; Jonsson, P. in *The Hydrogen Bond*; Schuster, P.; Zundel, G.; Sandorfy, C. Eds.; North-Holland: New York, 1976, Chapter 8. (i) Review of hydrogen bonding and its classification. Gilli, P.; Bertolasi, V.; Ferretti, V., Gilli, G. *J. Am. Chem. Soc.*, **1994**, *116*, 909. (l) Steed, J. W.; Tocher, D. A. *J. Chem. Soc. Chem. Commun.*, **1991**, *146,* 1609. (m) Winter, C. H.; Sheridan, P. H.; Heeg, M. J.; *Inorg. Chem.* **1991**, *30*, 1962. (n) Alster, P. L.; Baeskjou, P. J.; Jannsen, M. D.; Kooijman, H.; Sicher-Roetman, A.; Spek, A. L.; van Koten, G. *Organometallics*, **1992**, *11*, 4124. (o) Fryzuk, M. D.; MacNeil, P. A.; Rettig, S. J. *J. Am. Chem. Soc.* **1987**, *109*, 2803. (p) Osterberg, C. E.; King, M. A.; Arif, A. M.; Richmond, T. G. *Angew. Chem., Int. Ed. Engl.* **1990**, *29*, 888. (q) Antolini, L.; Benedetti, A.; Fabretti, A. C.; Giusti, A. *Inorg. Chem.* **1988**, *27*, 2192. (r) Osterberg, C. E.; Arif, A. M.; Richmond, T. G. *J. Am. Chem. Soc.* **1988**, *110*, 6903.

(23) A reinvestigation of the solvolytic behavior of *trans*-$Rh(PPh_3)_2(CO)(OTf)\cdot H_2O$ shows evidence that H_2O does not displace the OTf^- ligand in CH_2Cl_2 solution: Svetlanova-Larsen, A.; Hubbard, J. L., *Inorg. Chem.* in press.

(24) The structure of the $[Cp^*Ru(NO)(CH_3)(THF)]^+$ cation (as the $B(3,5\text{-}(CF_3)_2C_6H_3)_4^-$ salt) shows a coordination geometry very similar to the $[Cp^\wedge Ru(NO)(OTf)(OH_2)]^+$ cation and a ∠Ru-N-O of 159°: Hubbard, J. L.; Yi, G.-B., manuscript in preparation.

(25) Burgess, J. *Metal Ions in Solution;* John Wiley & Sons: New York-London-Sydney-Toronto, 1978

(26) Cp* conversions to the tetramethylfulvene complexes in transition metals: (a) Werner, H.; Crisp, G.T.; Jolly, P.W.; Kraus, H.-J.; Krüger, C. *Organometallics*, **1983**, *2*, 1369. (b) Parkin, G.; Bercaw, J.E. *Polyhedron* **1988**, *7,* 2053. (c) Pattiasina, J.W.; Hissink, C.E.; de Boer, J.L.; Meetsma, A.; Teuben, J.H. *J. Am. Chem. Soc.*, **1985**, *107*, 7758. (d) Straus, D.A.; Zhang, C.; Tilley, T.D. *J. Organomet. Chem.* **1989**, *369*, C13. (e) Einstein, F.W.B.;

Jones, R.H.; Zhang, X.; Yan, X.; Nagelkerke, R.; Sutton, D. *J. Chem. Soc. Chem. Commun.*, **1989**, 1424. (f) Glueck, D.S.; Bergman, R.G. *Organometallics*, **1990**, *93*, 2862.

(27) Scheflan, L.; Jacobs, M. *The Handbook of Solvents;* Van Nostrand: New York, 1953, p.112.

(28) Seidler, M.D.; Bergman, R.G. *J. Am. Chem. Soc.* **1984**, *106*, 6110.

(29) Van Geet, A. L. *Anal. Chem* **1970**, *42*, 679.

(30) Yi, G.-B., Thesis, Utah State University, 1992.

(31) SHELXL-93 is available from: Siemens Analytical X-ray Instruments, 6300 Enterprise Lane, Madison, WI 53719; or directly from G. Sheldrick, Institut für Anorganische Chemie,der Universität, Tammannstrasse 4, D-37077 Göttingen, Germany: gsheldr@shelx.uni-ac.gwdg.de

CHAPTER 3

AN EVALUATION OF TRIFLATE DISPLACEMENT BY WATER IN CH_2Cl_2 SOLUTION: THE COMPARISON OF *trans*-[Rh(CO)(PPh_3)$_2$(OSO_2CF_3)] AND THE CRYSTALLINE SALT *trans*-[Rh(CO)(PPh_3)$_2$(OH_2)][OTf][1]

Abstract

The complex *trans*-[Rh(CO)(PPh_3)$_2$(OH_2)][OTf] crystallizes from a wet CH_2Cl_2/hexane solution of *trans*-[Rh(CO)(PPh_3)$_2$(OTf)] (OTf = $OSO_2CF_3^-$). Analytical single-crystal X-ray data confirm the presence of a bound H_2O ligand and an outersphere OTf$^-$ in the solid state. X-ray data for *trans*-[Rh(CO)(PPh_3)$_2$(OH_2)][OTf] (173 K) ($C_{38}H_{32}O_5F_3SP_2Rh$): monoclinic space group *C* 2/c, *a* = 23.401 (8), *b* = 9.1222 (4), *c* = 17.047 (6), β = 107.03 (3)°, V = 3479 (2) Å^3, R1 = 0.1057 on F^2. The ν_{CO} absorption for the Nujol mull of the salt is 2008 cm^{-1}. Analytically pure *trans*-[Rh(CO)(PPh_3)$_2$(OTf)] is obtained by azeotropic distillation or freeze-drying of the hydrate in benzene and the solid-state IR spectrum of this material shows a ν_{CO} of 1988 cm^{-1}. The appearance of a single ν_{CO} absorption at 1996 cm^{-1} for either of these materials in rigorously dry CH_2Cl_2 indicates *trans*-[Rh(CO)(PPh_3)$_2$(OTf)] to be the only detectable species in CH_2Cl_2 solution. This conclusion is also supported by ^{19}F and ^{31}P NMR spectroscopy as well as conductivity measurements. Comparison to the related *trans*-[Rh(CO)(PPh_3)$_2$(OH_2)][BF_4] complex shows OTf$^-$ to be a better ligand than BF_4^- in CH_2Cl_2.

Introduction

During the course of our studies of the organometallic chemistry of the electrophilic [Cp*Ru(NO)]$^{+2}$ fragment, we have determined that dissociation of OTf$^-$ from Cp*Ru(NO)(OTf)$_2$ to give the corresponding solvento-cations is somewhat exothermic but entropically costly due to the

---

[1]Coauthored by Anna Svetlanova-Larsen and John L. Hubbard. Reprinted in part with permission from *Inorg. Chem.* **1996**, *35*, 3073. Copyright 1996 American Chemical Society.

solvent reorganization required for the formation of the product ion pairs (Cp* = η-$C_5(CH_3)_5$; OTf = $OSO_2CF_3^-$).[1] Thus, we find that in a homogeneous H_2O-saturated CH_2Cl_2 solution of $Cp^*Ru(NO)(OTf)_2$, the major species in solution is the neutral ditriflate complex with only small amounts of $[Cp^*Ru(NO)(OTf)(OH_2)]^+$ and $[Cp^*Ru(NO)(OH_2)]^{+2}$ being present.[1b,2]

The nature of weakly coordinating ions is important in the discussion of coordination unsaturation and catalytic reactivity.[3,4] We continue to be interested in the equilibria of OTf^- displacement by coordinating solvents and weak ligands. In concert with our work on $Cp^*Ru(NO)(OTf)_2$, some previous work has shown OTf^- to be a "moderately strong" ligand.[5] For example, a kinetic study of the $M(CO)_5(OTf)$ complexes (M = Mn, Re) showed substitution of OTf^- by oxygen donor solvents in CH_2Cl_2 to occur for M = Mn but not for M = Re.[6] If one considers OTf^- to be a fairly good ligand, the report that *trans*-$[Rh(CO)(PPh_3)_2(OH_2)][OTf]$ persists in solution with no detectable traces of the parent complex *trans*-$[Rh(CO)(PPh_3)_2(OTf)]$ would be counterintuitive[7] even though the dissociation of OTf^- in the "basic" d^8 Rh complexes might be expected to be more favorable than in electrophilic d^6 complexes like $Cp^*Ru(NO)(OTf)_2$.[7,8] Prompted by the rather sketchy analytical details reported for *trans*-$[Rh(CO)(PPh_3)_2(OH_2)][OTf]\cdot H_2O$[9] and the importance of square planar rhodium complexes in catalytic reactions,[10] we embarked on a reinvestigation of this case to see if H_2O actually displaces the OTf^- ligand in CH_2Cl_2. The results of this study show that OTf^- is a better ligand than H_2O in CH_2Cl_2.

Results

Characterization of *trans*-$[Rh(CO)(PPh_3)_2(OH_2)][OTf]$. The combustion analysis for the crystalline material isolated from the reaction of *trans*-$[Rh(CO)(PPh_3)_2(Cl)]$ with AgOTf in benzene agrees with the formula "$[Rh(CO)(PPh_3)_2(OTf)]\cdot H_2O$." The use of more than 1 equiv of AgOTf in the reaction leads to significant contamination of the product with AgOTf.[11] The presence of unreacted AgOTf in the product is easily detected by a broadening of the ^{19}F NMR signal, the depression of the melting point from 178°C, and the reduction of the carbon content.

The single-crystal structure determination for crystals of "$[Rh(CO)(PPh_3)_2(OTf)]\cdot H_2O$" shows consistency with the analytical formulation. The calculated crystal density of 1.57 g/cm^3 is the same as the density determined by flotation in CCl_4/hexane. The molecular structure of the complex unambiguously shows a *trans*-arrangement of the PPh_3 ligands (Fig 3-1, Table 3-1). Despite disorder of the CO and H_2O ligands, the molecular structure clearly shows the presence of an outersphere OTf^- ion (see Experimental Section). Henceforth, we will refer to this material as *trans*-$[Rh(CO)(PPh_3)_2(OH_2)][OTf]$.

The IR spectrum of *trans*-$[Rh(CO)(PPh_3)_2(OH_2)][OTf]$ in a Nujol mull shows a strong ν_{CO} absorption at 2008 cm^{-1}. A CH_2Cl_2 solution of *trans*-$[Rh(CO)(PPh_3)_2(OH_2)][OTf]$ shows a ν_{CO} absorption at 1996 cm^{-1}. The ^{19}F NMR spectrum of this CH_2Cl_2 solution shows a single sharp resonance at δ -78.5 and the ^{31}P NMR spectrum shows a doublet at δ 28.2 (J = 125 Hz). The presence of water in the homogeneous CH_2Cl_2 solutions does not alter the IR spectrum or the ^{19}F, ^{31}P, and ^1H NMR spectra. The molar conductivity of a 0.02 **M** solution of *trans*-$[Rh(CO)(PPh_3)_2(OH_2)][OTf]$ in CH_2Cl_2 is 2.0 (1) $\Omega^{-1}cm^{-1}mol^{-1}$. For comparison, the molar conductivity of a 0.01 **M** solution of *trans*-$[Rh(CO)(PPh_3)_2(Cl)]$ in CH_2Cl_2 is 1.5 (1) $\Omega^{-1}cm^{-1}mol^{-1}$.

Isolation of *trans*-$[Rh(CO)(PPh_3)_2(OTf)]$. Analytically pure *trans*-$[Rh(CO)(PPh_3)_2(OTf)]$ is obtained by the azeotropic removal of water from a benzene solution prepared with *trans*-$[Rh(CO)(PPh_3)_2(OH_2)][OTf]$ or by freeze-drying the benzene solution under high vacuum. The IR spectrum of microcrystalline *trans*-$[Rh(CO)(PPh_3)_2(OTf)]$ in Nujol shows a ν_{CO} absorption at 1988 cm^{-1} and the ν_{CO} absorption appears at 1996 cm^{-1} when the complex is dissolved in both rigorously dry CH_2Cl_2 and in H_2O-saturated CH_2Cl_2. The ^1H, ^{19}F, and ^{31}P NMR signals of *trans*-$[Rh(CO)(PPh_3)_2(OTf)]$ in rigorously dry CH_2Cl_2 are identical to those observed for *trans*-$[Rh(CO)(PPh_3)_2(OH_2)][OTf]$ and do not change upon the addition of H_2O. The solid residue remaining after removal of the H_2O-saturated CH_2Cl_2 shows a ν_{CO} absorption at 2008 cm^{-1} in Nujol.

Reactivity of *trans*-$[Rh(CO)(PPh_3)_2(OH_2)][OTf]$. Addition of $[Ph_3PNPPh_3]Cl$ to a CH_2Cl_2 solution of *trans*-$[Rh(CO)(PPh_3)_2(OH_2)][OTf]$ causes an immediate shift of the ^{19}F NMR resonance

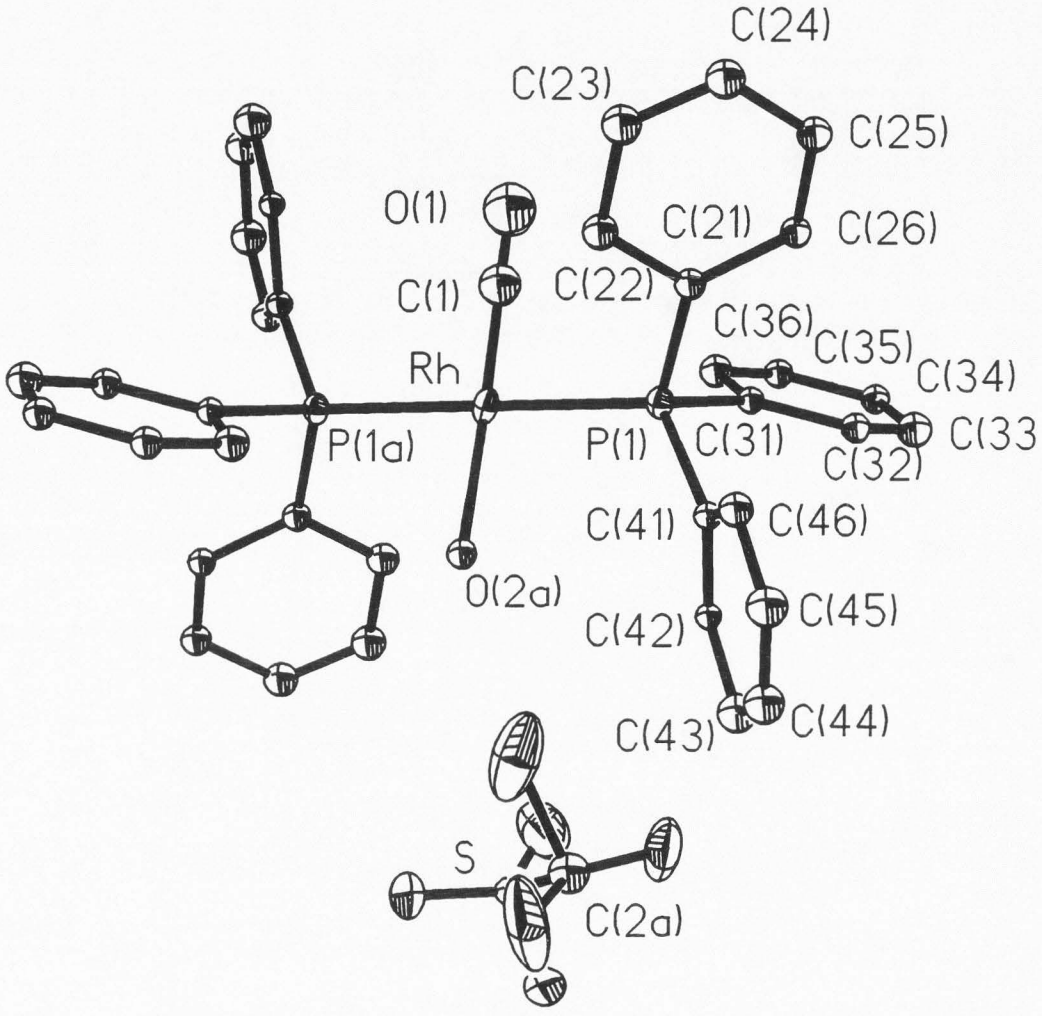

Figure 3-1. Molecular structure of *trans*-[$Rh(PPh_3)_2(CO)(OH_2)$][OTf]. Selected bond distances (Å): Rh-P(1) 2.333 (4); Rh-C(1) 1.70 (1); Rh-O(1) 2.00 (1); P(1)-C(21) 1.81 (2); P(1)-C(31) 1.84 (1); P(1)-C(41) 1.81 (2); C(1)-O(1) 1.05 (1); selected bond angles (°): C(1)-Rh-P(1) 90 (3); O(2)-Rh-P(1) 87.4 (7); Rh-C(1)-O(1) 177 (3).

Table 3-1. Crystallographic data for *trans*-[Rh(CO)(PPh_3)$_2$(OH_2)][OTf].

Chemical formula	$C_{38}H_{32}O_5F_3SP_2Rh$
Formula Wt, amu	822.6
a	9.122 (4) Å
b	23.401 (8) Å
c	17.047 (6) Å
β	107.03 (3)°
V	3479 (2) Å^3
Z	4
Space group	monoclinic, *C*2/c (#15)
T	173 K
λ	0.71073 (Mo Kα)
ρ (obsd)	1.57 g/cm^3
ρ (calcd)	1.57 (2) g/cm^3
μ	0.70 mm^{-1}
R (F^2) [I > 2σ(I)]	R1[a] = 0.1057, wR2[b] = 0.1740
R (F^2) (all data)	R1[a] = 0.2126, wR2[b] = 0.2308
GOF[c] on F^2	1.108

[a]$R1 = \Sigma||F_o|-|F_c||\Sigma|F_o|$ [b]$wR2 = |\Sigma[w(F_o^2-F_c^2)]^2]/\Sigma[w(F_o^2)^2]]^{1/2}$
[c]$GOF = [\Sigma[w(F_o^2-F_c^2)^2]/(n-p)]^{1/2}$ where n = no. of reflections, p = no. of parameters refined; $w=1/[\sigma^2(Fo^2)+(0.0326P)^2 + 224.2319P]$ where $P=(Fo^2+2Fc^2)/3$

from δ -78.52 to δ -78.60. The appearance of a ν_{CO} IR absorption at 1976 cm^{-1} and a new doublet at δ 26.9 (J = 127 Hz) in the ^{31}P NMR spectrum of this solution corresponds to a complete conversion to *trans*-$[Rh(CO)(PPh_3)_2(Cl)]$[12] and free OTf^-.

Addition of 1 equiv of pyridine to *trans*-$[Rh(CO)(PPh_3)_2(OH_2)][OTf]$ dissolved in CH_2Cl_2 causes the initial δ -78.52 ^{19}F NMR resonance to shift to δ -78.60. This represents the complete conversion to *trans*-$[Rh(CO)(PPh_3)_2(py)][OTf]$ as indicated by a new doublet in the ^{31}P NMR spectrum at δ 31.8 (J = 129 Hz) and a single ν_{CO} absorption at 2009 cm^{-1}.[13] Subsequent addition of 1 equiv of $[Ph_3PNPPh_3]Cl$ to this solution does not cause any change in ^{19}F NMR spectrum, but the presence of a mixture of *trans*-$[Rh(CO)(PPh_3)_2(py)][OTf]$ and *trans*-$[Rh(CO)(PPh_3)_2(Cl)]$ is indicated by their characteristic ^{31}P signals and their ν_{CO} absorptions at 2009 cm^{-1} and 1976 cm^{-1}.

Comparative Characteristics of *trans*-$[Rh(CO)(PPh_3)_2(OH_2)][BF_4]$. The CH_2Cl_2 solutions of *trans*-$[Rh(CO)(PPh_3)_2(OH_2)][BF_4]$[7] deteriorate rapidly at ambient temperature, necessitating their spectral evaluation within 1 h of preparation. In CH_2Cl_2, the ν_{CO} absorption for *trans*-$[Rh(CO)(PPh_3)_2(OH_2)][BF_4]$ appears at 1999 cm^{-1} and the ^{31}P NMR spectrum shows a doublet at δ 31.1 (J = 128 Hz). Addition of pyridine results in the shift of the ^{31}P NMR resonance downfield to δ 31.8 (J = 129 Hz) and the appearance of a single ν_{CO} absorption at 2009 cm^{-1}. The molar conductance of 0.01 **M** solution of *trans*-$[Rh(CO)(PPh_3)_2(OH_2)][BF_4]$ in CH_2Cl_2 is 12 (1) $\Omega^{-1}cm^{-1}mol^{-1}$.

Discussion

In contrast to an earlier report,[7] the results of our study show that *trans*-$[Rh(CO)(PPh_3)_2(OTf)]$ does not undergo OTf^- substitution by H_2O in CH_2Cl_2. The 20 cm^{-1} difference in the ν_{CO} absorptions for analytically pure *trans*-$[Rh(CO)(PPh_3)_2(OH_2)][OTf]$ and *trans*-$[Rh(CO)(PPh_3)_2(OTf)]$ clearly illustrates the difference between cationic *trans*-$[Rh(CO)(PPh_3)_2(OH_2)]^+$ and neutral *trans*-$[Rh(CO)(PPh_3)_2(OTf)]$ in the solid state. However, the presence of a single carbonyl-containing species in CH_2Cl_2 in solutions prepared from either *trans*-$[Rh(CO)(PPh_3)_2(OH_2)][OTf]$ or *trans*-$[Rh(CO)(PPh_3)_2(OTf)]$ is compelling evidence that *trans*-

[Rh(CO)(PPh$_3$)$_2$(OTf)] is the only detectable complex in solution. The H_2O is easily removed by azeotropic distillation in benzene. The ^{31}P NMR signals of *trans*-[Rh(CO)(PPh$_3$)$_2$(OTf)] in CH_2Cl_2 shift to ca. 3 ppm to lower field upon the addition of pyridine and identical ^{31}P NMR signals are generated when pyridine is added to *trans*-[Rh(CO)(PPh$_3$)$_2$(OH$_2$)][BF$_4$]. This shows that pyridine displaces both H_2O and OTf$^-$, giving the *trans*-[Rh(CO)(PPh$_3$)$_2$(py)]$^+$ ion from two different starting points. The similarity of the ^{31}P NMR signals of *trans*-[Rh(CO)(PPh$_3$)$_2$(OTf)] and *trans*-[Rh(CO)(PPh$_3$)$_2$(Cl)] is consistent with these complexes being neutral species in solution. The similarity of the downfield ^{31}P NMR signals from CH_2Cl_2 solutions of *trans*-[Rh(CO)(PPh$_3$)$_2$(OH$_2$)][BF$_4$] and *trans*-[Rh(CO)(PPh$_3$)$_2$(py)][OTf] is consistent with the presence of the *trans*-[Rh(CO)(PPh$_3$)$_2$(OH$_2$)]$^+$ and *trans*-[Rh(CO)(PPh$_3$)$_2$(py)]$^+$ cations in solution. The conductivity measurements lead to the same conclusion as the ^{31}P NMR data. The low electrolytic character of *trans*-[Rh(CO)(PPh$_3$)$_2$(OTf)] and *trans*-[Rh(CO)(PPh$_3$)$_2$(Cl)] suggests they dissolve in CH_2Cl_2 as neutral complexes, whereas the significantly higher molar conductivity of *trans*-[Rh(CO)(PPh$_3$)$_2$(OH$_2$)][BF$_4$] shows the presence of the *trans*-[Rh(CO)(PPh$_3$)$_2$(OH$_2$)]$^+$ and [BF$_4$]$^-$ ions in the CH_2Cl_2 solution.

While ^{19}F NMR spectroscopy is especially important in the study of the Cp*Ru(NO)(OTf)$_2$,[1] the small chemical shift difference between bound and free OTf$^-$ precludes the application of ^{19}F NMR spectroscopy as a quantitative probe of the equilibria in the Rh cases.[14] Nevertheless, a measurable shift of the ^{19}F NMR signal occurs when Cl$^-$ or pyridine is added to solutions of *trans*-[Rh(CO)(PPh$_3$)$_2$(OTf)] in CH_2Cl_2. Since no shift in the ^{19}F NMR signal occurs when Cl$^-$ is added to *trans*-[Rh(CO)(PPh$_3$)$_2$(py)][OTf], this evidence supports OTf$^-$ being bound to Rh when *trans*-[Rh(CO)(PPh$_3$)$_2$(OH$_2$)][OTf] is dissolved in CH_2Cl_2.

The present study shows the previous assessment of the equilibria in eq 1 to be incorrect. Our inability to detect the presence of any cationic *trans*-[Rh(CO)(PPh$_3$)$_2$(OH$_2$)]$^+$ in CH_2Cl_2 leads to a K_{eq} of at least 10^2 based on a minimum detection limit of 1% in the NMR spectra.

$$K_{eq} \geq 10^2 \qquad \text{(eq 1)}$$

trans-$[Rh(CO)(PPh_3)_2(OH_2)]^+ + OTf^- \rightleftarrows$ *trans*-$[Rh(CO)(PPh_3)_2(OTf)] + H_2O$

It is important to note that the relatively high ν_{CO} absorption energy of *trans*-$[Rh(CO)(PPh_3)_2(OTf)]$ in CH_2Cl_2 might lead to the incorrect interpretation that a cationic complex is present in solution. As reported for several other cases, the ν_{NO} or ν_{CO} absorptions of OTf^- complexes fall at 23-50 cm^{-1} *higher* energy than their Cl^- analogues.[1,5] For example, the ν_{CO} absorptions for (η-$C_5(CH_3)_5$)$Fe(CO)_2OTf$ are 23 cm^{-1} higher than for (η-$C_5(CH_3)_5$)$Fe(CO)_2Cl$.[15] The strongly electron-withdrawing SO_2CF_3 moiety on the OTf^- donor O-atom likely reduces the π-donor ability of OTf^- compared to Cl^-.

In summary, we have shown that solid *trans*-$[Rh(CO)(PPh_3)_2(OH_2)][OTf]$ precipitates preferentially from wet CH_2Cl_2 or benzene solutions rather than anhydrous *trans*-$[Rh(CO)(PPh_3)_2(OTf)]$. In CH_2Cl_2 solution, however, the OTf^- ligand is a substantially better ligand than water, leading to *trans*-$[Rh(CO)(PPh_3)_2(OTf)]$ as the only detectable species. Triflate displacement from Rh by H_2O does not occur to a significant extent in CH_2Cl_2 or benzene. Thus, the OTf^- ion in these solvents cannot be classified as a weak ligand in the same category as BF_4^-.

Experimental

General. Standard Schlenk techniques were employed for routine experiments unless otherwise indicated. A Vacuum Atmospheres Dry-Lab glovebox with an N_2-atmosphere containing less than 1 ppm H_2O and 1 ppm O_2 was utilized for the preparation and handling of anhydrous materials. CH_2Cl_2 was rigorously dried using PbNa alloy and transferred in glassware that was dried in a 160°C oven. The concentration of H_2O in homogeneous H_2O-saturated CH_2Cl_2 was determined to be 0.198 g/ 100 mL CH_2Cl_2.[16] The nitrogen reaction atmosphere was purified by passing through scavengers for water (Aquasorb, Mallinckrodt) and oxygen (Catalyst R3-11, Chemical Dynamics, So. Plainfield, NJ). Organic solvents were distilled under nitrogen over appropriate drying agents prior

to use.[17] All other chemical reagents were used as received from Aldrich unless stated otherwise. Infrared spectra were recorded on a Mattson Polaris-Icon FT-spectrometer. The ^{31}P, ^{1}H, ^{13}C, and ^{19}F NMR spectra were recorded on a Bruker ARX-400 NMR spectrometer operating at 162 MHz (^{31}P), 400 MHz (^{1}H), and 376.2 MHz (^{19}F). The residual solvent peak of $CDCl_3$ was used as the internal NMR standard (^{1}H δ 7.24). ^{19}F chemical shifts were referenced externally to CCl_3F (δ 0.0)[17] or internally to 3,5-bis(trifluoromethyl)benzene (δ -63.20 in $CDCl_3$). ^{1}H NMR spectra in CH_2Cl_2 were measured using solvent presaturation techniques and were shimmed and referenced to the signals from $CDCl_3$ sealed inside a 1.5-mm capillary located concentrically inside the 5-mm NMR tube. The chemical shifts reported for the complexes in CH_2Cl_2 are identical to those in CD_2Cl_2. Conductivity measurements were performed on a YSI Model 31A conductivity bridge. For comparison purposes, a 0.02 **M** solution of $[Ph_3PNPPh_3]Cl$ in CH_2Cl_2 has a molar conductance of 50 (1) $\Omega^{-1}cm^{-1}mol^{-1}$. Melting points were measured with a Mel-Temp device (Laboratory Devices) in open capillaries and are uncorrected. Combustion analyses were performed by Atlantic Microlab, Inc., Norcross, GA.

Synthesis of *trans*-[Rh(CO)(PPh$_3$)$_2$(OH$_2$)][OTf]. A mixture of *trans*-[Rh(CO)(PPh$_3$)$_2$(Cl)] (0.13 g, 0.20 mmol) and AgOTf (0.05 g, 0.20 mmol) in 10 mL of benzene (not rigorously dried) was stirred vigorously for 12 h. The reaction was deemed complete when the 1976 cm^{-1} signal of the starting chloride complex was no longer detectable by IR spectroscopy. The solution was filtered, taken to dryness *in vacuo* and the residue was redissolved in 5 mL of dichloromethane. Addition of 5 mL of hexane followed by storage at -70°C for 12 h produced lemon-yellow crystalline *trans*-[Rh(CO)(PPh$_3$)$_2$(OH$_2$)][OTf] (120 mg, 0.15 mmol, 79 %). IR ν_{CO} (CH_2Cl_2, cm^{-1}): 1996vs, (Nujol mull, cm^{-1}) 2008vs; ^{1}H NMR (CH_2Cl_2): δ 7.45 (m, 10 H), δ 7.6 (m, 20 H); ^{31}P NMR ($CDCl_3$): δ 29.5 (d, J = 125 Hz), (CH_2Cl_2): δ 28.2 (J = 125 Hz); ^{19}F NMR (CH_2Cl_2): δ -78.52 Anal. Calcd for $RhP_2C_{38}H_{30}O_4F_3S{\cdot}H_2O$: C, 55.48; H, 3.92. Found: C, 55.43; H, 3.98; mp 178-180 °C.

Synthesis of *trans*-[Rh(CO)(PPh$_3$)$_2$(OTf)]. A Schlenk-distillation apparatus was filled with a solution prepared from *trans*-[Rh(CO)(PPh$_3$)$_2$(OH$_2$)][OTf] (0.150 g, 0.19 mmol) and 20 mL of rigorously dried benzene. Distillation resulted in the removal of H_2O in the early cloudy distillate

fractions. After the distillate became clear, the remaining solvent was removed *in vacuo* to leave a quantitative yield of *trans*-[Rh(CO)(PPh_3)$_2$(OTf)] as a yellow powder. IR ν_{CO} (Nujol mull, cm^{-1}): 1988vs. The IR and NMR spectral properties of Rh(CO)(PPh_3)$_2$(OTf) in CH_2Cl_2 solution are identical to those described above for *trans*-[Rh(CO)(PPh_3)$_2$(OH_2)][OTf]. Anal. Calcd for $RhP_2C_{38}H_{30}O_4F_3S$: C, 56.72; H, 3.76. Found: C, 56.54; H, 3.95; mp 169-170°C.

An alternative method of preparing *trans*-[Rh(CO)(PPh_3)$_2$(OTf)] was to freeze-dry the benzene solution of *trans*-[Rh(CO)(PPh_3)$_2$(OH_2)][OTf] under high vacuum using a liquid-nitrogen trap. The residue that remained had an IR absorption at 1988 cm^{-1}.

X-ray Structural Analysis of *trans*-[Rh(CO)(PPh_3)$_2$(OH_2)][OTf]. A weakly diffracting, but acceptable crystal was found after the examination of numerous candidates. The specimen selected was centered vertically at 173 K on a Siemens P4 Autodiffractometer. The computer centering of 25 random reflections revealed the monoclinic lattice with a = 23.401 (8) Å, b = 9.1222 (4) Å, c = 17.047 (6) Å; β = 107.03 (3)°, V = 3479 (2) Å^3. Data collection of $0 \leq h \leq 26$, $0 \leq k \leq 10$, $-19 \leq l \leq 19$ for a primitive lattice showed a *C*-lattice by the systematic absences $h + k \neq 2n$. The presence of a *c* glide plane was indicated by the systematic absences h0l, h00, and 00l when $h \neq 2n$ and $l \neq 2n$. Solution and refinement of the structure was carried out on an IBM-compatible 486 personal computer using the SHELXS-86[18] and SHELXL-93[19] programs from Sheldrick.[20] Selection of the space group *C*2/c and the use of Patterson methods led to the location of the Rh atom at the special position (0.5, 0.0, 0.0). The P atom and the C atoms of the phenyl rings were clearly visible in the first difference map. The unique PPh_3 group showed no sign of disorder. Three peaks of approximately equal weight were located along a vector that formed a ca. 90° angle to the Rh-P vector. These peaks were successfully modeled isotropically as a 1:1 disorder of a CO ligand and an H_2O ligand.

After the Rh and P peaks, the next largest peak was located 5.5 Å from the Rh atom. This peak was situated in the center of three smaller peaks that formed a ca. three-fold symmetric trigonal pyramid. Application of the crystal symmetry operations generated four symmetry-related peaks that,

overall, formed a staggered ethane-like fragment that was assigned as an end-to-end disordered $SO_3CF_3^-$ moiety. Upon assigning the large peak as a S atom with a site-occupation factor = 0.5, the largest peak in the subsequent difference map was located 0.96 Å from the S position and just off the vector between S and the position of its symmetry equivalent S(a). Overall, the pattern appeared to be the partially resolved superposition of the C atom (from the CF_3 group) and the S atom (of the SO_3 group). Therefore, the best approximation of the disordered $SO_3CF_3^-$ resulted from a model where both the S and C(2) atoms where given site-occupation factors of 0.5 and the F(1), F(2), and F(3) atoms were assigned site-occupation factors of 1.0 each in order to approximately account for both the superposition of the F and O atoms.

Despite the disorder in the CO, H_2O, and $SO_3CF_3^-$ positions, refinement of the structure to 10.57% was possible. The density of the crystals was determined to be 1.57 (2) g/cm^3 by flotation in a CCl_4/hexane mixture. The calculated density for four molecules of *trans*-$[Rh(CO)(PPh_3)_2(OH_2)][OTf]$ per unit cell is 1.57 g/cm^3.

Supporting Information Available. Tables of crystallographic data, collection parameters, atomic coordinates, and equivalent isotropic displacement parameters, complete listing of bond distances and bond angles, anisotropic displacement parameters, and H-atom coordinates (5 pages). This material is contained in many libraries on microfiche, immediately follows this article in the microfilm version of the journal, and can be ordered from the ACS; see any current masthead page for ordering information.

References

(1) (a) Burns, R. M.; Hubbard, J. L. *J. Am. Chem. Soc.*, **1994**, *116*, 9514. (b) Svetlanova-Larsen, A.; Zoch, C.R.; Hubbard, J.L. *J. Am. Chem. Soc.*, submitted.

(2) Lewis acidic metal ions like Al^{+3} are noted for their reactivity in water to give acidic solutions containing polynuclear μ-OH complexes; see: Burgess, J. *Metal Ions in Solution;* John Wiley & Sons: New York-London-Sydney-Toronto, 1978.

(3) (a) Lawrance, G. A. *Chem. Rev.* **1986**, *86*, 17 and references therein. (b) Beck, W.; Sunkel, K.; *Chem. Rev.* **1988**, *88*, 1405 and references therein. (c) Blosser, P. W.; Gallucci, J. C.; Wojcicki, A. *Inorg. Chem.* **1992**, *31*, 2376.

(4) Humphrey, R. B.; Lamanna, W. M.; Brookhart, M.; Husk, G. R. *Inorg. Chem.* **1983**, *22*, 3355.

(5) (a) Hollis, T. K.; Robinson, N. P.; Bosnich, B. *Organometallics*, **1992**, *11*, 2645. (b) Hollis, T. K.; Robinson, N. P.; Bosnich, B. *J. Am. Chem. Soc.*, **1992**, *114*, 5464. (c) Bonnesen, P. V.; Puckett, C. L.; Honeychuck, R. V.; Hersh, W. H.; *J. Am. Chem. Soc.* **1989**, *111*, 6070. (d) Honeychuck, R. V.; Bonnesen, P.V.; Farahi, J.; Hersh, W. H.; *J. Org. Chem.* **1987**, *52*, 5293. (e) Odenkirk, W.; Rheingold, A. L.; Bosnich, B. *J. Am. Chem. Soc.*, **1992**, *114*, 6392. (f) Haggin, J. *Chem. & Eng. News,* **1994,** *10*, 28. (g) Wang, L.; Flood, T. C. *J. Am. Chem. Soc.*, **1992**, *114*, 3169. (h) Wang, C.; Ziller, J. W.; Flood, T. C. *J. Am. Chem. Soc.*, **1995**, *117*, 1647. (i) Wang, L.; Lu, R. S.; Bau, R.; Flood, T. C. *J. Am. Chem. Soc.*, **1993**, *115*, 6999. (j) Darensbourg, D. J.; Stafford, N. W.; Joo, F.; Reibenspies, J. H. *J. Organomet. Chem.* **1995**, *488*, 99. (k) McGrath, D. V.; Grubbs, R. H. *Organometallics*, **1994**, *13*, 224.

(6) (a) Nitschke, J.; Schmidt, S. P.; Trogler, W. C. *Inorg. Chem.* **1985**, *24*, 1972. (b) Trogler, W. C. *J. Am. Chem. Soc.*, **1979**, *101*, 6459.

(7) Branan, N.M.; Hoffman, N.W.; McElroy, E.A.; Prokopuk, N.; Salazar, A.B.; Robbins, M.J.; Hill, W.E.; Webb, T.R. *Inorg. Chem.* **1991**, *30*, 1200.

(8) (a) Werner, H. *Pure Appl. Chem.* **1982**, *54*, 177. (b) Werner, H. *Angew. Chem., Int. Ed. Engl.* **1983**, *22*, 927.

(9) Neither the work in ref. 3 or references therein reported the combustion analysis, mp, and solid-state IR ν_{CO} data for the Rh-OTf complex. Branan, D.M.; Hoffman, N.W.; McElroy, E.A.; Ramage, D.L.; Robbins, M.J; Eyler, J.R.; Watson, C.H.;

deFur, P.; Leary, J.A. *Inorg. Chem.* **1990**, *29*, 1915.

(10) Collman, J. P.; Hegedus, L. S.; Norton, J. R.; Finke, R. G. *Principals of Organotransition Metal Chemistry*; University Science Books: Mill Valley, CA, 1987; chapters 10-12 and references therein.

(11) This reaction can be successfully performed in fluorobenzene with 1 equiv. of AgOTf according to the published procedure for the synthesis of $(PPh_3)_2Ir(CO)(OTf)$: Liston, D.J.; Lee, Y.J.; Scheidt, W.R.; Reed, C.A. *J. Am. Chem. Soc.*, **1989**, *111*, 6643.

(12) Evans, D.; Osborn, J.A.; Wilkinson, G. *Inorg. Synth.*, **1968**, *11*, 99.

(13) Reddy, G.K.N.; Ramesh, B.R. *J. Organomet. Chem.* **1975**, *87*, 347.

(14) Small differences between the ^{19}F NMR signals of bound and free OTf^- occur in related square planar complexes: (a) Stang, P. J.; Huang, Y. H.; Arif, A. M. *Organometallics* **1992**, *11*, 231. (b) Stang, P. J.; Cao, D. H.; Poulter, G. T.; Arif, A. M. *Organometallics*, **1995**, *14*, 1110. (c) Bennet, B. L.; Birnbaum, J.; Roddick, D. M. *Polyhedron*, **1995**, *14*, 187.

(15) Hubbard, J. L.; McVicar, W. L. *J. Organomet. Chem.* **1992**, *429*, 369.

(16) Scheflan, L.; Jacobs, M. *The Handbook of Solvents;* Van Nostrand, New York, 1953; p.112.

(17) Gordon, A. J.; Ford, R. A. *The Chemist's Companion*; John Wiley & Sons: New York, 1972; pp. 25, 433.

(18) Sheldrick, G. M. *Acta Cryst.* **1990,** *A46*, 467-473.

(19) Sheldrick, G. M. *J. Appl. Crystallogr.*, submitted; SHELXL-93 scattering factors from: *International Tables for X-ray Crystallography* Vol. C; Ed. A. J. C. Wilson, Kluwer Academic Publishers: Dordrect, 1992; Tables 6.1.1.4 (pp. 500-502, neutral atom scattering factors), 4.2.6.8 (pp. 219-222, f′,f′′), and 4.2.4.2 (pp. 193-199, absorption coefficients).

(20) SHELXL-93 is available from: Siemens Analytical X-ray Instruments, 6300 Enterprise Lane, Madison, WI 53719, or directly from G. Sheldrick, Institüt für Anorganische Chemie,der Universität, Tammannstrasse 4, D-37077 Göttingen, Germany: gsheldr@shelx.uni-ac.gwdg.de

CHAPTER 4

REACTIVITY OF THE ELECTROPHILIC $[(\eta\text{-}C_5(CH_3)_5Ru(NO)]^{2+}$ COMPLEXES WITH ALCOHOLS: COORDINATION EQUILIBRIA AND ALCOHOL OXIDATION KINETICS

Abstract

The ditriflate complex Cp*Ru(NO)$(OTf)_2$ (**1**) exists in equilibrium with coordinated alcohol species in CH_2Cl_2 solutions in the presence of 1-2 equiv of alcohol (Cp* = η-$C_5(CH_3)_5$; OTf = OSO_2CF_3; ROH = MeOH, EtOH, *i*-PrOH).

$$2\ ROH + \mathbf{1} \underset{K_1}{\rightleftarrows} [Cp^*Ru(NO)(OTf)(ROH)]^+ + ROH + OTf^- \underset{K_2}{\rightleftarrows} [Cp^*Ru(NO)(ROH)_2)]^{+2} + 2\ OTf^-$$

The ^{19}F NMR spectra of these solutions are temperature dependent, allowing for the determinations of the thermodynamic values of ΔH and ΔS. The alcohol complex salts in these cases are not isolable and revert to the starting complex **1** upon solvent removal in vacuo. The reaction of **1** with 3 equiv of HO-CH_2CH_2-OH in $CHCl_3$ results in the crystallization of the chelate-stabilized complex salt [Cp*Ru(NO)(HO-CH_2CH_2-OH)][2OTf] (**2**). Complex salt **2** exists in the equilibrium in $ClCH_2$-CH_2Cl solution.

$$\mathbf{2}^{+2} + 2OTf^- \underset{K_{eq}}{\rightleftarrows} \mathbf{1} + HO\text{-}CH_2CH_2\text{-}OH$$

Thermodynamic values ΔH and ΔS are determined from the analysis of the ^{19}F NMR spectra. X-ray structural data for **2** (173 K), ($C_{14}H_{21}NO_9F_6S_2Ru$): monoclinic $P2_1/c$ space group, a = 8.604 (2) Å, b = 30.681 (6) Å, c = 8.904 (2) Å, β = 91.04 (2)°, Z = 4, R/R_w = 0.0341/0.0497. Treatment of complex **1** with neat i-PrOH results in the rapid quantitative formation of the Ru(0) complex [Cp*Ru(μ-NO)]$_2$ and $(CH_3)_2C{=}O$. Formation of H_2 and $CHDCl_2$ is detected when the reaction between **1** and *i*-PrOH occurs in $CDCl_3$, indicating formation of a short-lived metal-hydride species.

Similar results are observed upon treatment of **1** with EtOH and MeOH, with formation of the acetaldehyde and formaldehyde, respectively. The kinetics of the oxidation of *i*-PrOH by complex **1** is studied by ^{1}H NMR spectroscopy methods in CH_2Cl_2. The reaction is first-order in complex **1** and in *i*-PrOH. The activation parameters obtained for the pseudo-first-order reaction of **1** and i-PrOH are $\Delta H^{\neq}_{obs}$ = 11.9 (5) kcal/mol, $\Delta S^{\neq}_{obs}$ = -24 (6) eu, and $\Delta G^{\neq}_{obs}(298)$ = 19 (2) kcal mol^{-1}. The kinetic isotope effect for the reaction of **1** with $(CD_3)_2CD$-OD at -11 °C is k_H/k_D = 2.0 (3). A mechanism for alcohol oxidation by electrophilic ruthenium (II) complexes via a β-hydrogen elimination step is proposed.

Introduction

The catalytic transformation of functional groups in organic molecules is a major target of research in modern organometallic chemistry. Soluble transition-metal complexes that can be tuned electronically and sterically by varying the metal and/or ligands provide broad opportunities for such transformations.[1] With such variations in reactivity, however, success with transition-metal catalysts seems to depend on serendipity to a large extent, due to a lack of background knowledge necessary for the invention of new catalytic processes.[2] Therefore, mechanistic studies of procatalytic reactions of transition-metal complexes constitute an important contribution to the development of catalysis.[3,4] Reports on transition-metal complex-mediated oxidation of alcohols have appeared in the literature.[5,6] Efficient procedures are developed for the enantioselective epoxidation of allyl alcohols employing *t*-butyl peroxide as the stoichiometric oxidant in the presence of catalytic amounts of vanadium, molybdenum, or titanium compounds.[7] Several researchers examined the formation and oxidative decomposition of alkoxo complexes, leading to metal hydrides and aldehydes or ketones, presumably via a β-hydrogen elimination step.[8,9] However, available mechanistic characterization of such processes is rather scarce.[10]

The present study deals with the reactivity of the Cp*Ru(NO)$(OTf)_2$ complex with alcohols. The triflate complexes have been shown to possess remarkable catalytic and stoichiometric reactivity

over a wide range of reaction conditions.[3-5] An important feature of the ruthenium triflate system under consideration is its aqueous solubility and electrophilicity, resulting in water binding and activation by the cationic $[Cp^*Ru(NO)]^{2+}$ fragment.[11] In concert with our previous investigation into aqueous organometallic chemistry of the [Cp*Ru(NO)] complexes, the present work is concerned with binding and oxidation of alcohols by ruthenium triflate complexes.[12] The study concentrates on the thermodynamic characterization of the triflate-alcohol coordination equilibrium and the kinetic aspects of the subsequent oxidation of alcohol. Isolation and crystallographic characterization of a new chelate-stabilized diol complex are also reported.

Results

Substitution of OTf^- in $Cp^*Ru(NO)(OTf)_2$ (1) by ROH (ROH = EtOH, MeOH, i-PrOH). Triflate ligands of the complex $Cp^*Ru(NO)OTf_2$ (**1**) undergo reversible substitution by simple alcohols in solution.[11] As monitored by ^{19}F NMR spectroscopy, the addition of 1.5 equiv of ROH (ROH = MeOH, EtOH, *i*-PrOH) to a solution of $Cp^*Ru(NO)(OTf)_2$ (**1**) in CH_2Cl_2 results in the decrease of the original δ -77.0 signal of bound OTf^- and the appearance of an upfield signal corresponding to free OTf^- (δ -78.6) and a downfield signal resulting from $[Cp^*Ru(NO)(OTf)(ROH)]^+$. Fig. 4-1 shows ^{19}F NMR spectra of a solution of **1** in the presence of 1.8 equiv of EtOH at various temperatures. The integral of the signal due to free OTf^- is greater than the integral of the signal from $[Cp^*Ru(NO)(OTf)(ROH)]^+$ in all cases, implying the presence of a third ^{19}F NMR silent complex $[Cp^*Ru(NO)(ROH)_2]^{2+}$.[12] Evidence for the ROH bound species is also found in the ^1H NMR spectra.[13] Fig. 4-2(A) shows the ^1H NMR spectrum of a CH_2Cl_2 solution of complex **1** with 2 equiv of EtOH at -20 °C. The resonance of the diastereotopic methylene group of the coordinated EtOH is observed as a multiplet appearing downfield from the methylene protons of free EtOH, with the bound hydroxyl signal appearing as a triplet at δ 8.15. Fig. 4-2(B) illustrates the temperature dependance of the intensity and line-width of the three overlapping Cp* signals between δ 1.87 and 1.89, assigned as $[Cp^*Ru(NO)(OTf)(EtOH)]^+$, complex **1**, and

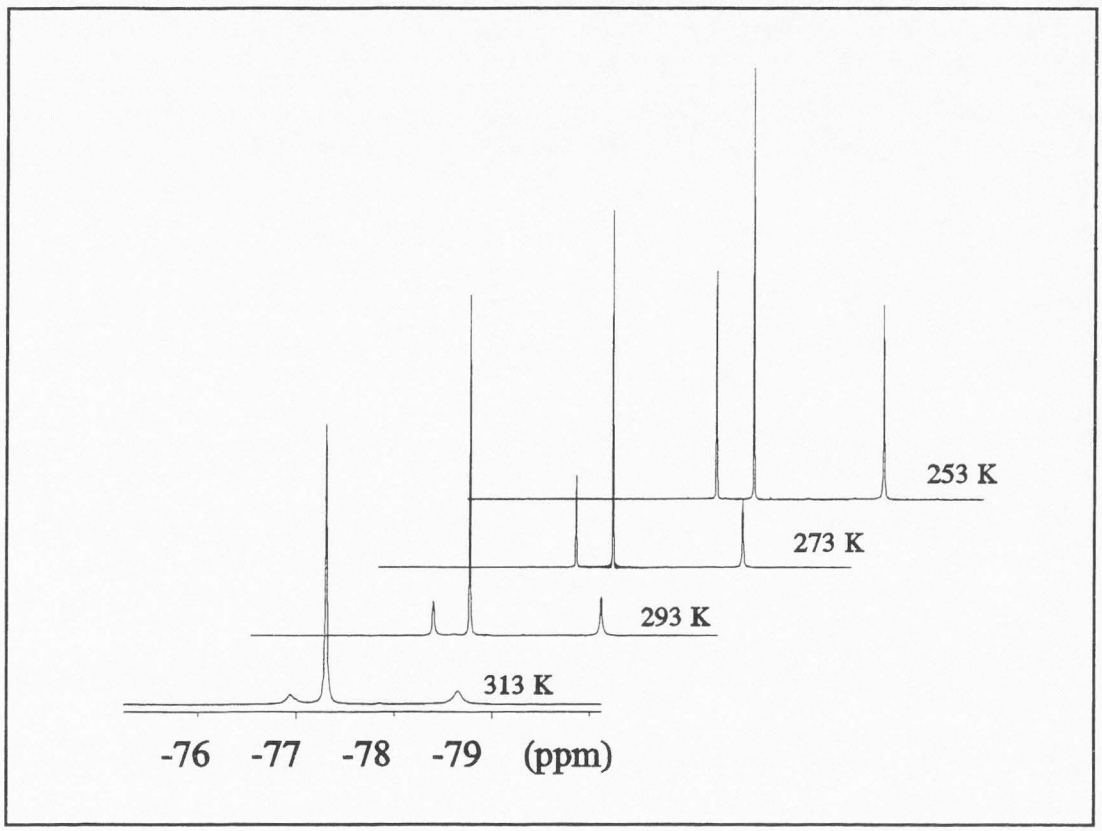

Figure 4-1. ^{19}F NMR spectrum of 1 in CH_2Cl_2 in the presence of 2 equiv EtOH at -20 °C.

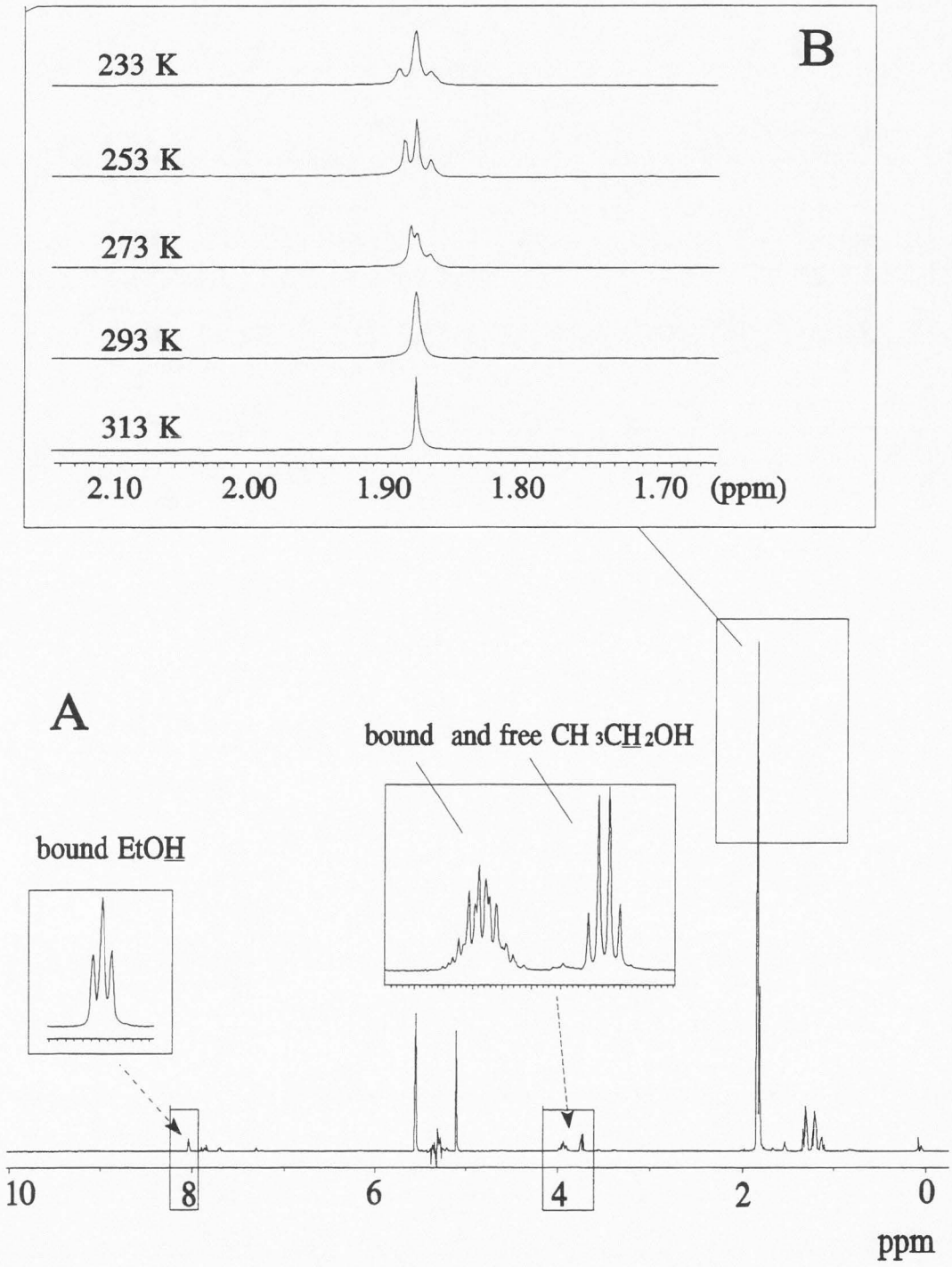

Figure 4-2. (A) ^{1}H NMR spectrum of **1** in CH_2Cl_2 in the presence of 2 equiv EtOH at -20 °C. (B) The Cp* resonance area of the ^{1}H NMR spectra at different temperatures.

$[Cp^*Ru(NO)(EtOH)_2]^{2+}$.

The van't Hoff analysis of the ^{19}F NMR spectra yields thermodynamic values of ΔH and ΔS for the two-step equilibrium process for the binding of MeOH, EtOH and *i*-PrOH according to eq 1 (see Tables 4-1 and 4-2, Fig. 4-3).

$$\underset{K_1}{} \qquad\qquad \underset{K_2}{} \qquad\qquad \text{(eq 1)}$$

$$2\ ROH + \mathbf{1} \rightleftarrows [Cp^*Ru(NO)(OTf)(ROH)]^+ + ROH + OTf^- \rightleftarrows [Cp^*Ru(NO)(ROH)_2)]^{+2} + 2\ OTf^-$$

The alcohol-coordinated complex salts do not precipitate from CH_2Cl_2/hexane mixtures at -78 °C and attempts to isolate these compounds by solvent removal in vacuo results in recovery of **1**.[11]

Synthesis and Characterization of $[Cp^*Ru(NO)(HO\text{-}CH_2CH_2\text{-}OH)][OTf]_2$ (2). Treatment of a $CHCl_3$ solution of complex **1** with 3 equiv of $HO\text{-}CH_2CH_2\text{-}OH$[13] results in a rapid color change from purple to red and precipitation of the $[Cp^*Ru(NO)(HO\text{-}CH_2CH_2\text{-}OH)][OTf_2]$ (**2**) as dark red single crystals. The ^1H NMR spectrum of a CH_2Cl_2 solution of **2** shows a major Cp* proton resonance at δ 1.93, two broad resonances of the diastereotopic methylene pairs of protons at δ 4.23 and 3.35, and a hydroxyl proton signal at δ 11.13 (*vide infra*).

The characterization of the complex salt **2** by single crystal X-ray analysis is summarized in Tables 4-3 and 4-4. Fig. 4-4 shows that the cation $\mathbf{2}^{+2}$ possesses a three-legged piano-stool geometry around the Ru-atom with average Ru-O distances of ca. 2.12 Å and a Ru-N-O angle of 159.8 (4)°. The ethylene glycol ligand forms a non-planar metallacyclic ring by chelating to the ruthenium atom. The non-bonded O(2)-O(6) and O(9)-O(3) distances of 2.6 Å are indicative of intramolecular hydrogen bonding between ethylene glycol and triflate ligands.[14] The triflate containing S(2) participates in intermolecular hydrogen bonding as indicated by F(5)-O(2b) and F(4a)-O(3) distances of 2.9 Å. A very weak intramolecular interaction is also found between the triflate containing S(1) and the Cp* ligand with O(4)-C(13) distance of 3.3 Å.

Minor amounts of **1** and free ethylene glycol are always present in the CH_2Cl_2 solution in

Table 4-1. Thermodynamic values determined by van't Hoff analysis of the ^{19}F NMR spectra according to eq 1.

ROH	ΔH_1, kcal/mol	ΔS_1, eu	ΔH_2, kcal/mol	ΔS_2, eu
MeOH	-2.5 (2)	-20 (10)	-2.0 (5)	-16 (9)
EtOH	-15 (1)	-40 (20)	-13 (1)	-40 (30)
i-PrOH	-10 (1)	-40 (20)	-6.5 (5)	-30 (10)

Table 4-2. K_1 and K_2 values for the eq 1 at variable temperatures.[a]

ROH	MeOH	MeOH		EtOH	EtOH		*i*-PrOH	*i*-PrOH
T,K	K_1	K_2	T,K	K_1	K_2	T,K	K_1	K_2
308	0.02	0.02	308	0.03	small[b]	278	0.03	0.01
303	0.05	0.03	305	0.06	0.001	273	0.05	0.02
293	0.11	0.04	293	0.11	0.004	268	0.09	0.03
283	0.25	0.05	285	0.20	0.01	261	0.12	0.05
273	0.54	0.07	273	0.68	0.05	258	0.22	0.06
263	1.11	0.11	263	1.94	0.07	250	0.35	0.07
253	2.14	0.20	249	5.31	0.17	243	0.58	0.12
243	3.95	0.27	237	26.5	0.62	238	0.96	0.14
233	7.32	0.32	227	150.0	5.28	230	2.17	0.26

[a] All the measurements were done in the presence of 1.5-2.0 equiv of ROH and [**1**] = 0.02-0.03 **M** in CH_2Cl_2.
[b] The value of the constant was below the sensitivity limit of the method.

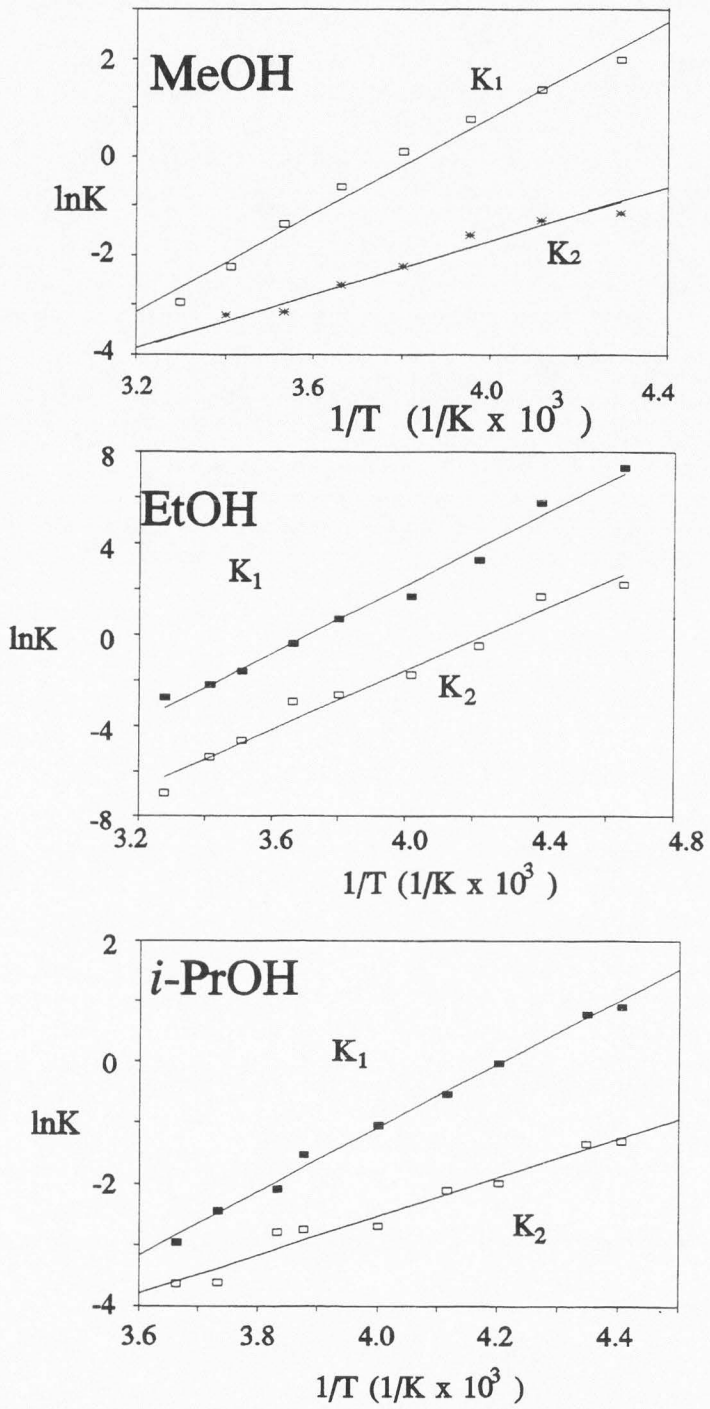

Figure 4-3. The van't Hoff plots for the equilibria of **1** with MeOH, EtOH and *i*-PrOH in CH_2Cl_2.

Table 4-3. Summary of crystallographic data for complex **2**.

Formula	$C_{14}H_{21}NO_9F_6S_2Ru$
Formula weight, amu	626.5
Crystal system	Monoclinic
Space group	$P2_1/c$
a (Å)	8.604 (2)
b (Å)	30.681 (6)
c (Å)	8.904 (2)
β (°)	91.04 (2)
V (Å^3)	2350.0 (9)
Z	4
T,K	173
μ (Mo Kα) (mm^{-1})	0.94
ρ_{calc} (g/cm^3)	1.771
final R, R_w	0.0341[a] 0.0497[b]

[a] $R = \Sigma \mid \mid Fo \mid - \mid F_c \mid \mid \; / \; \Sigma \mid F_o \mid$ [b] $R_w = [\Sigma w(\mid F_o \mid - \mid F_c \mid)^2 / \Sigma w \mid F_o \mid ^2]^{1/2}$; $w = 1/\sigma^2(\mid F_o \mid)$

Table 4-4. Selected geometric data for **2**.

Bond distances (Å)		Angles (°)	
Ru-N	1.779 (4)	N-Ru-O(2)	101.3(2)
Ru-O(2)	2.117 (3)	N-Ru-O(3)	108.4(2)
Ru-O(3)	2.120 (3)	O(2)-Ru-O(3)	75.2(1)
Ru-Cp^*_{cent}	1.85	Ru-N-O(1)	159.8(4)
N-O(1)	1.149 (6)	Ru-O(2)-C(6)	112.5(3)
O(2)-C(6)	1.440 (6)	Ru-O(3)-C(7)	115.8(3)
O(3)-C(7)	1.454 (6)	O(2)-C(6)-C(7)	106.6(4)
C(6)-C(7)	1.470 (8)	O(3)-C(7)-C(6)	107.4(4)
S(1)-O(4)	1.426 (4)	O(4)-S(1)-O(5)	116.9(3)
S(1)-O(5)	1.431 (4)	O(4)-S(1)-O(6)	114.5(3)
S(1)-O(6)	1.458 (4)	O(5)-S(1)-O(6)	113.4(2)
S(1)-C(8)	1.810 (6)	O(4)-S(1)-C(8)	103.7(3)
C(8)-F(1)	1.308 (8)	O(5)-S(1)-C(8)	104.1(3)
C(8)-F(2)	1.326 (8)	O(6)-S(1)-C(8)	101.8(3)
C(8)-F(3)	1.337 (7)	S(1)-C(8)-F(1)	111.5(4)
		S(1)-C(8)-F(2)	111.7(4)
S(2)-O(7)	1.422 (4)	F(1)-C(8)-F(2)	108.2(5)
S(2)-O(8)	1.428 (4)	S(1)-C(8)-F(3)	110.6(4)
S(2)-O(9)	1.454 (4)	F(1)-C(8)-F(3)	107.3(5)
S(2)-C(9)	1.829 (6)	F(2)-C(8)-F(3)	107.3(5)
C(9)-F(4)	1.315 (7)		
C(9)-F(5)	1.321 (7)	O(7)-S(2)-O(8)	116.9(2)
C(9)-F(6)	1.335 (7)	O(7)-S(2)-O(9)	113.6(2)
		O(8)-S(2)-O(9)	113.9(2)
O(3)--O(9)	2.61	O(7)-S(2)-C(9)	104.0(3)
O(2)--O(6)	2.58	O(8)-S(2)-C(9)	103.8(3)
O(3)--F(4a)	2.86	O(9)-S(2)-C(9)	102.3(2)
O(4)--C(13)	3.28	S(2)-C(9)-F(4)	111.2(4)
F(5)--O(2b)	2.93	S(2)-C(9)-F(5)	111.2(4)
		F(4)-C(9)-F(5)	108.0(5)
		S(2)-C(9)-F(6)	111.0(4)
		F(4)-C(9)-F(6)	108.5(5)
Cp^*_{cent} = centroid of η-$C_5(CH_3)_5$ ligand		F(5)-C(9)-F(6)	

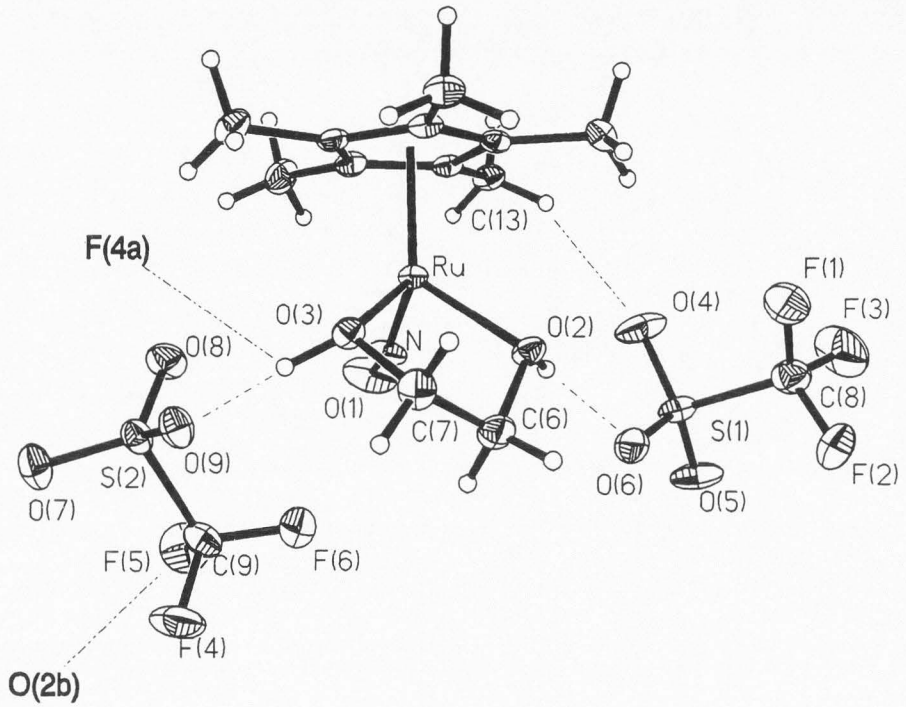

Figure 4-4. Thermal ellipsoid plot for complex salt **2**. The dashed lines represent weak intra- and intermolecular interactions via hydrogen bonding.

equilibrium with **2** (eq 5-2), as indicated by the Cp* resonance of **1** at δ 1.89 in ^{1}H NMR spectrum and a bound OTf resonance of **1** at δ -77.0 in ^{19}F NMR spectrum.

$$[Cp^*Ru(NO)(HO\text{-}CH_2CH_2\text{-}OH)]^{+2} + 2\ OTf^- \overset{K_{eq}}{\rightleftarrows} \mathbf{1} + HO\text{-}CH_2CH_2\text{-}OH \qquad \text{(eq 2)}$$

The van't Hoff analysis of the ^{19}F NMR spectra for this equilibrium gives $\Delta H = 5.5(5)$ kcal/mol, $\Delta S = 20(5)$ eu (Table 4-5, Fig. 4-5).[12]

Alcohol Oxidation by Complex 1. Treatment of **1** with neat i-PrOH results in the rapid quantitative formation of a dark red precipitate, identified as $[Cp^*Ru(\mu\text{-}NO)]_2$ by ^{1}H and ^{13}C NMR spectroscopy methods.[15,16] An equimolar amount of acetone is simultaneously produced in this reaction according to eq 3.

$$\underset{\text{Ru(II)}}{Cp^*Ru(NO)(OTf)_2} + i\text{-}PrOH \xrightarrow{-2HOTf} 1/2\ \underset{\text{Ru(0)}}{[Cp^*Ru(\mu\text{-}NO)]_2} + CH_3C(O)CH_3 \qquad \text{(eq 3)}$$

The above reaction also proceeds in CH_2Cl_2 and $CDCl_3$ solutions, where formation of the dimeric $[Cp^*Ru(\mu\text{-}NO)]_2$ can be monitored by ^{1}H NMR due to the appearance of the characteristic Cp* resonance (δ 1.65 in CH_2Cl_2). Generation of molecular H_2 is detected by the appearance of the singlet at δ 4.60 in ^{1}H NMR spectrum when the reaction between **1** and *i*-PrOH occurs in $CDCl_3$ (confirmed by passing gaseous H_2 through the same sample), along with formation of $CHDCl_2$ (triplet of singlets of equal intensity at δ 5.33, resulting from the spin-spin coupling between proton and deuterium nuclei). After the reaction of **1** with *i*-PrOH in CH_2Cl_2 is complete, the red color of the solution due to $[Cp^*Ru(\mu\text{-}NO)]_2$ darkens within 2-3 h at ambient temperature. In the ^{1}H NMR spectrum the Cp* proton resonance at δ 1.65 decreases, while a new signal at δ 1.83 assigned as $Cp^*Ru(NO)Cl_2$ appears simultaneously. The rate of this process increases in the presence of air,

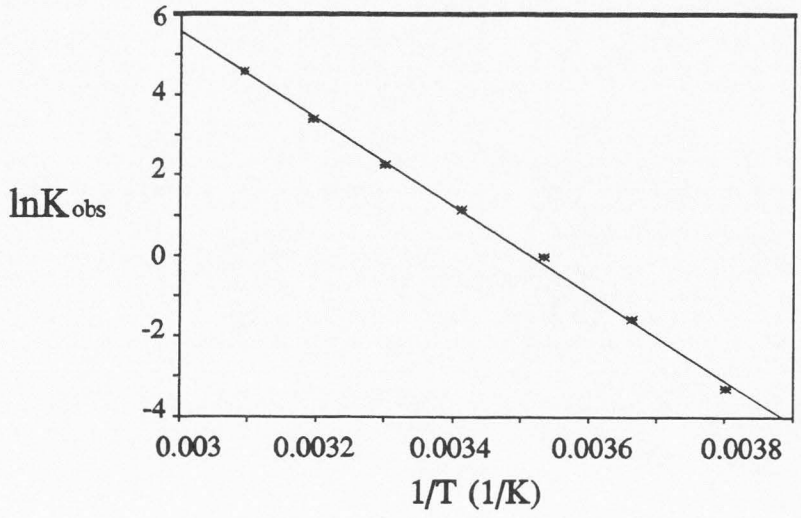

Figure 4-5. The van't Hoff plot for the equilibrium between **1** and **2** in $ClCH_2CH_2Cl$.

Table 4-5. K_{eq} values for eq. 2 at different temperatures.

T,K	K
333	256
323	91.9
313	29.8
303	9.44
293	3.17
283	0.97
273	0.21
263	0.04

higher temperatures, and at lower starting concentrations of **1**. Similar reactions occur between **1** and neat EtOH and MeOH, resulting in the generation of $[Cp^*Ru(\mu\text{-}NO)]_2$ in both cases and the formation of acetaldehyde and formaldehyde, respectively. In the reaction with EtOH in CH_2Cl_2, acetaldehyde and acetal formation is easily detected in the ^1H NMR spectrum of the solution.[17] In experiments performed with $CH_3C^{13}H_2OH$ in $CDCl_3$signals at δ 99.48 and 60.68 are observed, indicating formation of acetal $CH_3{}^{13}CH(O{}^{13}CH_2CH_3)_2$.[17] In the reaction with MeOH, formaldehyde is not observed in the ^1H NMR spectrum, so studies with ^{13}C-labeled MeOH help to identify the reaction products. Characteristic signals of dimethoxymethane, the product of the reaction between formaldehyde and MeOH, are observed in the ^{13}C NMR spectrum in $CDCl_3$ at δ 97.50 and 55.04.[17] An unidentified intermediate with the Cp* proton resonance at δ 1.78 is observed in the reaction with MeOH at 0 °C. This intermediate converts to the dimeric $[Cp^*Ru(\mu\text{-}NO)]_2$ complex within 30 min at ambient temperature.

Kinetics of the *i*-PrOH Oxidation by Complex 1. Kinetics of the oxidation reaction in CH_2Cl_2 solutions of **1** in the presence of ca. 100 equiv of *i*-PrOH are followed by monitoring the rate of disappearance of the Cp* signal of the Ru(II) species. The amount of Ru(II) complexes in solution is estimated as a total integral of the Cp* signal at δ 1.87-1.89 (area shown on Fig. 4-2[B]), corresponding to the starting complex **1** together with its alcohol substituted derivatives. The product $[Cp^*Ru(\mu\text{-}NO)]_2$ exhibits a Cp* signal 0.25 ppm upfield from that of **1**, while the $(CH_3)_2C{=}O$ proton signal appears at δ 2.14. The analysis of the concentration-time profiles for the Ru(II) species shows that the reaction is first order in **1** from -47 to -11 °C (Table 4-6 (experiments numbered 1-6), Fig. 4-6[A]).[18] A plot of ln[**1**] versus time does not deviate from the linearity during five half-lives at -19 °C. Activation parameters determined for this process are $\Delta H^{\neq}_{obs}$ = 11.9 (5) kcal/mol, $\Delta S^{\neq}_{obs}$ = -24 (6) eu, and $\Delta G^{\neq}_{obs}(298)$ = 19 (2) kcal mol^{-1} (Fig. 4-6[B]).

In experiments numbered 7-10 (Table 4-6), the starting concentration of **1** is varied from 0.0065 **M** to 0.016 **M**, yielding the same values of k_{obs} within experimental error. In experiments numbered 11-16 (Table 4-6), the concentration of *i*-PrOH is varied from 0.02 **M** to 2.0 **M**. Fig. 4-7

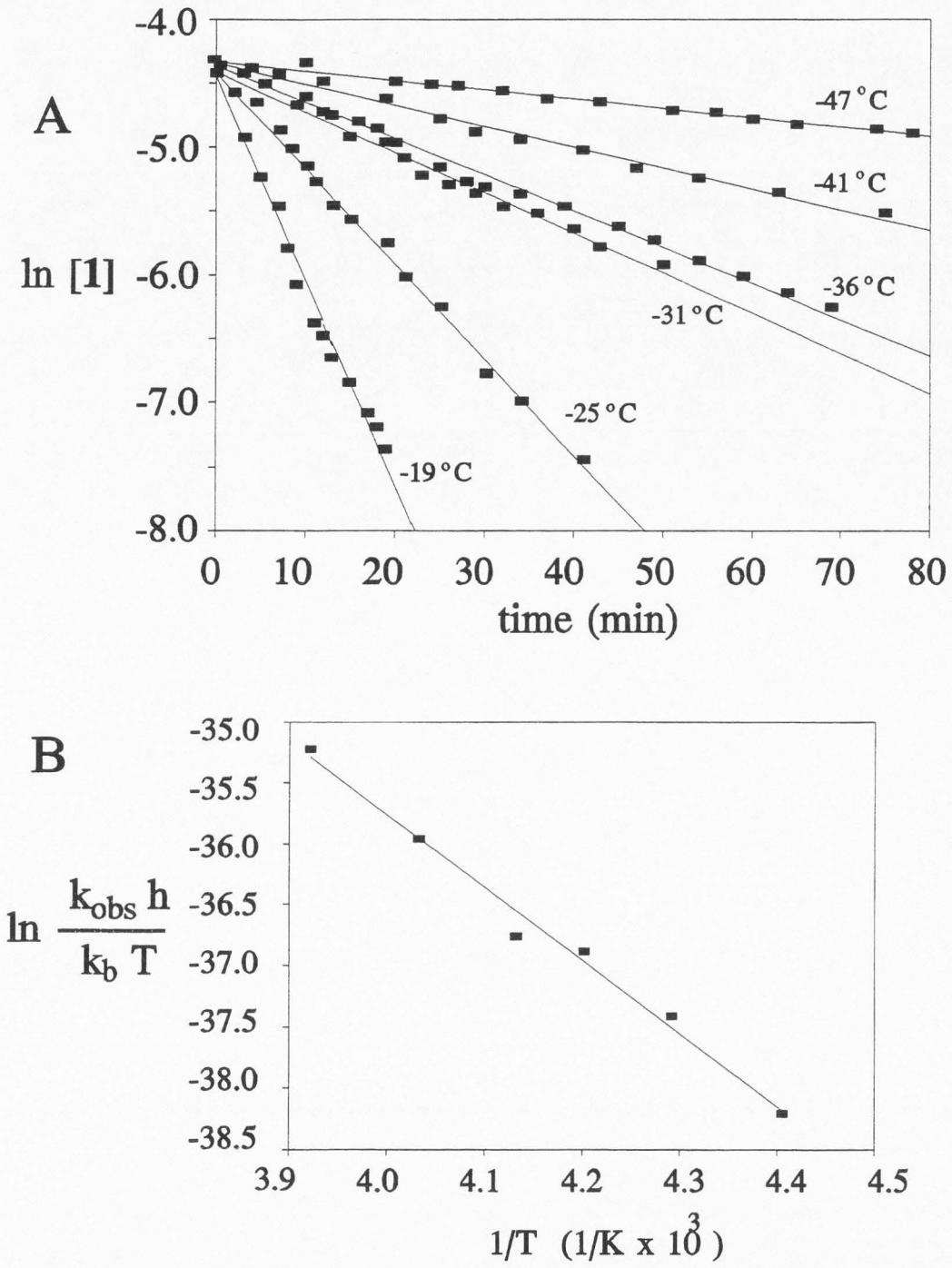

Figure 4-6. (A) Pseudo-first-order plots for the reaction of **1** with *i*-PrOH in CH_2Cl_2 (see Table 4-6, exp. 1-6); (B) Eyring plot for the reaction of **1** with *i*-PrOH in CH_2Cl_2.

Table 4-6. Observed rate constants for the reaction of **1** with *i*-PrOH in CH_2Cl_2.

No.	[**1**], **M** x 10^{-2}	[*i*-PrOH], **M**	T, °C	k_{obs}[a], s^{-1}
1	0.014	2.1	-47	1.2×10^{-4}
2	0.014	2.1	-41	2.7×10^{-4}
3	0.014	2.1	-36	4.7×10^{-4}
4	0.014	2.1	-31	5.2×10^{-4}
5	0.014	2.1	-25	1.2×10^{-3}
6	0.014	2.1	-19	2.3×10^{-3}
7	0.016	1.5	-11	1.8×10^{-3}
8	0.013	1.5	-11	1.8×10^{-3}
9	0.0065	1.5	-11	2.0×10^{-3}
10	0.009	1.5	-11	1.9×10^{-3}
11	0.014	0.02	-19	0[b]
12	0.014	0.059	-19	3.8×10^{-4}
13	0.014	0.087	-19	7.2×10^{-4}
14	0.014	1.4	-19	1.0×10^{-3}
15	0.014	1.8	-19	1.2×10^{-3}
16	0.014	2.0	-19	1.8×10^{-3}

[a] The variation in the reproducibility of k_{obs} is 15%.
[b] No change in the integral value of **1** observed during 24 h.

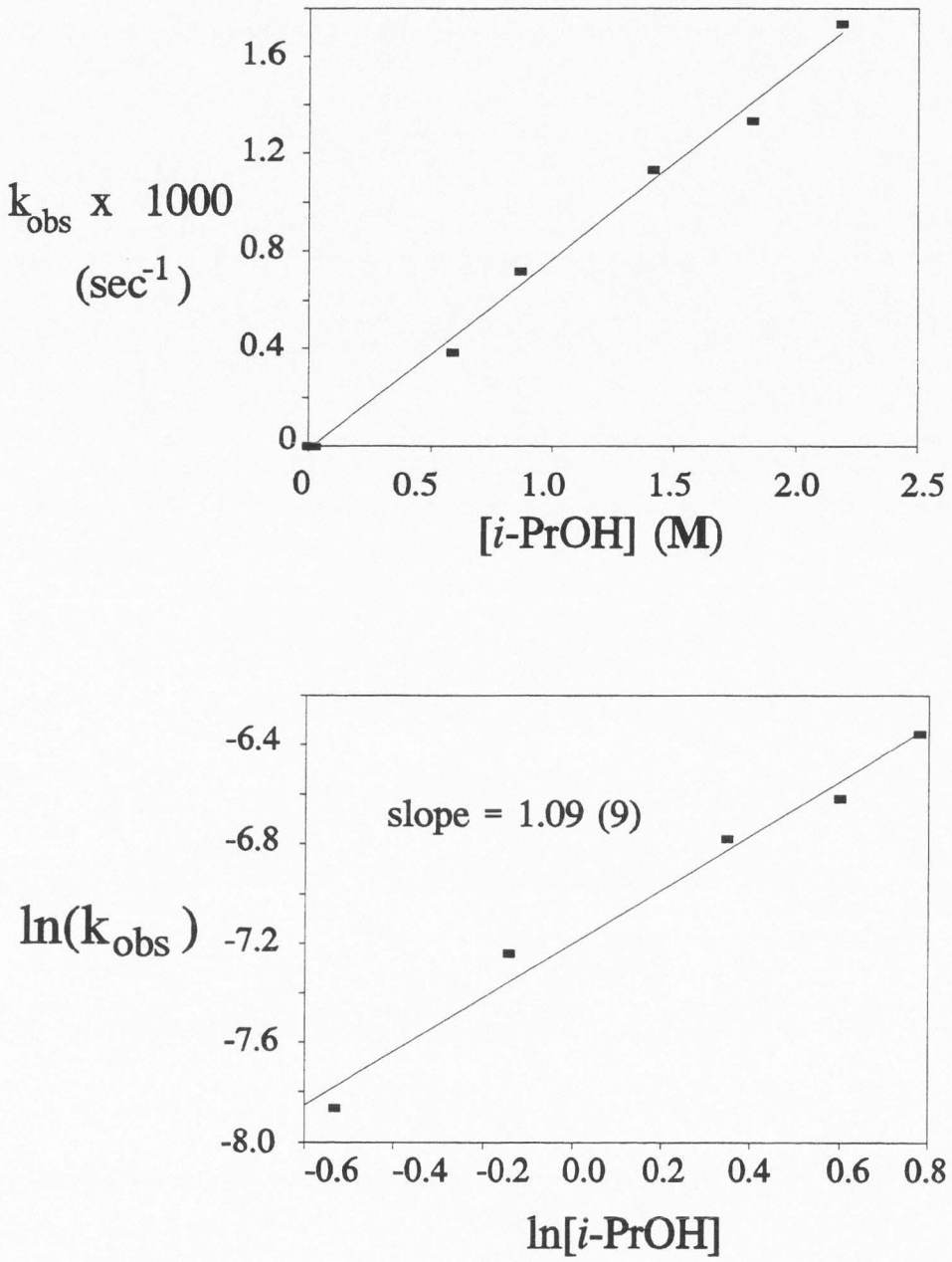

Figure 4-7. Effect of different concentrations of *i*-PrOH on the values of k_{obs}.

shows a plot of the pseudo-first-order k_{obs} vs [*i*-PrOH] and its logarithmic version. The slope of $\ln k_{obs}$ versus ln[*i*-PrOH] on the latter plot was determined to be 1.09 (9). The oxidation reaction proceeds faster in the presence of higher concentrations of *i*-PrOH, and is immeasurably slow in the presence of ≤ 2 equiv of *i*-PrOH per molecule of **1** (no change in the total integral value of Cp* resonance of **1** and alcohol substituted derivatives was observed after 24 h).

Kinetic Isotope Effect. The effect of deuterium substitution on the rate is determined by comparing the reaction of **1** with *i*-PrOH and with $(CD_3)_2CD\text{-}OD$.[19] The obtained value of $k_{obs,H}/k_{obs,D}$ is 2.0 (3) at -11 °C (see Fig. 4-8[A]). The kinetic isotope effect of the reaction of **1** with *i*-PrOD (only the hydroxyl proton deuterium substituted) versus *i*-PrOH is indistinguishable from unity.

Kinetics of Oxidation of EtOH by Complex 1 in CH_2Cl_2. The analysis of the rate of the reaction of **1** with 2.2 **M** EtOH in CH_2Cl_2, monitored by ^1H NMR, yields the pseudo-first-order rate constant k_{obs} of 5.1×10^{-4} s^{-1}. The effect of deuterium substitution on the rate is determined by comparing the reaction of **1** with *i*-PrOH and with CD_3CD_2CDOD.[19] The obtained value of $k_{obs,H}/k_{obs,D}$ is 6.8 (9) at -11 °C (see Fig. 4-8[B]). The kinetic isotope effect of the reaction of **1** with EtOD (only the hydroxyl proton is deuterium substituted) versus EtOH is indistinguishable from unity.

Discussion

Substitution of Coordinated OTf^- in Solution in the Presence of Alcohols and Ethylene Glycol. Triflate has been shown to bind tightly to the $[Cp^*Ru(NO)]^{+2}$ fragment by X-ray methods.[12] In CH_2Cl_2 solution in the presence of 1-2 equiv of alcohol, triflate dissociation is detected by NMR spectroscopy and mono- and di-alcohol bound species are formed according to eq 1. Complex **1** remains the major species in solution. The van't Hoff analysis demonstrates that release of triflate is an exothermic process, with negative ΔS values due to the required reorganization of the solvent around newly formed ionic particles.[12,20,21] This situation is similar to the displacement of OTf^- in

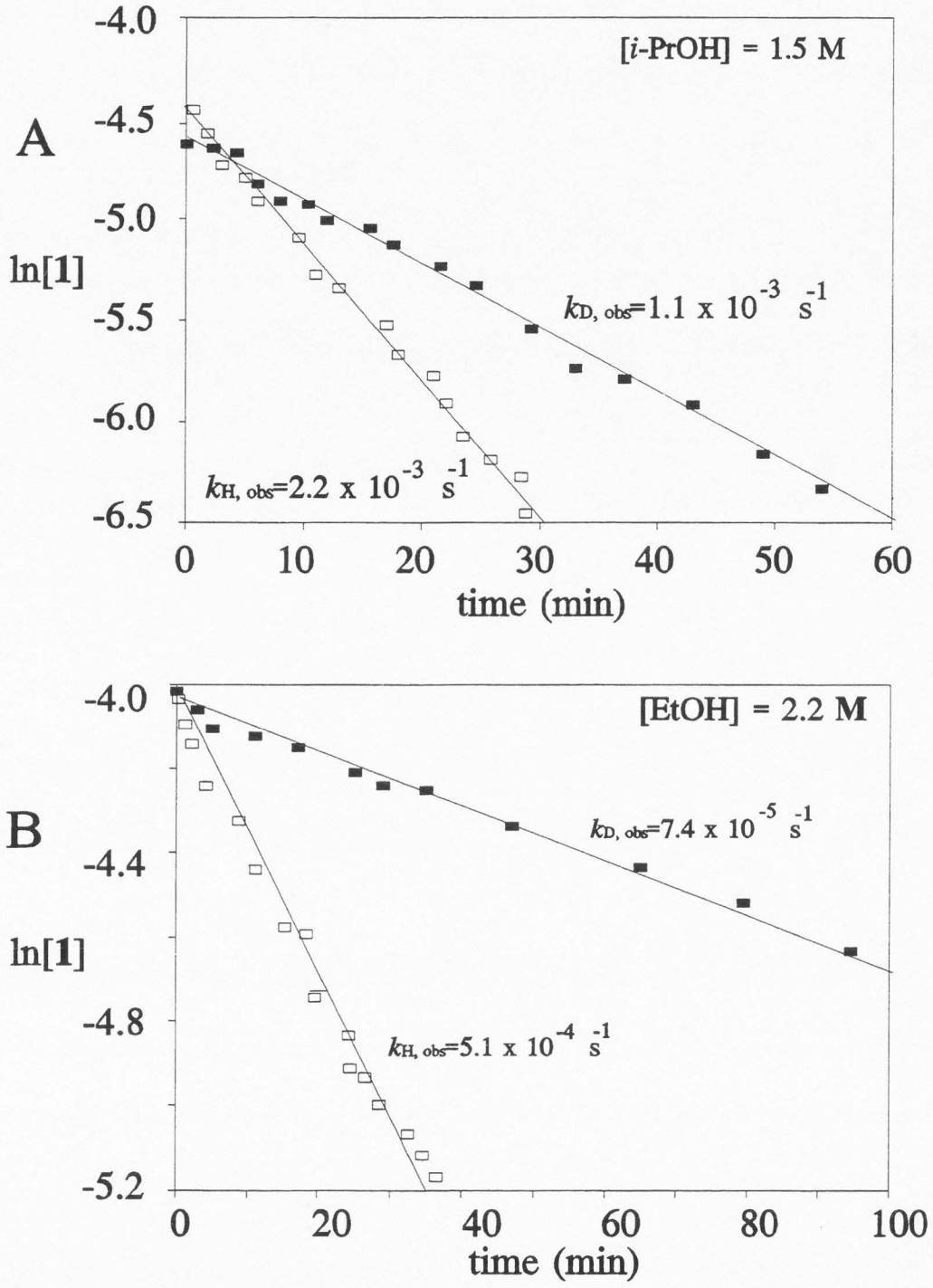

Figure 4-8. Pseudo-first order plots for the reaction of 1 with (A) *i*-PrOH and perdeutirated *i*-PrOD in CH_2Cl_2 at -11 °C (concentration of alcohol in both experiments is 1.5 M) and (B) EtOH and perdeutirated EtOD in CH_2Cl_2 at -11 °C (concentration of alcohol in both experiments is 2.2 M).

1 by H_2O ligands in CH_2Cl_2, where the negative ΔS values reflect the need for solvent reorganization around formed ion pairs.[12] The equilibrium between alcohol-bound and alcohol-free species is reached so quickly that kinetic studies of the binding process cannot be carried out by NMR methods.

Diol-coordinated complex salt **2** is a chelate stabilized version of $[Cp^*Ru(NO)(ROH)_2][OTf]_2$. Dissociation of ethylene glycol from complex $\mathbf{2}^{+2}$ with formation of minor amounts of starting complex **1** occurs in CH_2Cl_2 solution in spite of the chelate stabilization effect. Since the process in eq 2 leads to elimination of the ions and formation of the neutral molecules, it is entropically favorable and is characterized by positive ΔS value. The open-ring intermediate where ethylene glycol ligand is mono-bound to the ruthenium center can be invoked, but apparently it is short lived and cannot be detected. The ratio of complex **1** to complex salt **2** increases with increasing dilution in order to satisfy the requirement of the constant value of K_{eq} for eq 2. The observed ν_{NO} value in the IR spectra of the CH_2Cl_2 solutions of **2** shifts from 1790 to 1850 cm^{-1}. The opposite effect is caused by gradual addition of ethylene glycol to solutions of **1**. These observations also illustrate the difference in the electron donation ability of ethylene glycol ligand compared to the triflate ligand.

Structural Features of Complex Salt 2. The overall solid-state structure of the cationic fragment of complex salt **2** consists of the three-legged "piano-stool" with two "legs" joined by the ethylene fragment of the HO-CH_2CH_2-OH molecule. The ∠ Ru-N-O is 159.8°, indicating the significant π-donation from the oxygens of ethylene glycol, resulting in the deviation from linear coordination of nitrosyl.[22] Two triflate counterions are closely associated to the cation via H-bonding interaction between O(2) and O(6) and between O(3) and O(9) atoms.[14] In response to the involvement of O(6) and O(9) in this additional interaction the corresponding S(1)-O(6) bonds are distinctly elongated compared to other S-O bonds in the triflate fragment (ca. 1.46 Å versus 1.43 Å). Secondary intermolecular interactions originate from hydrogen bonding between the fluorine atoms of triflate of one molecule and hydroxyl hydrogens of the ethylene glycol ligand of another molecule.

These interactions result in the formation of extended planes of layered packing in the crystals of **2**. Only one of the two triflates in each molecule participates in the intermolecular hydrogen bonding. The SO_3 group of the second triflate is effectively chelated between O(2) of the ethylene glycol and C(13) of the Cp* ligand through O(6) and O(4) atoms.

Alcohol Oxidation by Complex 1. Alcohols serve as effective reducing agents in the reaction with **1**, resulting in the 2-electron reduction to the Ru(0) complex $[Cp^*Ru(\mu\text{-}NO)]_2$ according to eq 3. The original synthetic method starting from $Cp^*Ru(NO)Cl_2$ requires excess of zinc dust as a reductant in dry ethanolic solutions.[15,16] The reaction between **1** and alcohols proceeds even in the presence of water. For example, in the 50-50 ethanol-water mixture the reduction of **1** occurs readily and $[Cp^*Ru(\mu\text{-}NO)]_2$ precipitates from the solution. When the same reaction occurs in pure EtOH, the final product remains dissolved in EtOH. Observation of $[Cp^*Ru(\mu\text{-}NO)]_2$ formation in the dilute CH_2Cl_2 or $CDCl_3$ solutions of **1** upon addition of alcohols at ambient temperature may be obscured by the apparent activation of $[Cp^*Ru(\mu\text{-}NO)]_2$ towards the chloride abstraction from the solvent and formation of ruthenium(I) and ruthenium(II) chloride complexes. An opposite transformation from $[Cp^*Ru(\mu\text{-}NO)]_2$ to **1** was reported to occur upon addition of 4 equiv of HOTf to a CH_2Cl_2 solution of $[Cp^*Ru(\mu\text{-}NO)]_2$ via a Ru(I) intermediate dimer according to eq 4.[11]

$$\underset{\text{Ru(0)}}{[Cp^*Ru(\mu\text{-}NO)]_2} \xrightarrow{2\ HOTf} \underset{\text{Ru(I)}}{[Cp^*Ru(OTf)(\mu\text{-}NO)]_2} \xrightarrow{2\ HOTf} \underset{\text{Ru(II)}}{Cp^*Ru(NO)(OTf)_2} \qquad \text{(eq 4)}$$

Coupled with the reaction of *i*-PrOH and **1**, the transformation in eq 4 completes the hypothetical procatalytic cycle for *i*-PrOH oxidation in which HOTf would play a role of the sacrificial reagent (Scheme 4-1). The difficulty in practical realization of this scheme is the preferential reaction of HOTf with *i*-PrOH (forming ester or dehydrating *i*-PrOH)[20] rather than with the $[Cp^*Ru(\mu\text{-}NO)]_2$ complex. The solution to this problem may be in finding a suitable two-phase system, where *i*-PrOH and complex **1** will be contained in another phase where the oxidation step

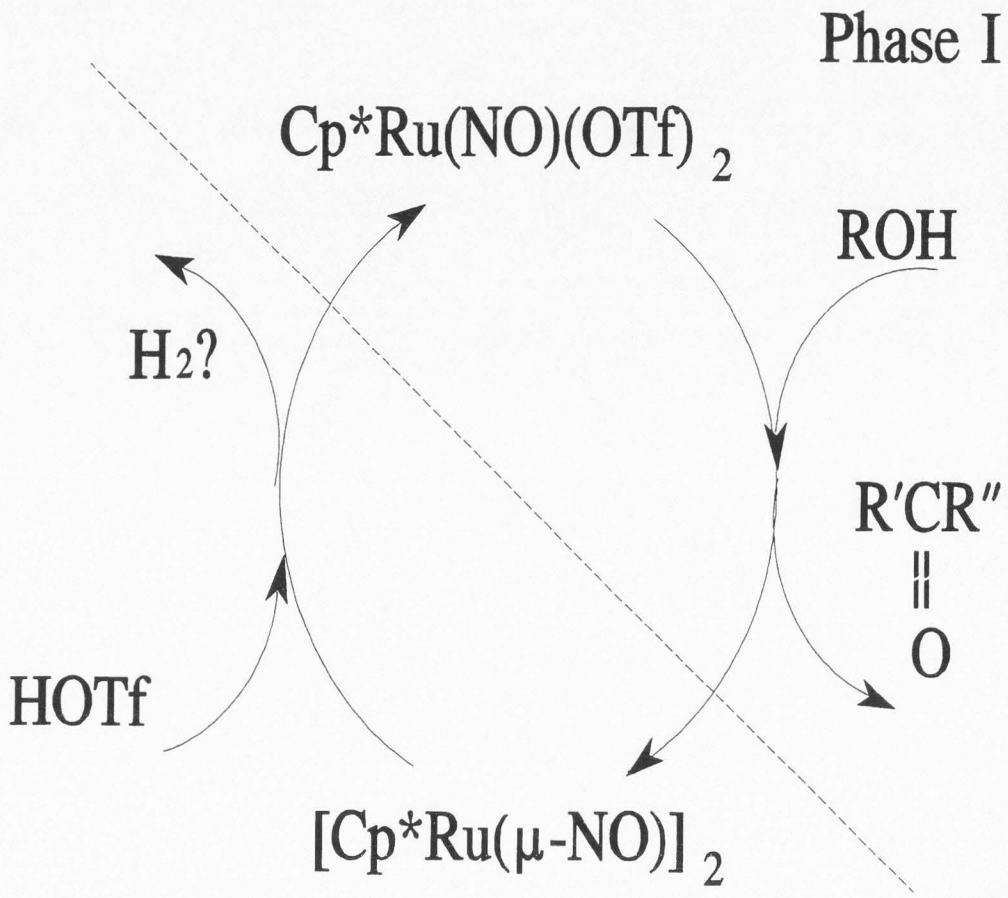

Scheme 4-1

occurs. The product $[Cp^*Ru(\mu\text{-}NO)]_2$ will be absorbed into the second phase, where the reaction with HOTf will convert it back to complex **1**, that in its turn will be absorbed by the first phase again, and so forth. The solubility properties of complexes **1** and $[Cp^*Ru(\mu\text{-}NO)]_2$ differ considerably, so in principle the separation between two solution phases based on this difference is not inconceivable. However, the development of the practical procedure for the catalysis will require further experimental work.

A related example of the ionic hydrogenation with a net result of formation of *i*-PrOH from acetone has been reported by Song et al.[5b] The formal sources of H^+ and H^- in this case are HOTf and $HW(CO)_3Cp$, respectively. A bound *i*-PrOH complex is isolated prior to the decomposition to free *i*-PrOH and $Cp(CO)_3W(OTf)$. In terms of this example the reaction between **1** and *i*-PrOH (eq. 3) should be classified as a case of **reversed** ionic hydrogenation, since it leads to the formation of acetone and unstable metal-hydride species (*vide infra*). The observation of H_2 and $CHDCl_2$ (from $CDCl_3$) formation are indicative of the presence of metal-hydride species.[11] Reactions of late transition metals with alcohols frequently lead to aldehydes or ketones and hydrido products without observation of an (alkoxo) intermediate.[6,7,23] Metal hydride-complexes are often very reactive and decompose with a release of H_2 and metal-metal bond formation.[24]

The results of the kinetic experiments show that the oxidation reaction of *i*-PrOH is first order in complex **1**. This is in spite of the fact that the major organometallic product of the reaction is dinuclear. Therefore, the formation of dimeric complexes is not a rate-determining step (RDS) in this reaction. The value of the kinetic isotope effect $k_{i\text{-}PrOH}/k_{(CD3)2CD\text{-}OD}$ of 2.0 suggests that C-H cleavage is probably involved in the RDS.[19] In a related study, the methanol-catalyzed decomposition of *mer-cis*-$HIr(OCH_3)Cl(PMe_3)_3$ to *mer-cis*-$H_2IrCl(PMe_3)_3$ and formaldehyde and its oligomers via β-hydrogen elimination step in a methanolic benzene solution is observed according to eq 5.[6a] A kinetic isotope effect of 2.4 is determined for β-hydrogen elimination in this iridium octahedral system. Activation parameters determined for this reaction in eq 5 are $\Delta H^{\neq}_{obs}$ = 24 kcal/mol, $\Delta S^{\neq}_{obs}$ = 0 eu, and $\Delta G^{\neq}_{obs}(298)$ = 24 kcal mol^{-1}.[6]

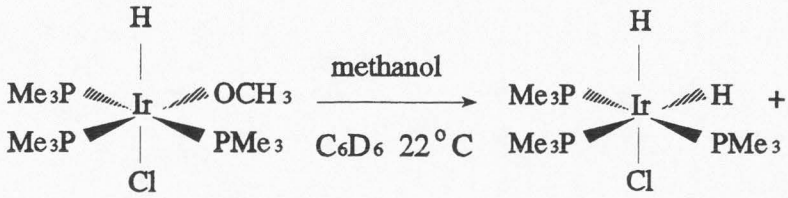

(eq 5)

Activation parameters determined for the oxidation reaction of *i*-PrOH with **1** cannot be compared directly to the results of Milstein's study. The observed activation parameters consist of a sum of the different equilibrium values of all the basic transformations occurring prior to the RDS plus the activation value for the RDS. Although the RDS in the decomposition of (methoxy)iridium complex may be similar to the RDS in the reaction of **1** and *i*-PrOH, other circumstances of these two reactions may differ significantly. The fast exchange of alcohol in the Ru case most probably affects the values of activation parameters. In the iridium system (eq 5), this exchange is not observed at all.[6a]

Possible Mechanism of the Alcohol Oxidation Reaction. An earlier mechanism of alcohol oxidation by complex **1** proposed by Zoch involved a β-hydrogen elimination step from the alcohol-coordinated complex.[11] The results of the present study are consistent with this hypothesis (see Scheme 4-2). The reaction mechanism consists of alcohol coordination to the ruthenium center; β-hydrogen elimination from the coordinated alcohol molecule, leading to the formation of aldehyde or ketone and metal hydride species; and reductive elimination from the metal hydride, resulting in the formation of the dimeric Ru(0) complex $[Cp^*Ru(\mu\text{-}NO)]_2$. In the first step (i), an alcohol molecule coordinates to the ruthenium center, liberating one triflate as a counterion. Alkoxide formation is not proposed here, since bound hydroxyl protons are detectable in the low-field region of the ^1H NMR spectrum. The binding process is facilitated by the presence of high concentrations of alcohol in solution. The dissociation of the second triflate generates a free coordination site (step ii), so β-hydrogen elimination from the bound alcohol molecule can occur, resulting in the release of an

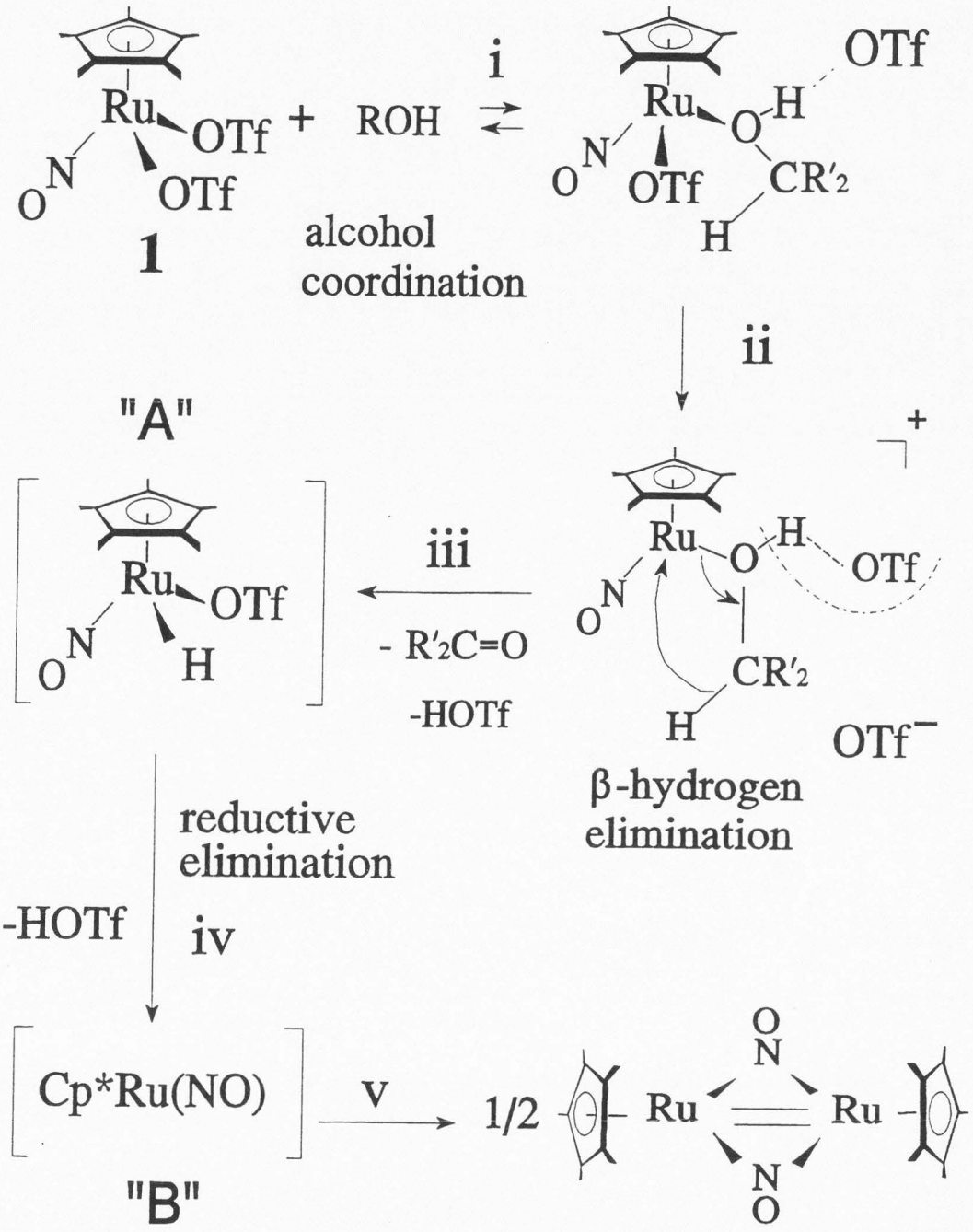
Ru
OTf
N
O
OTf
1
+ ROH
i
alcohol
coordination
OTf
H
CR′2
ii
"A"
iii
- R′2C=O
-HOTf
+
OTf⁻
β-hydrogen
elimination
reductive
elimination
-HOTf
iv
Cp*Ru(NO)
v
1/2
"B"

Scheme 4-2.

aldehyde or ketone molecule and the formation of a metal-hydride species A (step iii). The formation of $CHDCl_2$ when the reaction is run in $CDCl_3$ clearly indicates the intermediacy of a ruthenium-hydride species. The results of kinetic studies (in particular, the determination of the first order in Ru(II) species and primary kinetic isotope effect value) support the suggestion that this process is involved in the RDS of the reaction. The key role in the proposed mechanism belongs to the mono-alcohol complex with an available coordination site. The fact that the reaction is also first order in *i*-PrOH and the observation that Cp*Ru(NO)(CH_3)(OTf) is incapable of alcohol oxidation (apparently, due to the blocked coordination site)[21] are consistent with the proposed scheme. The released hydroxyl proton may be absorbed in a close ionic pair with triflate anion at this point, effectively forming triflic acid. The observation of HOTf generation is obviously obscured by the high concentration of alcohol in solution. In step iv of Scheme 4-2 the elimination of HOTf from the short-lived metal-hydride species **A** results in a 2-electron reduction of the metal center[1] and generation of the neutral and coordinatively unsaturated Ru(0) intermediate [Cp*Ru(NO)] (species "B").[15,16] Rapid coupling of two [Cp*Ru(NO)] fragments generates the final dimeric product, [Cp*Ru(μ-NO)]$_2$ (step v). Species **A** and **B** are expected to be very reactive and therefore not likely to be observable by NMR methods. The fact that Ru(I) complexes are not isolated from the reaction of **1** with *i*-PrOH is an indication, that the reductive elimination from species **A** occurs via a 2-electron rather than 1-electron route.

Experimental

General. Standard Schlenk techniques were employed in all procedures. The nitrogen reaction atmosphere was purified by passing through scavengers for water (Aquasorb, Mallinckrodt) and oxygen (Catalyst R3-11, Chemical Dynamics, So. Plainfield, NJ). Organic solvents were distilled under nitrogen over appropriate drying agents prior to use. The water used was purified and deionized (NANO-pure Ultrapure Water System) and saturated with N_2 gas prior to use. All chemical reagents were used as received from Aldrich unless stated otherwise. Infrared spectra were

recorded on a Mattson Polaris-Icon FT-spectrometer.

The ^{1}H, ^{2}H, ^{13}C and ^{19}F NMR spectra were recorded on a Bruker ARX-400 NMR spectrometer operating at 400 MHz (^{1}H), 61.42 MHz (^{2}H), 100.62 Mhz (^{13}C), and 376.2 Mhz (^{19}F). The residual solvent peak of $CDCl_3$ was used as the internal NMR standard (^{1}H δ 7.24; ^{13}C δ 77.0 ppm), as well as the residual peak of HDO (^{1}H δ 4.70). Spectra were recorded at 298 K unless otherwise stated. ^{19}F chemical shifts were referenced externally to $CFCl_3$ (δ 0.0)[25] or internally to 3,5-bis(trifluoromethyl)benzene (δ -63.2); a relaxation delay of 12 s ($> 5T_1$) was used to optimize the integration. Free OTf^- appears at δ -78.6 in CH_2Cl_2 and δ -78.0 in H_2O, regardless of the counterions present. NMR spectra in CH_2Cl_2 and H_2O were measured using solvent presaturation techniques and were shimmed and referenced to the signals from $CDCl_3$ sealed inside a 1.5-mm capillary located concentrically inside the 5-mm NMR tube. When necessary, 5-mm NMR tubes with resealable Teflon valves were used (Brunfeld Co., Bartlesville, OK). The chemical shifts reported for the complexes in CH_2Cl_2 and H_2O are identical to those in the analogous deuterated solvents. The equilibrium and kinetic studies utilized ^{19}F and ^{1}H NMR spectroscopy. The temperature inside the VT-NMR probe was calibrated according to literature procedures.[26] For van't Hoff analyses, the samples were allowed to thermally equilibrate at the desired temperatures before spectra were recorded (15-120 min).

Melting points were measured with a Mel-Temp device (Laboratory Devices) in open capillaries and are uncorrected. Combustion analysis was performed by Atlantic Microlab, Inc., Norcross, GA.

Synthesis of [Cp*Ru(NO)(HO-CH_2CH_2-OH)][OTf]$_2$ (2). Ten μL of HO-CH_2CH_2-OH (0.213 mmol, 3 equiv) was added to a stirred solution of 40 mg of **1** (0.071 ml)[12] in 10 ml of $CHCl_3$. A red precipitate formed within 5 min and the initially purple solution became almost colorless. The supernatant was decanted and the precipitate recrystallized from a CH_2Cl_2/hexane mixture at -40 °C yielding 30 mg (0.050 mmol, 70%) of analytically pure complex **2**. X-ray quality crystals were grown by slow evaporation of $CDCl_3$ solution. The $CHCl_3$ solvent used in this

reaction should be completely free from EtOH traces; otherwise isolation of the crystalline **2** becomes difficult due to the reaction between **1** and EtOH.[13] ^{1}H NMR (CH_2Cl_2): δ 1.93 (s) (15H, Cp*); δ 1.88 (s) (15H, Cp* minor amounts of **1** in equilibrium with **2**); δ 4.23 (broad) (2H, HO-CHH_a-CHH_a-OH); δ 3.35 (broad) (2H, HO-CH_bH-CH_bH-OH); δ 11.13 (2H, 2OH) ; ^{13}C NMR (CH_2Cl_2): δ 119.8 (q, $OSO_2\underline{C}F_3$, $J_{C\text{-}F}$ = 318.4 Hz); δ 113.9 ($\underline{C}_5Me_5$); δ 67.8 (HO-$\underline{C}H_2$-$\underline{C}H_2$-OH), δ 9.6 ($C_5\underline{Me}_5$) ; ^{19}F{^{1}H} NMR (CH_2Cl_2): δ -78.6; IR (nujol) ν_{NO} 1820 cm^{-1} (vs); mp 131°C; Anal. Calcd for $C_{14}H_{21}NO_9RuS_2F_6$ (626): C, 26.80; H, 3.40; N, 2.20; Found: C, 26.82; H, 3.43; N, 2.18.

Reaction of 1 with i-PrOH. *I*-PrOH (10 mL) was added via syringe to a Schlenk flask charged with 100 mg (0.177 mmol) of solid **1** and a stir-bar. A red precipitate formed after 5 min of stirring. The solution was filtered through a frit under N_2 and the solid was washed with cold hexane and dried in vacuo, yielding 44 mg of $[Cp^*Ru(NO)]_2$ (0.082 mmol, 93 %). ^{1}H NMR (C_6D_6, CH_2Cl_2) and ^{13}C NMR (C_6D_6) spectra are identical to published data.[15]

K_{eq} Calculations for the OTf Substitution in 1 by ROH and OH-CH_2CH_2-OH. The K_{eq} determination for eq 1 and 2 from ^{19}F NMR spectra are performed according to the procedures described elsewhere.[12] Substitution reactions with alcohols were studied in the presence 1.7-2 equiv alcohols to avoid oxidation processes.

Kinetics Experiments. A CH_2Cl_2 solution of **1** was prepared in the glovebox using standard dilution techniques and a Fisher/Ainsworth (1 mg) balance. A Hamilton microliter syringe was used to add solutions at room temperature to 5-mm Pyrex NMR tubes, and the height of the solution in the tubes was checked for consistency. Usually each tube contained 500 μL of a 0.014 **M** solution of **1**. The solutions of alcohols in CH_2Cl_2 of the desired concentration was also prepared in the glove box and placed in separate vials. Prior to monitoring the reaction between **1** and alcohol, the NMR tube containing the solution of **1** in CH_2Cl_2 was placed in a Dewar with hexane-liquid N_2 slush for 2 min. The prechilled alcohol solution in CH_2Cl_2 (usually 150 μL) was added to the tube via syringe through a septum. The tube was shaken several times to achieve homogeneity of the solution and quickly placed in the NMR probe, maintained at the desired temperature. Spectra were recorded

using at least five T_1 periods between pulses to assure reliable quantitative results. The total integral over the signals of the starting **1** and alcohol coordinated complexes was used to deduce the amount of Ru(II) species present in solution. In all cases, integrals and peak-heights were referenced to an internal standard signal of C_6H_6 that was added to the CH_2Cl_2 used in the sample preparation. In each set of experiments, the acquisition parameters were left constant. The intervals between the acquisition of individual data sets single spectra were changed as needed. The reaction was followed at -47 °C for ca. two half-lives of **1**, at -41 °C for ca. two half-lives of **1**, at -36 °C for ca. three half-lives of **1**, at -31 °C for ca. three half-lives of **1**, at -25 °C for ca. four half-lives of **1**, at -19 °C for ca. five half-lives of **1**. In these experiments there was no deviation from the first-order dependence of the rate on [**1**]. In all reactions only starting material and $[Cp^*Ru(\mu\text{-}NO)]_2$ were observed at the end of the experiments. The presence of acetone was detected by its characteristic singlet at δ 2.14. The values of rate constants were reproducible with 10-15 % inaccuracy.

References

(1) Collman, J. P.; Hegedus, L. S.; Norton, J. R.; Finke, R. G. *Principles of Organotransition Metal Chemistry*; University Science Books: Mill Valley, CA, 1987; Chapter 1.

(2) Rouhi, A.M. *Chem. & Eng. News,* **1995**, *6*, 32.

(3) Diels-Alder reaction catalysis: (a) Hollis, T. K.; Robinson, N. P.; Bosnich, B. *Organometallics*, **1992**, *11*, 2645. (b) Hollis, T. K.; Robinson, N. P.; Bosnich, B. *J. Am. Chem. Soc.*, **1992**, *114*, 5464. (c) Bonnesen, P. V.; Puckett, C. L.; Honeychuck, R. V.; Hersh, W. H.; *J. Am. Chem. Soc.* **1989**, *111*, 6070. (d) Honeychuck, R. V.; Bonnesen, P.V.; Farahi, J.; Hersh, W. H.; *J. Org. Chem.* **1987**, *52*, 5293; Odenkirk, W.; Rheingold, A. L.; Bosnich, B. *J. Am. Chem. Soc.*, **1992**, *114*, 6392.

(4) (a) Agbossou, S. K.; Smith, W. W.; Gladysz, J. A. *Chem. Ber.*, **1990**, *123*, 1293. (b) Song, J. S.; Szalda, D. J.; Bullock, R. M.; Lawrie, C. J. C.; Rodkin, M. A.; Norton, J. R. *Angew. Chem., Int. Ed. Engl.* **1992**, *31,* 1233. (c) Zhang, N.; Mann, C.M.; Shapley,

P.A. *J. Am. Chem. Soc.* **1988**, *110*, 6591. (d) Trost, B.M.; Indolese, A.F.; Müller, T.J.J.; Treptow, B. *J. Am. Chem. Soc.*, **1995**, *117*, 615.

(5) (a) Dobson, A.; Robinson, S. D.; *Inorg. Chem.* 1977, *16*, 137. (b) Jung, C. W.; Garrou, P. E.; *Organometallics* **1982**, *1*, 658. (c) Che, C. M.; Tang, W. T.; Wong, W. T.; Lai, T. F.; *J. Am. Chem. Soc.* **1989**, *111*, 9048. (d) Muller, J. G.; Acquaye, J. H.; Takeuchi, K. J. *Inorg. Chem.* **1992**, *31*, 4552. (e) Smith, D. P.; Griffin, M. T.; Olmstead, M. M.; Maestre, M. F.; Fish, R.H. *Inorg. Chem.* **1993,** *32,* 4677. (f) Winter, C. H.; Sheridan, P. H.; Heeg, M. J.; *Inorg. Chem.* **1991**, *30*, 1962. (g) Appelt, A.; Ariaratnam, V.; Willis, A. C.; Wild, S. B. *Tetrahedron: Asymmetry* **1990**, *1*, 9.

(6) (a) Blum, O.; Milstein, D. *J. Am. Chem. Soc.*, **1995**, *117*, 4582. (b) Hoffman, D.M.; Lappas, D.; Wierda, D.A. *J. Am. Chem. Soc.*, **1989**, *111*, 1531.

(7) (a) Carey, F. A.; Sundberg, R. J. *Advanced Organic Chemistry;* Plenum Press: New York, 3rd Ed, 1993; Chapter 12 "Oxidations," pp. 627-628 and references therein. (b) Sharpless, K. B.; Michaelson, R. C. *J. Am. Chem. Soc.*, **1973**, *95*, 6136. (c) Gao, Y.; Hanson, R.M.; Klunder, J. M.; Ko, S. Y.; Masamune, H.; Sharpless, K. B. *J. Am. Chem. Soc.*, **1987**, *109*, 1987.

(8) Bryndza, H.E.; Calabrese, J.C.; Marsi, M.; Roe, D.C.; Tam, W.; Bercaw, J.E.; *J. Am. Chem. Soc.*, **1986**, *108*, 4805

(9) (a) Blum, J.; Sasson, Y.J.; *J. Chem. Soc. Chem. Commun.*, **1974**, 300. (b) Bullock, R. M.; Song, J.-S. *J. Am. Chem. Soc.*, **1994**, *116*, 8602. (c) Milstein, D.; *J. Am. Chem. Soc.*, **1986**, *108*, 3525

(10) (a) Ikaria, T.; Yamamoto, A. *J. Organomet. Chem.* **1976**, *120*, 257. (b) Evans, J.; Schwart, J.; Urquhart, P.W. *J. Organomet. Chem.* **1974**, *81*, C37. (c) Yamamoto, T.; Yamamoto, A.; Ikeda, S. *Bull. Chem. Soc. Jpn.*, **1972**, *45*, 1104. (d) Reger, D.L.; Culbertston, E.C. *J. Am. Chem. Soc.*, **1976**, *98*, 2789. (e) Evitt, E.R.; Bergman, R.G. *J. Am. Chem. Soc.*, **1979**, *101*, 3973. (f) Bryndza, H.E.; Evitt, E.R.; Bergman, R.G. *J. Am.*

Chem. Soc., **1980**, *102*, 4948.

(11) Zoch, C.R., Dissertation, Utah State University, 1993.

(12) Svetlanova-Larsen, A.; Zoch, C.R; Hubbard, J.L., *J. Am. Chem. Soc.*, submitted.

(13) Perrin, D.D.; Armarego,W. L. F. *Purification of Laboratory Chemicals;* Pergamon Press: New York, 1988; p. 121.

(14) (a) Olovsson, I.; Jonsson, P. in *The Hydrogen Bond*; Schuster, P.; Zundel, G.; Sandorfy, C. Eds.; North-Holland: New York, 1976, Chapter 8. (b) Review of hydrogen bonding and its classification: Gilli, P.; Bertolasi, V.; Ferretti, V., Gilli, G. *J. Am. Chem. Soc.*, **1994**, *116*, 909.

(15) Hubbard, J.L.; Morneau, A.; Burns, R.M.; Zoch, R.Z. *J. Am. Chem. Soc.*, **1991**, *113*, 9176.

(16) Chang, J.; Bergman, R.G. *J. Am. Chem. Soc.*, **1987**, *109*, 4298.

(17) Pouchert, J.C.; Behnke, J. *The Aldrich Library of ^{13}C and ^{1}H FT NMR Spectra*, Aldrich, Inc.: New York, 1993; v. 1, p. 727-750.

(18) Moore J.W.; Pearson, R.G. *Kinetics and Mechanism*; John Wiley & Sons: New York, 3rd Ed., 1981; Chapter 2.

(19) Melander, L.; Saunders, W.H. *Reaction Rates of Isotopic Molecules*; John Wiley & Sons: New York, 1980; Chapters 5, 6.

(20) March, J. A *Advanced Organic Chemistry* Wiley-Interscience Publication, John Wiley & Sons: New York-Chichester-Brisbane-Toronto-Singapore, 1987; Sections 17-1, 10-33.

(21) Hubbard, J.L.; Burns R.M. *J. Am. Chem. Soc.*, **1994**, *116*, 9514.

(22) The π-donor stabilization of the coordinatively unsaturated metal centers: (a) Rothfuss, H.; Huffman, J. C.; Caulton, K. G. *J. Am. Chem. Soc.*, **1994**, *116*, 187. (b) Gusev, D. G.; Kulhman, R.; Rambo, J. R.; Berke, H.; Eisenstein, O.; Caulton, K. G. *J. Am. Chem. Soc.*, **1995**, *117*, 281. (c) Johnson, T. J.; Folting, K.; Streib, W. E.; Martin, J. D.; Huffman, J. C.; Jackson, S. A.; Eisenstein, O.; Caulton, K. G. *Inorg. Chem.* **1995**, *34*, 488. (d)

Caulton, K. G. *New J. Chem.* **1994**, *18*, 25.

(23) Kaesz, H.D.; Saillant, R.B. *Chem. Rev.* **1972**, *72*, 231.

(24) Bryndza, H.E.; Tam, W. *Chem. Rev.* **1988**, *88*, 1163.

(25) Gordon, A.S.; Ford, R.A. *The Chemists Companion*; John Wiley & Sons: New York, 1972; 288.

(26) Van Geet, A. L. *Anal. Chem* **1970**, *42*, 679.

CHAPTER 5

ALKYL HALIDE, METAL HALIDE, AND METAL(HALOMETHYL) COMPLEX LIGATION TO THE $[Cp^*Ru(NO)(CH_3)]^+$ FRAGMENT

Abstract

Treatment of a CH_2Cl_2 solution of $Cp^*Ru(NO)(CH_3)_2$ with $[H(OEt_2)_2][BAr4']$ at low temperature results in formation of a reactive CH_2Cl_2 bound complex salt $[Cp^*Ru(NO)(CH_3)(ClCH_2Cl)][BAr_4']$ (**1**) as observed by ^{13}C NMR spectroscopy ($[BAr_4'] = [[(3,5\text{-}(CF_3)_2C_6H_3)_4B]$). Treatment of a $CDCl_3$ solution of the complex salt $[Cp^*Ru(NO)(CH_3)(THF)][BAr_4']$ (**2**) with 1 equiv of RI leads to the formation of complex salts $[Cp^*Ru(NO)(CH_3)(IR)][BAr_4']$ **3-6**, characterized by spectroscopic methods in solution (R = CH_3, **3**; C_2H_5, **4**; CH_2I, **5**; $CH_2Cr(Cp)(NO)_2$, **6**). Complexes **3-6**$^+$ quickly decompose in $CDCl_3$ solutions with formation of the dinuclear complex salt $[Cp^*Ru(NO)(\mu\text{-}I)]_2$ $[2BAr_4']$ (**7**). X-ray structural data for *cis*-complex salt **7** (173 K), ($[C_{43}H_{28}NOBF_{24}ICl_3Ru]$): triclinic space group $P\bar{1}$, a = 13.021 (2) Å, b = 13.091 (2) Å, c = 16.409 (2) Å, α = 88.37 (2) °, β = 82.68 (2)°, γ = 66.34 (2)°, Z = 2, R/R_w = 0.0535/0.0591. Treatment of complex **2** with 1 equiv $CpCr(NO)_2I$ results in formation and precipitation of $[Cp^*Ru(NO)(CH_3)(\mu\text{-}I)Cr(Cp)(NO)_2][BAr_4']$ (**8**). X-ray structural data for **8** (173 K), ($C_{48}H_{35}N_3O_3IBCrRuF_{24}$): monoclinic space group $P2_1/n$, a = 12.560 (5) Å, b = 27.75 (1) Å, c = 16.80 (1) Å, β = 109.90 (4)°, Z = 2, R/wR2(on F^2) = 0.1247/2834. Molecular structure and spectroscopic properties of heteronuclear Ru-Cr complex salt **8**, containing direct M-I-M' link, allow for evaluation of the comparative strength of $[CpCr(NO)_2]^+$ and $[Cp^*Ru(NO)(CH_3)]^+$ as Lewis acids competing for the bridging iodine atom.

Introduction

The oxidative addition of an alkyl halide to a coordinatively unsaturated metal complex is a key step in a variety of important catalytic and stoichiometric processes.[1] Although several mechanisms have been documented, prior alkyl halide coordination step is possible in nearly all cases.[1]

Thus, characterization of new complexes containing a direct M-XR linkage should improve our mechanistic understanding of these reactions. Another important aspect of these complexes is that they are expected to offer a rich coordination chemistry, since halocarbons have ligand strengths far weaker than other main group alkyls such as amines, phosphines, ethers, and sulfides.[2] Because they possess weakly solvated coordination sites, halocarbon complexes may have very high catalytic activity.

Stable alkyl halide complexes have become recently available due to the work of several groups.[2-10] A very recent report describes a new iridium(III) CH_2Cl_2-coordinated complex with a BAr_4' counterion that carries out exceptionally selective C-H activation under very mild conditions.[10] The optically resolved organometallic Lewis acid $[CpRe(NO)(PPh_3)(ClCH_2Cl]^+$ exhibits an extraordinary selectivity for the binding of one enantiomer of rhenium halide complexes $[CpRe(NO)(PPh_3)(I)$.[4] Gladysz et al. have also shown that alkyl halide ligands in rhenium complexes are dramatically activated toward nucleophilic attack.[5]

We set out to generate and characterize alkyl halide complexes utilizing the Lewis acidity of the cationic fragment generated by the dissociation of THF from the complex salt $[Cp^*Ru(NO)(CH_3)(THF)][BAr_4']$ ($[BAr_4'] = [[(3,5\text{-}(CF_3)_2C_6H_3)_4B]$).[6] Herein we report the synthesis, reactivity, and structural studies of a number of complexes containing a direct Ru-XR linkage, where R is alkyl, metalloalkyl, or another metal center.

Results

Generation of $[Cp^*Ru(NO)(CH_3)(ClCH_2Cl)][BAr_4']$ (1). Mixing of equimolar amounts of $Cp^*Ru(NO)(CH_3)_2$ and $[H(OEt_2)_2][BAr_4']$ in CH_2Cl_2 at -80 °C results in immediate CH_4 evolution. The ^{13}C NMR spectra immediately recorded at -80 °C show the formation of a new complex $[Cp^*Ru(NO)(CH_3)(ClCH_2Cl)][BAr_4']$ (**1**) as demonstrated by a signal from the coordinated $ClCH_2Cl$ ligand at δ 72.4 (Fig. 5-1). The ^{13}C NMR spectra with gated decoupling of protons show the CH_2-group as a triplet at δ 72.4 (J_{CH} = 171 Hz). Further characterization of complex **1** is not possible due to decomposition in solution to a mixture of unidentified products upon warming. The ^1H NMR

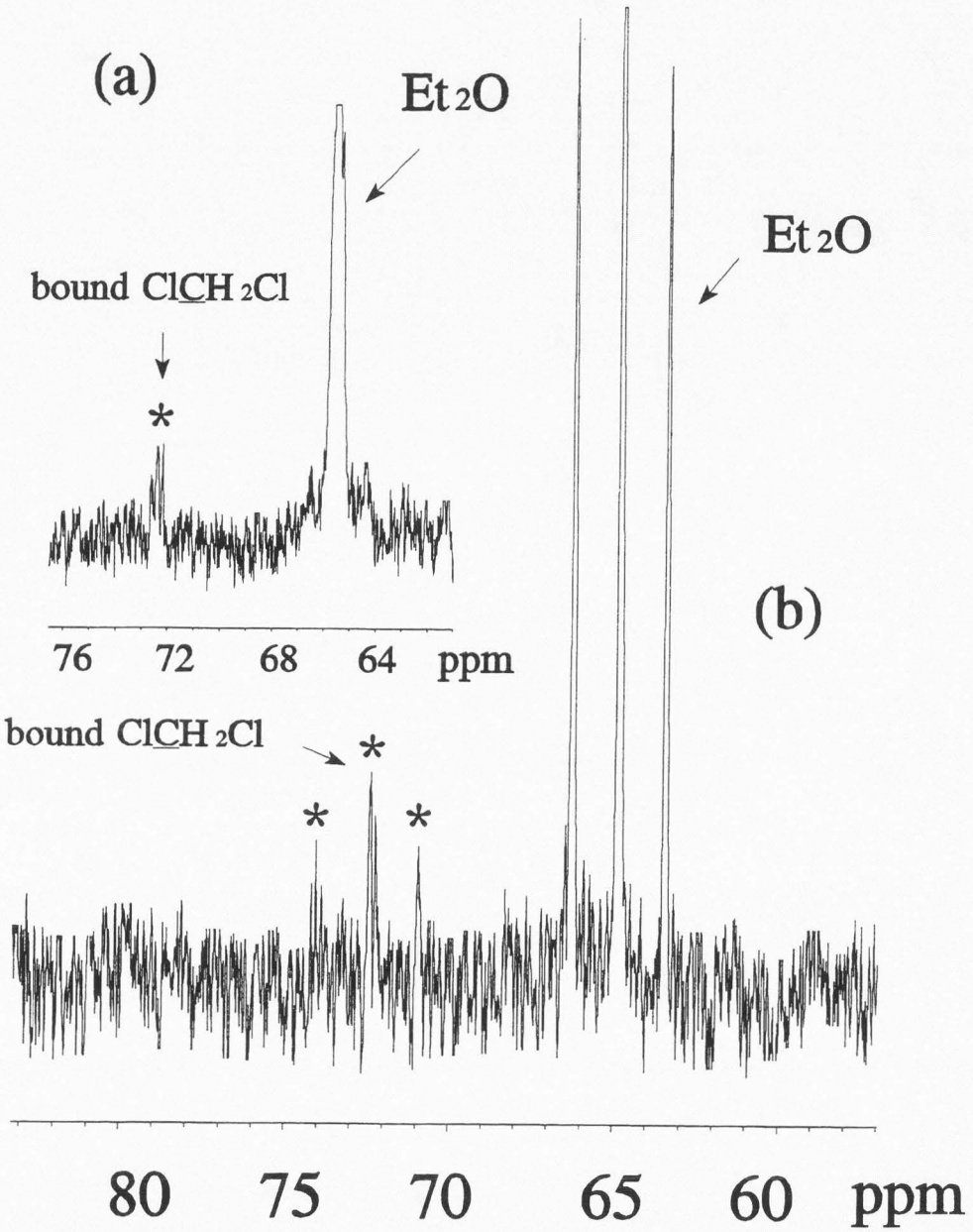

Figure 5-1. Proton decoupled (a) and proton coupled (b) ^{13}C NMR spectrum of CH_2Cl_2 solution of complex **8** at -85 °C. Signals of the bound $ClCH_2Cl$ are marked with stars.

spectrum of this mixture is not informative due to the domination of the Et_2O resonances in the region of interest.

Generation and Spectroscopic Characterization of Complexes [Cp*Ru(NO)(CH_3)(IR)][BAr_4'] (3-6). As monitored by ^1H NMR spectroscopy the treatment of [Cp*Ru(NO)(CH_3)(THF)][BAr_4'] (**2**)[6,7] with 1 equiv of RI in $CDCl_3$ at ambient temperature results in the immediate change of color of the solution from brown to orange and quantitative formation of the complex salts [Cp*Ru(NO)(CH_3)(IR)][BAr_4'] (**3-6**) as monitored by ^1H NMR (R = CH_3, **3**; C_2H_5, **4**; CH_2I, **5**; $CH_2Cr(Cp)(NO)_2$, **6**; see Scheme 5-1). The ^1H NMR spectra of **3-6** show the appearance of the new Cp* and CH_3 signals (Table 5-1). For **4-6**, an AB pattern for the resonances of diastereotopic methylene protons of the coordinated RI ligands appears. The new species $\mathbf{3}^+$-$\mathbf{6}^+$ persist in $CDCl_3$ solutions for several days at -40 °C, but decompose within 2-3 h at room temperature (*vide infra*).

Isolation and Characterization of the Dinuclear Complex [Cp*Ru(NO)(μ-I)]$_2$2BAr_4'(7). Attempts to isolate complex salts **3-6** as solids result in decomposition in $CDCl_3$ solutions to [Cp*Ru(NO)(μ-I)]$_2$[2BAr_4'] (**7**) as a dark crystalline residue within 2-3 h. Analysis of the ^1H NMR spectrum of the $CDCl_3$ solution where decomposition of complex salt **4** occurred shows the presence of CH_4 (singlet at δ 0.19), EtOH (triplet at δ 1.22 and quartet at δ 3.69 in 3:2 integral ratio), and Et_2O (triplet at δ 1.18 and quartet at δ 3.45 in 3:2 integral ratio). Analysis of the ^1H NMR spectrum of the $CDCl_3$ solution where decomposition of complex salt **3** occurred also shows the presence of CH_4 (singlet at δ 0.19) and a small amount of MeOH (resonance at δ 3.47). Complex salt **7** exhibits a ν_{NO} at 1833 cm^{-1} in the IR spectrum. The ^1H NMR spectrum of CD_2Cl_2 solution of analytically pure **7** shows a major Cp* resonance at δ 2.14 and a minor Cp* resonance at δ 2.11 (ca. 100:5 integral ratio).

X-ray quality crystals of **7** are isolated by slow evaporation of a $CDCl_3$ solution formed upon addition of 1 equiv EtI to complex salt **2** at room temperature. X-ray structural data for **7** at 173 K are presented in Tables 5-2 and 5-3. The thermal ellipsoid plot is shown in Fig. 5-2. The structure is

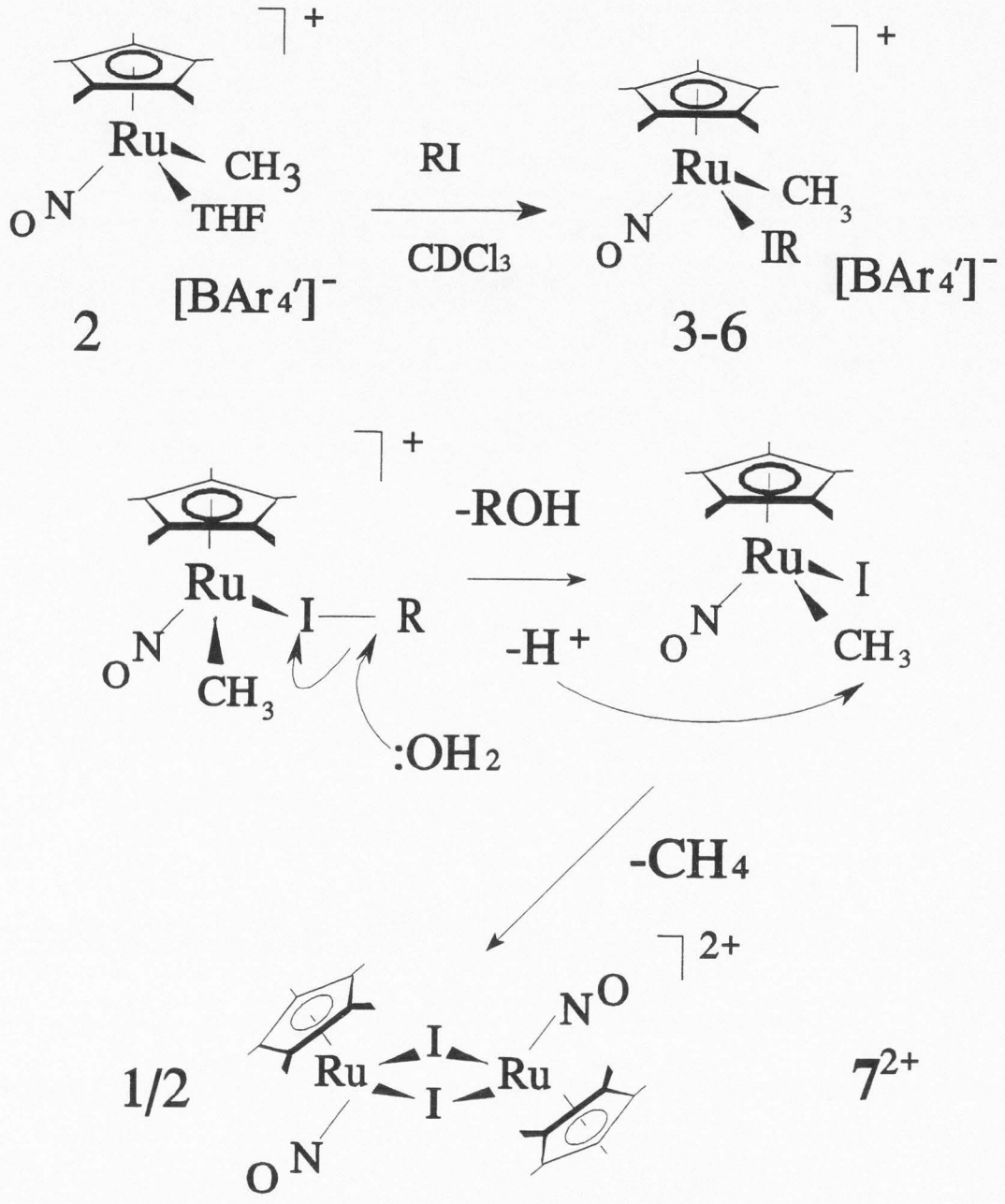

R = CH_3, (3); CH_2CH_3, (4); CH_2I, (5); $CH_2Cr(NO)_2Cp$, (6).

Scheme 5-1

Table 5-1. ^{1}H NMR spectroscopic characterization of bridging iodine complexes 3^+-6^+, 8^+.

Compound Formula	Signals in ^{1}H NMR spectrum in $CDCl_3$
3^+ 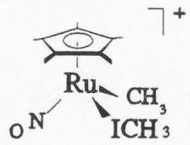	δ 2.39 (s, ICH₃); δ 1.83 (s, Cp*); δ 1.20 (s,CH₃)
4^+ 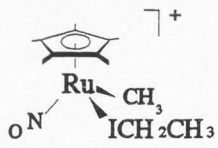	δ 3.54 (q, J=7.2 Hz, ICHH'); δ 3.46 (q, J=7.5 Hz, ICHH'); δ 1.83 (s, Cp*); δ 1.66 (t, J=7.2 Hz, CH₂CH₃); δ 1.23 (s, CH₃).
5^+ 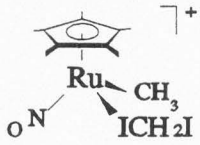	δ 4.23 (d, J=6.3 Hz, ICHH'); δ 4.09 (d, J=6.3 Hz, ICHH'); δ 1.87 (s, Cp*); δ 1.23 (s, CH₃).
6^+ 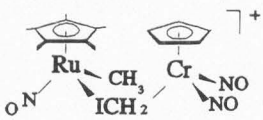	δ 5.70 (s, Cp); δ 3.44 (d, J=6.6 Hz, ICHH'); δ 3.32 (d, J=6.6 Hz, ICHH'); δ 1.84 (s, Cp*); δ 1.20 (s, CH₃).
8^+ 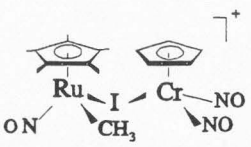	δ 5.73 (s, Cp); δ 1.83 (s, Cp*); δ 1.34 (s,CH₃)

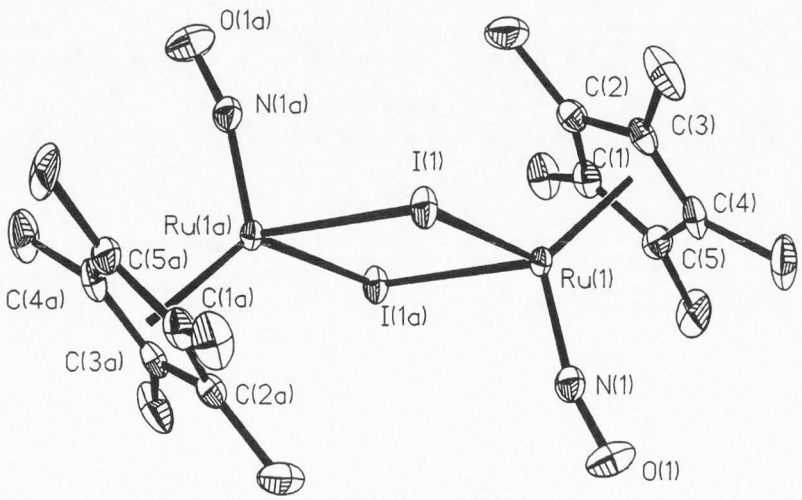

Figure 5-2. Thermal ellipsoid plot for complex 7^{2+}.

Table 5-2. Selected geometric parameters for complex 7^{2+}.

Bond lengths (Å)		Bond angles (°)	
I(1)-Ru(1)	2.699 (1)	Ru(1)-I(1)-Ru(1A)	97.6(1)
I(1)-Ru(1A)	2.702 (1)	I(1)-Ru(1)-N(1)	100.2(2)
Ru(1)-I(1A)	2.702 (1)	I(1)-Ru(1)-I(1A)	82.4(1)
N(1)-O(1)	1.155 (10)	N(1)-Ru(1)-I(1A)	101.3(3)
Ru(1)-Ru(1a)	4.062	Ru(1)-N(1)-O(1)	164.3(8)
I(1)-I(1a)	3.562		
Ru--Cp^*_{cent}	1.868		

Table 5-3. Summary of crystallographic data for complexes **7** and **8**.

Formula	$C_{43}H_{28}NOBF_{24}ICl_3Ru$, **7**	$C_{48}H_{35}N_3O_3BF_{24}ICrRu$, **8**
Formula Wt, amu	1375.8	1448.54
Crystal system	Triclinic	Monoclinic
Space group	$P\bar{1}$	$P2_1/n$
a (Å)	13.021 (2)	12.560 (5)
b (Å)	13.091 (2)	27.75 (1)
c (Å)	16.409 (2)	16.80 (1)
α (°)	88.37 (2)	90
β (°)	82.68 (2)	109.90 (4)
γ (°)	66.34 (2)	90
V (Å^3)	2540.2 (7)	5506.3 (7)
Z	2	2
T,K	173	173
μ (Mo Kα) (mm^{-1})	1.20	1.16
ρ_{calc} (g/cm^3)	1.799	1.747
final R, R_w	0.0535[a] 0.0591[b]	0.1247[a] 0.2834[c]

[a] $R = \Sigma \mid \mid Fo \mid - \mid F_c \mid \mid \; / \; \Sigma \mid F_o \mid$ [b] $R_w = [\Sigma w(\mid F_o \mid - \mid F_c \mid)^2 / \Sigma w \mid F_o \mid ^2]^{1/2}$; $w = 1/\sigma^2(\mid F_o \mid)$

[c] $wR2 = \mid \Sigma[w(F_o^2-F_c^2)]^2]/\Sigma[w(F_o^2)^2]]^{1/2}$

a *trans*-symmetric dimer containing a Ru(μ-I)$_2$Ru core with a Ru(1)-Ru(1a) distance of 4.06 Å, a Ru-I distance of 2.70 Å, and I-I(a) distance of 3.56 Å. The inversion center in the molecule makes each half of the molecule structurally identical. The value of ∠ Ru-N-O angle is 164.3°. The [Ru_2I_2] core is perfectly planar. The distance between Ru atom and the centroid of the Cp* ring is 1.87 Å. The angle between Ru-N bond and the plane of the [Ru_2I_2] core is 104.4°. There are no interactions closer than 7.5 Å observed between cationic complex 7^{2+} and the [BAr_4'] counterion.

Synthesis and Characterization of Heterobimetallic Complex [Cp*Ru(NO)(CH_3)(μ-I)Cr(Cp)($CO)_2$][BAr_4'] (8). Addition of 1 equiv $CpCr(NO)_2I$ to a $CDCl_3$ solution of complex salt **2** results in quantitative formation of Cp*Ru(NO)(CH_3)(μ-I)Cr(Cp)($CO)_2$][BAr_4'] (**8**) as monitored by ^{1}H NMR spectroscopy. The ^{1}H NMR spectrum in $CDCl_3$ shows appearance of the new signals of Cp (δ 5.73), Cp* (δ 1.83) and CH_3 (δ 1.34) protons. IR spectrum of **8** in CH_2Cl_2 displays three ν_{NO} signals at 1833 cm^{-1} (Cr-NO_{sym}), 1784 cm^{-1} (Ru-NO) and 1733 cm^{-1} (Cr-$NO_{antisym}$).

Dark brown crystals of **8** for X-ray analysis grow from CH_2Cl_2/toluene mixtures at -40°C. After numerous attempts, the data set was collected at 173 K. X-ray parameters for $\mathbf{8}^+$ are summarized in Tables 5-3 and 5-4. The structure of complex $\mathbf{8}^+$ is shown in Fig. 5-3. The iodine atom bridges the Ru and Cr atoms with Ru-I and Cr-I distances of ca. 2.73 Å and 2.65 Å, respectively. The Ru-N-O angle is 172° and the two Cr-N-O angles are 172° and 176°. The distance between the ruthenium atom and the Cp* centroid is 1.92 Å. The chromium atom is located 1.84 Å from the Cp centroid. The distance between Cr and Ru atoms is 4.24 Å and the Ru-I-Cr bond angle is 108°. The [Cp^*_{cent}-Ru--Cr-Cp_{cent}] torsion angle is 68° and the I-Ru-N bond angle is 103°.

Reactivity of 8 with [Ph_3PNPPh_3]Cl. Addition of 10-fold excess of [Ph_3PNPPh_3]Cl to a $CDCl_3$ solution of **8** results in the appearance of new signals at δ 5.71, δ 1.76, and δ 1.90, that are attributed to $CpCr(NO)_2Cl$, Cp*Ru(NO)(CH_3)Cl, and Cp*Ru(NO)(CH_3)I, respectively. The IR spectrum of this mixture shows overlapped ν_{NO} absorbances for $CpCr(NO)_2Cl$, Cp*Ru(NO)(CH_3)Cl, and Cp*Ru(NO)(CH_3)I.[8]

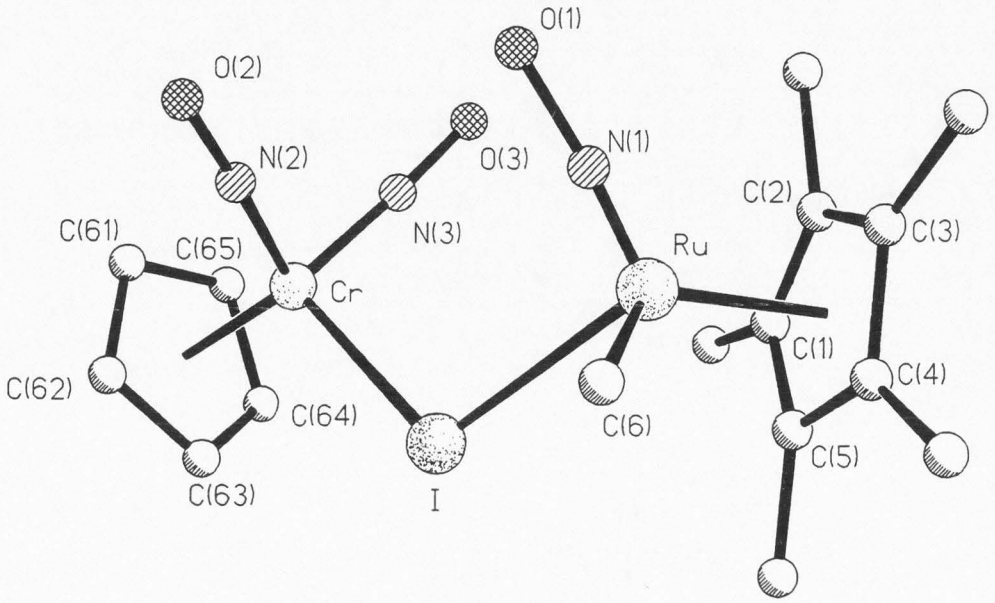

Figure 5-3. X-ray structure of the cation $\mathbf{8}^{+}$.

Table 5-4. Selected geometric parameters for the cation $\mathbf{8}^{+}$.

Bond lengths (Å)		Bond angles (°)	
I-Ru	2.727 (6)	Ru-I-Cr	107.6 (2)
I-Cr	2.652 (7)	I(1)-Ru(1)-N(1)	100.2(2)
Ru(1)-I(1A)	2.702 (1)	Ru-N(1)-O(1)	172.3 (4)
N(1)-O(1)	1.155 (10)		
Ru--Cr	4.342	$Cp^*_{cent}Ru$--Cr-Cp_{cent}(tors)	67.6
Ru--Cp^*_{cent}	1.923		
Cr--Cp_{cent}	1.842		

Discussion

Generation of CH_2Cl_2-Coordinated Complex 1. Deprotonation of $Cp^*Ru(NO)(CH_3)_2$ with $[H(OEt_2)_2][BAr_4']$ results in the generation of the CH_2Cl_2 coordinated complex salt **1** as monitored by ^{13}C NMR spectroscopy. The chemical shift of the resonance exhibited by the coordinated CH_2Cl_2 ligand of complex $\mathbf{1}^+$ at δ 76.2 is very similar to that found for the reactive intermediate $[CpRe(NO)(PPh_3)(ClCH_2Cl)]^+$ (δ 72.4) observed in ^{13}C NMR spectrum at -85 °C.[9] The $^1J_{CH}$ value observed in the proton coupled ^{13}C spectrum of species **1** is 171 Hz, which is also comparable to the J_{CH} value of 186 Hz, observed for the rhenium system.[9] Free Et_2O is still present in the solution after the reaction is complete, i.e., species **1** is not an ether-coordinated complex (Fig. 5-1). Thus, the proposed formulation for species **1** is $[Cp^*Ru(NO)(CH_3)(ClCH_2Cl)][BAr_4']$. Related iridium complex $[Cp^*Ir(PMe_3)(CH_3)(ClCH_2Cl)][BAr_4']$ has been recently isolated and structurally characterized.[3d] Similar to complex salt **1**, the iridium complex is stable only at low temperatures. The iridium system is capable of facile C-H bond activation in functionalized substrates like Et_2O with the loss of methyl group and iridium hydride formation. Similar transformation may be responsible for the observed decomposition of **1** in solution upon warming, especially since Et_2O is initially present in the reaction mixture. Ruthenium hydride species are expected to be very reactive and hence short lived. However, these issues, including C-H bond activation reactivity of species **1** with other substrates, must be resolved by further experimentation.

Alkyl Iodide Binding and Activation by the $[Cp^*Ru(NO)(CH_3]^+$ Fragment in Complexes 3-6. The results establish that a range of alkyl iodides readily form adducts with the Lewis acid $[Cp^*Ru(NO)(CH_3)]^+$. The formation of alkyl iodide complex salts **3-6** generated in quantitative spectroscopic yield in the presence of only 1 equiv of RI in CH_2Cl_2 in solution shows that RI are stronger bases than THF in complex $\mathbf{2}^+$. Complexes $\mathbf{3}^+$-$\mathbf{6}^+$ are less stable than the analogous complexes $[Cp^*Re(NO)(PPh_3)(IR)][BF_4]$ that were isolated as analytically pure powders.[5] The decreased stability of complexes $\mathbf{3}^+$-$\mathbf{6}^+$ can be explained by the presence of a methyl ligand, which is

more susceptible to various chemical transformations at the metal center than a phosphine ligand. The loss of the methyl ligand leads to the formation of dimeric complex 7^{+2} (Scheme 5-1), while the decomposition of rhenium alkyl-iodide complexes lead to the dinuclear μ-iodo complex $[[Cp^*Re(NO)(PPh_3)]_2(\mu\text{-}I)][BF_4]$, where each metal center retains its phosphine ligand.[5]

Analysis of the ^1H NMR spectrum of the $CDCl_3$ solution where decomposition of complex salts **3** and **4** occurred shows the presence of CH_4 and MeOH (for **3**) and EtOH (for **4**). Based on this observation, it may be proposed that decomposition occurs with the assistance of water impurities in the solvent. Scheme 5-1 shows nucleophilic attack of the water molecule to the coordinated alkyl iodide ligand, leading to the cleavage of the C-I bond with displacement of iodine by hydroxyl group and release of an alcohol molecule. The CH_3 group is protonated to give CH_4, resulting in the generation of the coordinatively unsaturated fragment $[Cp^*Ru(NO)(I)]^+$. Coupling of the two $[Cp^*Ru(NO)(I)]^+$ fragments results in the formation of the dimeric complex 7^{2+}.

Structural Features of Complex Salt 7. The complex cation 7^{2+} possesses a *trans* configuration and the Ru-I-Ru angle (ca. 98°) is considerably smaller than the [Ru-I-Cr] bond angle in complex 8^+ and the [M-I-M] angle in the related complexes $[CpFe(CO)_2]_2(\mu\text{-}I)^+$ and $[CpRe(PPh_3)(NO)](\mu\text{-})^+$.[5,10] In the cation $[Cp^*Ru(NO)(\mu\text{-}OH)]_2^{+2}$ the [Ru-O-Ru] angle is 103 ° with the Ru-Ru distance considerably smaller (ca. 3.24 Å) due to the shorter Ru-O bonds versus Ru-I bonds. Small amount of sterically hindered *cis*-isomer of complex **7** is present in equilibrium with *trans*-isomer, as shown by ^1H and ^{13}C NMR spectroscopy. Similar *cis-trans* isomerization equilibrium was observed for the closely related $[Cp^*Ru(NO)(\mu\text{-}Cl)]_2^{+2}$ complex.[6]

Competitive Lewis Acidity of Ruthenium and Chromium Metal Centers in Complex 8. The Ru-I-Cr linkage in complex 8^+ allows for the evaluation of the comparative Lewis acid strength of ruthenium and chromium centers. The ν_{NO} values in the IR spectrum of complex 8^+ show that chromium center gains cationic character compared to the starting $CpCr(NO)_2I$, since there is a definite shift of ν_{NO} values to the higher wave numbers (from 1815, 1691 cm^{-1} to 1833, 1733 cm^{-1},

Scheme 5-2).[8] The ruthenium center exhibits an opposite trend in the shift of the ν_{NO} value, compared to ν_{NO} value of starting complex **2** (1784 versus 1792 cm^{-1}), and hence the cationic character of the ruthenium center is decreasing.

Absence of $CpCr(NO)_2I$ in the product mixture after the reaction of complex $\mathbf{8}^+$ with excess $[Ph_3PNPPh_3]Cl$ suggests that the cleavage of the metal-iodine bond occurs preferably in Cr-I fragment (Scheme 5-3). This indicates that the iodine atom binds more strongly to ruthenium than to chromium. Thus, the conclusion may be drawn, that the $[Cp^*Ru(NO)(CH_3)]^+$ fragment is a stronger Lewis acid than the $[CpCr(NO)_2]^+$ fragment with regard to the binding of the bridging iodine atom. Scheme 5-3 shows two representations of the cationic part of complex **8** illustrating the stronger Ru-I binding.

The X-ray structure of complex $\mathbf{8}^+$ confirms the bridging position of iodine between two metal centers. The Ru-I bond legth is slightly longer than in the dimeric complex $\mathbf{7}^{+2}$. Both Cp and Cp* groups are situated below Cr-Ru-C(6) plane, while all three NO groups are pointing away from this plane. Fig. 5-4 shows the projection along Ru-Cr vector with Cp* and Cp ligands fixed in the slightly distorted gauche conformation (torsion angle Cp^*_{cent}-Ru--Cr-Cp_{cent} ca. 68°). The M-I-M angle in the analogous $[CpRe(PPh_3)(NO)]I[BF_4]$ is ca. 114°.[5] Apparently, the lower steric requirements on the ruthenium and chromium ligands results in the smaller Ru-I-Cr angle (ca. 108 Å). Comparable M-I-M angle of 111° is found in $[CpFe(CO)_2]_2I[BF_4]$.[10]

Experimental

General. Standard Schlenk techniques were employed in all syntheses. The nitrogen reaction atmosphere was purified by passing through scavengers for water (Aquasorb, Mallinckrodt) and oxygen (Catalyst R3-11, Chemical Dynamics, So. Plainfield, NJ). Organic solvents were distilled under nitrogen over appropriate drying agents prior to use. All chemical reagents were used as received from Aldrich unless stated otherwise. Infrared spectra were recorded on a Mattson Polaris-Icon FT-spectrometer. Melting points were measured with a Mel-Temp device (Laboratory Devices)

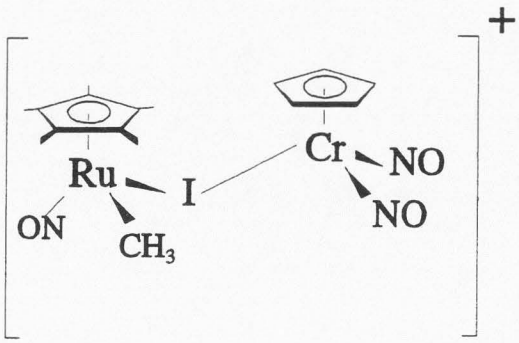

ν_{NO} (cm^{-1}): 1833 (Cr-NO_{sym}); 1784 (Ru-NO); 1733 (Cr-NO $_{antis}$)

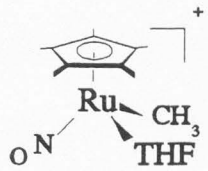

νNO

1792 cm^{-1}

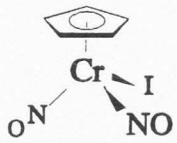

νNO

1815 cm^{-1}
1691 cm^{-1}

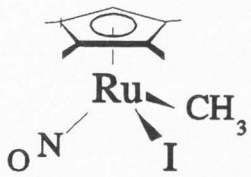

1735 cm^{-1}

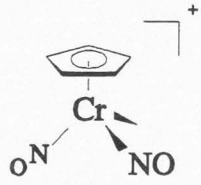

BF_4^-

1841 cm^{-1}
1741 cm^{-1}

Scheme 5-2.

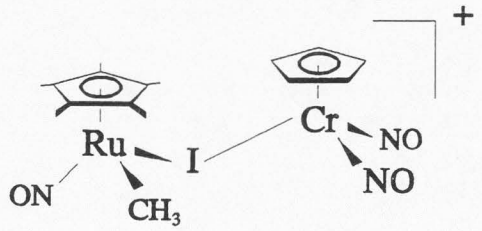

excess [PPN]Cl

$CpCr(NO)_2Cl$ +

$Cp^*Ru(NO)_2(CH_3)(I)$ +

$Cp^*Ru(NO)_2(CH_3)(Cl)$

no $CpCr(NO)_2I$ observed

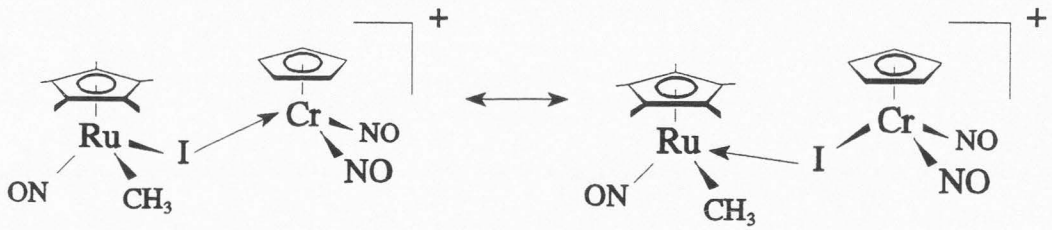

more favorable

Scheme 5-3.

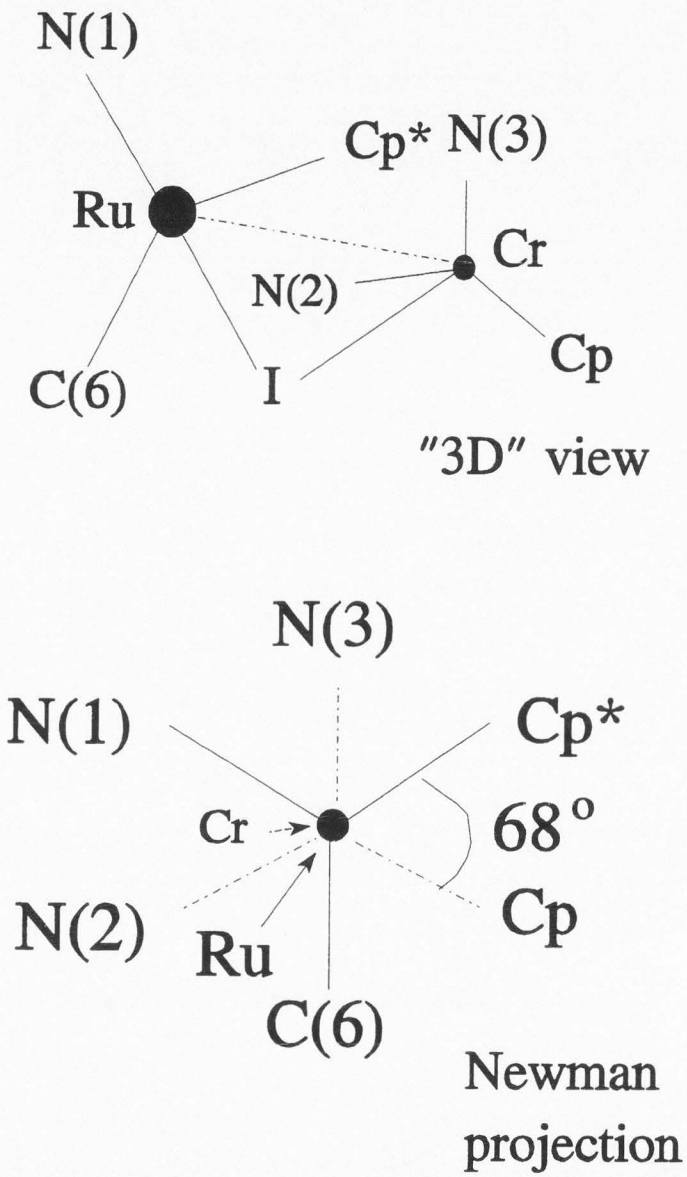

Figure 5-4. Schematic view down the Ru-Cr vector in complex 8^{+}.

in open capillaries and are uncorrected. Combustion analyses were performed by Atlantic Microlab, Inc., Norcross, GA.

The ^{1}H and ^{13}C NMR spectra were recorded on a Bruker ARX-400 NMR spectrometer operating at 400 MHz (^{1}H), 61.42 MHz (^{2}H), 100.62 Mhz (^{13}C), and 376.2 Mhz (^{19}F). The residual solvent peak of $CDCl_3$ was used as the internal NMR standard (^{1}H δ 7.24; ^{13}C δ 77.0 ppm), as well as the residual peak of HDO (^{1}H δ 4.70). Spectra were recorded at 298 K unless otherwise stated. ^{1}H NMR spectra in CH_2Cl_2 were measured using solvent presaturation techniques and were shimmed and referenced to the signals from $CDCl_3$ sealed inside a 1.5-mm capillary located concentrically inside the 5-mm NMR tube. When necessary, 5-mm NMR tubes with resealable Teflon valves were used (Brunfeld Co., Bartlesville, OK). The chemical shifts reported for the complexes in CH_2Cl_2 are identical to those in the analogous deuterated solvents.

Generation of Complex 1. A 5-mm NMR tube was charged with $Cp^*Ru(NO)(CH_3)_2$[11] (0.025 g, 0.089 mmol) and $HBAr_4'$ (0.064 g, 0.089 mmol). The tube was cooled to -78 °C, and CH_2Cl_2 (1.0 mL) was added by syringe through the septum. The tube was shaken and placed in a -80 °C NMR probe. ^{1}H and ^{13}C NMR spectra were recorded immediately (see text for data).

Reaction of $Cp^*Ru(NO)(CH_3)(THF)(BAr_4')$ with Alkyl Iodides. Generation of Complexes 3-6. Alkyl iodides CH_3I, CH_2I_2 and EtI were purified on the 1x3 cm column with Al_2O_3 prior to use. $CpCr(NO)_2(CH_2I)$ was synthesized according to published procedure.[7,8] One equiv of RI was added to a stirred solution of $[Cp^*Ru(NO(CH_3)(THF)][BAr_4']$ **2**[12] (0.050 g, 0.036 mmol) in CH_2Cl_2 (10 mL). The color change from brown to orange was observed within 5 min. The solvent was removed in vacuo. The oily residues were used to characterize complexes **3-6** spectroscopically. ^{1}H NMR for complexes **3-6** ($CDCl_3$): $[Cp^*Ru(NO)(CH_3)(ICH_3)][BAr_4']$ (**3**): δ 7.67 (b, 8H, BAr_4'); δ 7.51 (b, 4H, BAr_4'); δ 2.39 (s, 3H, ICH_3); δ 1.83 (s, 15H, Cp*); δ 1.20 (s, 3H, CH_3). $[Cp^*Ru(NO)(CH_3)(ICH_2H_3)][BAr_4']$ (**4**): δ 7.67 (b, 8H, BAr_4'); δ 7.51 (b, 4H, BAr_4'); δ 3.54 (q, J=7.2 Hz, IC<u>H</u>H'); δ 3.46 (q, J=7.5 Hz, ICH<u>H</u>'); δ 1.83 (s, 15H, Cp*); δ 1.66 (t, J=7.2 Hz, 3H,

$CH_2C\underline{H}_3$); δ 1.23 (s, 3H, CH_3). [Cp*Ru(NO)(CH_3)(ICH_2I)][BAr_4'] (**5**): δ 7.67 (b, 8H, BAr_4'); δ 7.51 (b, 4H, BAr_4'); δ 4.23 (d, J=6.3 Hz, IC$\underline{H}$H'); δ 4.09 (d, J=6.3 Hz, ICH$\underline{H}$'); δ 1.87 (s, 15H, Cp*); δ 1.20 (s, 3H, CH_3). [Cp*Ru(NO)(CH_3)(ICH_2)($Cr(NO)_2Cp$][BAr_4'] (**6**): δ 7.67 (b, 8H, BAr_4'); δ 7.51 (b, 4H, BAr_4'); δ 5.70 (s, 5H, Cp); δ 3.44 (d, J=6.6 Hz, IC$\underline{H}$H'); δ 3.32 (d, J=6.6 Hz, ICH$\underline{H}$'); δ 1.84 (s, 15H, Cp*); δ 1.20 (s, 3H, CH_3). IR (ν_{NO}, cm^{-1}, thin film): 1800 (identical for **2-4**).

Synthesis of [Cp*Ru(NO)(μ-I)]$_2$ [2BAr$_4$'] (7). EtI (3.5 μL, 0.040 mmol) was added to a stirred solution of Cp*Ru(NO)(CH_3)(THF)(BAr_4')[17] (0.050 g, 0.036 mmol) in $CHCl_3$ (10 mL). The color of the solution changed from brown to orange within 3 min. The stirring stopped and the solution was left on the air lightly capped for slow evaporation. Brown-orange crystals of **7** formed within 3 h at ambient temperature, were washed by hexanes, and were dried in vacuo (isolated yield 22 mg, 47%). X-ray quality crystals were grown by slow evaporation in $CDCl_3$. ^{1}H NMR (CD_2Cl_2): δ 7.67 (b, 8H, BAr_4'); δ 7.51 (b, 4H, BAr_4'); δ 2.14 (s) (15H, Cp*-trans, major isomer); δ 2.11 (s) (15H, Cp*-cis, minor isomer); IR (nujol) ν_{NO}: 1833 cm^{-1}; ^{13}C NMR ($CDCl_3$): δ 161.7 (q, J_{C-B}=50Hz, C_{ipso}), δ 135.30(s, C_{ortho}), δ 129.1 (q,J_{C-F}=32Hz, C_{meta}), δ 124.50 (q, J_{C-F}=275Hz, CF_3), δ117.4 (s, C_{para}), δ 108.1(s, $C_5(CH_3)_5$ skeletal C); δ 11.39 ($C_5\underline{Me}_5$-trans, minor); δ 11.29 ($C_5\underline{Me}_5$-cis, major). mp 195°C; Anal. Calcd for $C_{48}H_{35}N_3O_3IBCrRuF_{24}$ (1448): C, 40.15; H, 2.17 N, 1.11; Found: C, 40.40; H, 2.32; N, 1.01.

Synthesis of [Cp*Ru(NO)(CH_3)(μ-I)Cr(NO)$_2$Cp][BAr$_4$'] (8). Solid $CpCr(NO)_2I$[12,16] (0.026 g, 0.074 mmol) was added to a stirred solution of Cp*Ru(NO)(CH_3)(THF)(BAr_4') (0.077 g, 0.062 mmol) in CH_2Cl_2 (10 mL). Reaction was completed after 15 min stirring at ambient temperature. The volume of solution was reduced twice in vacuo, layered with toluene, and placed at -40 °C in a freezer. Dark brown single crystals of **8** formed after 24 h and were isolated by decantation and drying in vacuo (isolated yield 0.054 g, 61%). ^{1}H NMR ($CHCl_3$): δ 1.34 (s) (3H, CH_3); δ 1.83 (s) (15H, Cp*); δ 5.73 (s) (5H, Cp); IR (nujol) ν_{NO}(cm^{-1}): 1733 ($Cr(NO)_{antisym}$), 1783 (Ru(NO)), 1832 ($Cr(NO)_{sym}$); mp 107°C; Anal. Calcd for $C_{48}H_{35}N_3O_3IBCrRuF_{24}$ (1448): C, 39.80; H, 2.43; N, 2.90;

Found: C, 39.87; H, 2.48; N, 2.94.

X-ray Structural Analysis of Complexes 7 and 8. A suitable specimen were selected and centered vertically at 173 K on a Siemens P4 Autodiffractometer equipped with the LT-2a temperature controller preset at -100 °C in each case for complexes **7** and **8.** The computer centering of 25 random reflections revealed the triclinic lattice with a = 13.021 (2) Å, b = 13.091 (2) Å, c = 16.409 (2) Å; α = 88.37 (2) °, β = 97.85 (2)°, γ = 66.34 (2) °; V = 2540 (7) Å^3 for complex **7**; and monoclinic lattice with a = 12.560 (5) Å, b = 27.75 (1) Å, c = 16.80 (1) Å; β = 109.90 (4)°, V = 5506.3 (7) Å^3 for complex **8**. Data collection of $0 \leq h \leq 14$, $-13 \leq k \leq 14$, $-18 \leq l \leq 18$ for complex **7** showed a $P\bar{1}$-lattice. Data collection of $0 \leq h \leq 14$, $0 \leq k \leq 27$, $-19 \leq l \leq 18$ for complex **7** showed a $P2_1/n$-lattice. Structure solutions for complexes **7** and **8** were performed using direct methods. Subsequent refinement of the structures were carried out on an IBM-compatible 486 personal computer using the SHELXS-86[13] and SHELXL-93[14] programs from Sheldrick.[15] Difference maps led to the location of all the non-hydrogen atoms of two independent molecules in the asymmetric units of complexes **7** and **8**; all non-hydrogen atoms were positioned in a riding model with fixed C-H distances and isotropic thermal parameters. Convergence led to final R/R_w values of 0.0535/0.0591 with 8424 data ($F > 2\sigma F$) and 551 parameters for complex **7**; and R/wR_2 values of 0.1247/0.2834 with 6415 data ($F^2 > 2\sigma F^2$) and 459 parameters for complex **8**.

References

(1) Collman, J. P.; Hegedus, L. S.; Norton, J. R.; Finke, R. G. *Principles of Organotransition Metal Chemistry*; University Science Books: Mill Valley, CA, 1987; Part III, 306-310 and references therein.

(2) Colsman, M. R.; Noirot, M. D.; Miller, M. M.; Anderson, O. P.; Strauss, S. H. *J. Am. Chem. Soc.*, **1988**, *110*, 1988.

(3) (a) Crabtree, R. H.; Faller, J. W.; Mellea, M. F.; Quirk, J. M. *Organometallics*, **1982**, *1*, 1361-1366. (b) Burk, M. J.; Segmuller, B.; Crabtree, R. H. *Organometallics*, **1987**, *6*,

2241-2246. (c) Crabtree, R. H.; Mellea, M. F.; Quirk, J. M. *J. Am. Chem. Soc.*, **1984**, *106*, 2913. (d) Arndtsen, B. A.; Bergman, R. G. *Science*, **1995**, *270*, 1970.

(4) Winter, C. H.; Arif, A. M.; Gladysz, J. A. *Organometallics*, **1989**, *8*, 219-225.

(5) Winter, C. H.; Veal, W. R.; Garner, C. M.; Arif, A. M.; Gladysz, J. A. *J. Am. Chem. Soc.*, **1989**, *111*, 4767.

(6) Yi, G.-B. Dissertation, Utah State University, 1995.

(7) Hubbard, J. L.; McVicar, W. K. *Organometallics*, **1990**, *9*, 2683.

(8) (a) Legzdins, P.; Hoyano, J. K.; Malito, J. T. *Inorg. Synth.* **1978**, *18*, 126. (b) Regina, F.J.;

(9) (a) Fernandez, J. M.; Gladysz, J. A. *Organometallics*, **1989**, *8*, 207. (b) Winter, C. H.; Arif, A. M.; Gladysz, J.A. *J. Am. Chem. Soc.*, **1987**, *109*, 7560. (c) Fernandez, J. M.; Gladysz, J. A. *Inorg. Chem.* **1986**, *25*, 2674. (d) Winter, C. H.; Gladysz, J. A. *J. Organomet. Chem.* **1988**, *354*, C33-C36. (e) Czech, P. T.; Gladysz, J. A.; Fenske, R. F. *Organometallics*, **1989**, *8*, 1806-1810. (f) Peng, T. -P.; Winter, C. H.; Gladysz, J. A. *Inorg. Chem.* **1994**, *33*, 2534. (g) Stang, P. J.; Huang, Y.-H., Arif, A. M. *Organometallics*, **1992**, *11*, 231-237. (h) Fernandez, J. M.; Gladysz, J. A. *Inorg. Chem.* **1986**, *25*, 2674. (d) Winter, C. H.; Gladysz, J. A. *J. Organomet. Chem.* **1988**, *354*, C33-C36.

(10) Fe-I dimer: Cotton, F. A.; Frenz, B. A.; White, A. J. *J. Organomet. Chem.* **1973**, *60*, 147.

(11) Seidler, M. D.; Bergman, R. G. *J. Am. Chem. Soc.*, **1984**, *106*, 6110.

(12) (a) Svetlanova-Larsen, A.; Hubbard J. L; unpublished results.(b) Svetlanova-Larsen, A.; Zoch, C. R.; Hubbard, J. L. *Organometallics*, in press.

(13) Sheldrick, G. M. *Acta Cryst.* **1990** *A46*, 467-473.

(14) Sheldrick, G. M. *J. Appl. Crystallogr.*, in press; SHELXL-93 scattering factors from: *International Tables for X-ray Crystallography* Vol. C ; Ed. A. J. C. Wilson, Kluwer Academic Publishers: Dordrect, 1992; Tables 6.1.1.4 (pp. 500-502, neutral atom scattering factors), 4.2.6.8 (pp. 219-222, f′,f′′), and 4.2.4.2 (pp. 193-199, absorption coefficients)

(15) SHELXL-93 is available from: Siemens Analytical X-ray Instruments, 6300 Enterprise Lane, Madison, WI 53719 or directly from G. Sheldrick, Institüt für Anorganische Chemie,der Universität, Tammannstrasse 4, D-37077 Göttingen, Germany: gsheldr@shelx.uni-ac.gwdg.de

CHAPTER 6

CATALYTIC OXIDATION OF THF TO γ-BUTYROLACTONE. SYNTHESIS AND CHARACTERIZATION OF THE $[Cp^*Ru(NO)(CH_3)(\gamma\text{-BUTYROLACTONE})]^+[BAr_4']^-$

Abstract

The aerobic treatment of a THF solution of $Cp^*Ru(NO)(CH_3)_2$ with $[H(OEt_2)_2][BAr_4']$ results in CH_4 evolution and the formation of the complex salt $[Cp^*Ru(NO)(CH_3)(\gamma\text{-butyrolactone})]^+[BAr_F]^-$ (**2**) ($[BAr_4'] = [(3,5\text{-}(CF_3)_2C_6H_3)_4B]$). X-ray data for complex **2** (173 K), ($C_{48}H_{35}NO_3BF_{24}Ru{\cdot}CH_2Cl_2$): monoclinic space group $P2_1/c$, a = 13.957 (4) Å, b = 21.740 (6) Å, c = 17.819 (4) Å, β = 97.85 (2)°, Z = 4, R/wR2(on F^2) = 0.0806/0.1961. The purified complex salts **2** and $[Cp^*Ru(NO)(CH_3)(THF)][BAr_4]$ (**1**) are found to catalyze oxidation of THF to γ-butyrolactone, with ca. 25 turnovers/day under 25 psig of oxygen at 20°C and 0.03 mol-% catalyst loading. Studies with $^{18}O_2$ show O_2 to be the source of the γ-butyrolactone carbonyl oxygen. The presence of peroxo species in THF solution is detected and 1,6-diol-diformate [CH(O)-$(CH_2)_6$-CH(O)] is identified as a byproduct of the radical rearrangement of hydroperoxy-THF. A radical mechanism is proposed for the oxidation of THF via hydroperoxy intermediate, which decomposes to give γ-butyrolactone with the assistance of the ruthenium complex. An alternative mechanism for the catalytic oxidation proposes the formation of a transient ruthenium-dioxygen species.

Introduction

Transition metals are widely employed to catalyze the stereospecific transfer of oxo groups from dioxygen to organic substrates in biological and industrial processes.[1] In the context of organic substrate oxidation, the oxidation of ethers is relevant to biological systems and of great synthetic interest. Several instances of catalytically assisted conversion of primary ethers to esters (or lactones) have been reported in recent years.[2-6] Two reports describe catalytic oxidation with molecular oxygen mediated by CO_2 in the presence of rhodium and iron complexes.[2,3] The ruthenium complex

$RuCl_2((CH_3)_2SO)_4)$, as well as RuO_4, catalytically assists oxidation of furans by $NaIO_4$ and $LiClO_4$.[4] Efficient ether oxidation by atmospheric oxygen is achieved in the presence of catalytic amounts of cobalt(III) complexes.[4] O'Halloran et al. observed that the Mn(III) alkoxide-bridged dimer $Li_2[MnL]_2$ undergoes air-oxidation to yield the terminal-oxo complex $[Mn^{(V)}(O)L]^-$, which participates in stoichiometric oxo-transfer reactions with THF.[5] In spite of these reports, information leading to the mechanistic understanding of the catalytic oxidation of THF with molecular oxygen is rather limited. The search for selective catalysts for oxidation still receives considerable attention.[6-8] In this context, structural and reactivity studies of transition metal complexes are significant due to their relation to complexes with catalytic properties. Carboxylic and carbonic acid ester complexes of rhenium have been extensively studied by Gladysz.[9-11] The synthetic approach to such complexes involves generation of the rhenium Lewis acid $[Cp^*Re(NO)(PPh_3)]^+$ with subsequent coordination of the desired ligand to the metal center.[12] The present work utilizes a synthetic method, which combines the Lewis acidity of the $[Cp^*Ru(NO)(CH_3)]^+$ fragment with the ability of the ruthenium center to catalyze THF conversion to γ-butyrolactone in the presence of O_2. Some details of the mechanism of the catalytic oxidation reaction are revealed as a result of this study.

Results

Synthesis and Characterization of [Cp*Ru(NO)(CH3)(γ-butyrolactone)][BAr_4'] (2). Addition of 1.1 equiv $[H(OEt_2)][BAr_4']$ to a THF solution of $Cp^*Ru(NO)(CH_3)_2$ results in immediate CH_4 evolution and formation of $[Cp^*Ru(NO)(CH_3)(THF)][BAr_4']$ (**1**) ($[BAr_4'] = [(3,5\text{-}(CF_3)_2C_6H_3)_4B]$).[13] When this reaction is carried out in the presence of O_2, the subsequent oxidation of THF to γ-butyrolactone occurs and $[Cp^*Ru(NO)(CH_3)(gBL)][BAr_4']$ (**2**) is formed in quantitative yield (gBL = γ-butyrolactone). The complex salt **2** is identified by the appearance of new Cp* and CH_3 resonances at δ 1.65 and δ 1.17, respectively, in the ^1H NMR spectrum in $CDCl_3$. The resonances of the coordinated γ-butyrolactone ligand appear as multiplets at δ 4.64, δ 2.72, and δ 2.33. The carbonyl ^{13}C resonance is observed at δ 190.0 in the ^{13}C NMR spectrum in $CDCl_3$.

Complex **2** shows $\nu_{C=O}$ at 1688 cm^{-1} and ν_{NO} at 1796 cm^{-1} in the IR spectrum.

Red-brown X-ray quality crystals of **2** are grown from a CH_2Cl_2-hexane mixture (5:1) at -40 °C. Structural parameters for the cationic fragment $\mathbf{2}^+$ at 173 K are presented in Tables 6-1, 6-2 and the thermal ellipsoid plot is shown in Fig. 6-1. The cationic complex possesses a three-legged piano-stool geometry with γ-butyrolactone ring η^1-bound via the carbonyl oxygen to the ruthenium center with a Ru-O(2) distance of 2.109 (7) Å. The ∠ Ru-N-O value is 172.7 (13)°. There is a ca. 2:1 disorder of the NO and CH_3 ligands around the ruthenium center, but no disorder of the O(3) and C(17) atoms in the γ-butyrolactone ring. The O(3) atom of the lactone ring is found in a *cis* conformation to the ruthenium atom relatively to the C=O bond. The C(16)-C(17) and C(16)-O(3) bond distances are 1.238 (14) and 1.529 (19), respectively. An alternative refinement model, where O(3) and C(17) atoms positions are switched to place O(3) atom in the *trans* position to the ruthenium atom, unsatisfactorily describes the structure and results in oversized thermal ellipsoids for these atoms (see Fig. 6-2 and Discussion section).

Coordination Equilibrium of Complexes 1, 2, THF and gBL in Solution. Complex **2** is also formed upon addition of γ-butyrolactone to a $CDCl_3$ solution of **1**, as indicated by the appearance of characteristic for **2** resonances at δ 1.65 (Cp*) and 1.17 (CH_3). When 1.5 equiv of gBL is added to 0.0083 **M** $CDCl_3$ solution of **1,** an equilibrium is observed according to eq 1. The ratio of complex **1** to complex **2** is 1:5 determined from the integral ratio of the corresponding methyl resonances at δ 1.33 and 1.17.

$$K_{298} = 6.3(6) \qquad \text{(eq 1)}$$

$$Cp^*Ru(NO)(CH_3)(THF)^+ + gBL \rightleftarrows Cp^*Ru(NO)(CH_3)(gBL)^+ + THF$$

The resonances of the Cp* groups in complexes **1** and **2** are nearly coincident at δ 1.66-1.65. Diastereotopic signals of bound THF are observed as two symmetrical broad multiplets at δ 3.77 and 3.65.[13]

Table 6-1. Summary of crystallographic data for complex **2**.

Formula	$C_{48}H_{35}NO_3BF_{24}Ru{\cdot}CH_2Cl_2$
Formula Wt, amu	1315.6
Crystal system	Monoclinic
Space group	$P2_1/c$
a (Å)	13.957 (4)
b (Å)	21.740 (6)
c (Å)	17.819 (4)
α (°)	90
β (°)	97.85 (2)
γ (°)	90
V (Å^3)	5356 (2)
Z	4
T,K	173
μ (Mo Kα) (mm^{-1})	0.517
ρ_{calc} (g/cm^3)	1.628
final R, wR_2	0.0806[a] 0.1961[b]

[a] $R = \Sigma \mid \mid Fo \mid - \mid F_c \mid \mid \; / \Sigma \mid F_o \mid$ [b] $wR2 = \mid \Sigma[w(F_o^2-F_c^2)]^2]/\Sigma[w(F_o^2)^2]]^{1/2}$ $w = 1/\sigma^2(\mid F_o \mid^2)$

Table 6-2. Selected geometric parameters of complex **2** (see Figure 6-1).

Bond lengths (Å)		Bond angles (°)	
Ru-N(1)	1.769 (10)	N(1)-Ru-C(6)	98.4 (6)
Ru-C(6)	2.11 (2)	N(1)-Ru-O(2)	100.0 (5)
Ru-O(2)	2.102 (7)	O(2)-Ru-C(6)	84.4 (6)
N(1)-O(1)	1.169 (14)	Ru-N(1)-O(1)	172.7 (13)
O(2)-C(16)	1.224 (11)	Ru-O(2)-C(16)	130.8 (7)
C(16)-C(17)	1.48 (2)	O(2)-C(16)-C(17)	127.9 (11)
C(16)-O(3)	1.307 (13)	O(2)-C(16)-O(3)	119.1 (10)
C(19)-C(18)	1.46 (2)	C(17)-C(16)-O(3)	112.9 (10)
C(19)-O(3)	1.49 (2)	C(16)-C(17)-C(18)	100.8 (14)
		C(19)-C(18)-C(17)	107.1 (12)
		C(18)-C(19)-O(3)	102.4 (13)
		C(16)-O(3)-C(19)	109.6 (10)
		Torsion angles	
		N(1)-Ru-O(2)-C(16)	35.1
		O(3)-C(16)-O(2)-Ru	4.2
		C(17)-C(16)-O(2)-Ru	178.2

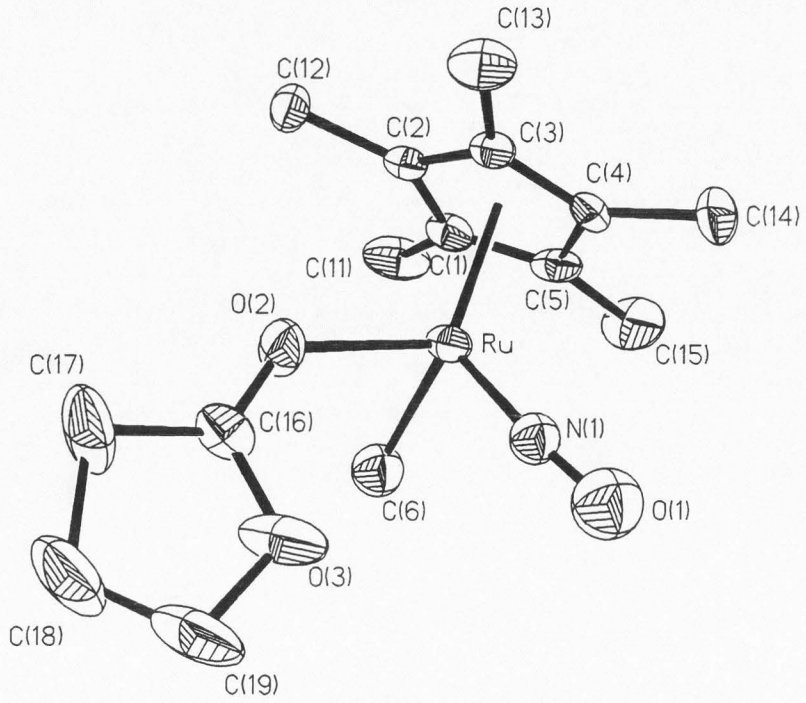

Figure 6-1. X-ray structure of complex $\mathbf{2}^{+}$. Thermal ellipsoid plot at 30% probability level.

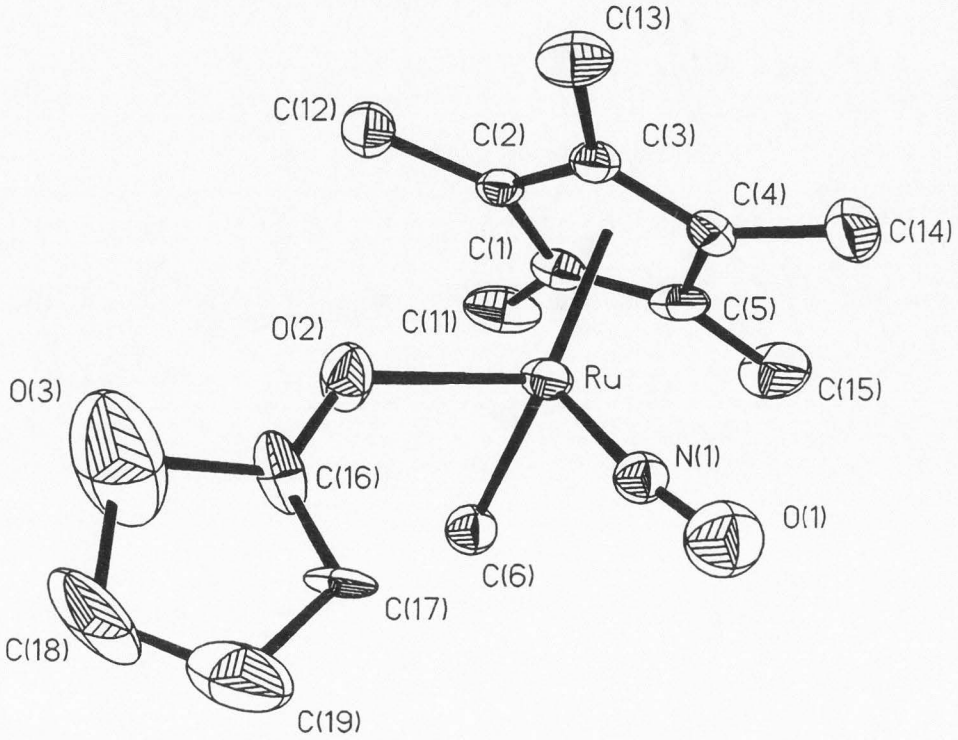

Figure 6-2. Incorrect X-ray model for complex 2^{+}. Thermal ellipsoid plot at 30% probability level.

Reaction of 1 with $[Ph_3PNPPh_3]Cl$. Addition of 20 equiv $[Ph_3PNPPh_3]Cl$ to a $CDCl_3$ solution of **2** results in immediate darkening of the solution. Formation of $Cp^*Ru(NO)(CH_3)Cl$ is observed by the appearance of a Cp* resonance at δ 1.77 and a CH_3 resonance at δ 1.34 in the ^1H NMR spectrum. The volatile part of the mixture transferred to another NMR tube on the vacuum line shows triplets at δ 4.34, δ 2.48 and a pentet at δ 2.25 in 2:2:2 integral ratio in the ^1H NMR spectrum. Comparison of the latter spectrum to that of an authentic γ-butyrolactone sample confirms liberation of γ-butyrolactone ligand from complex **2**.

Catalytic Oxidation of THF in the Presence of $Cp^*Ru(NO)(CH_3)(THF)][BAr_F]$ (2). As monitored by ^1H NMR spectroscopy, the treatment of a $7x10^{-5}$ **M** solution of **1** in THF with 1 atm of O_2 results in generation of γ-butyrolactone. After 48 h, generation of γ-butyrolactone ceases and neither complex **1** nor **2** is observed in the ^1H NMR spectrum. The molar ratio of the formed γ-butyrolactone versus the original amount of complex **2** is 10:1. When a similar experiment is carried out under 25 psig of O_2, the molar ratio of the formed γ-butyrolactone versus the original amount of complex **2** found after 24 h is 25:1, as measured by ^1H NMR spectroscopy. Reducing the concentration of **1** twice in the original solution results in the decrease of the production of gBL to 20 turnovers per molecule of **1**. Generation of gBL reaches only 10 turnovers after 48 h treatment with 25 psig O_2 in a 10:90 mixture of CH_2Cl_2:THF that is $7x10^{-5}$ **M**, respectively. The turnover numbers are 5 and 2 in the 20:80 and 25:75 mixtures of CH_2Cl_2:THF, which are $7x10^{-5}$ **M**. Generation of γ-butyrolactone cannot be detected during 48 h by ^1H NMR spectroscopy in a similar experiment when a 50:50 mixture of CH_2Cl_2:THF is used. No new species are observed by ^1H NMR spectroscopy over a 48-h period when a $7x10^{-5}$ **M** solution of **2** is stirred under N_2 atmosphere. Any organometallic products of the reaction that are left after the removal of the volatiles *in vacuo* are not tractable. They exhibit very broad unresolved resonances at δ 1.5-2.2 in the ^1H NMR spectrum and characteristc ν_{NO} signal is not found in the IR spectrum.

The formation of small amounts of 1,6-hexanediol-diformate always accompanies the formation of gBL (5-7 % of 1,6-hexandiol-diformate, as compared to the amount of produced γ-

butyrolactone, measured by ^{1}H NMR integration). The presence of 1,6-hexandiol-diformate is more evident in the IR spectrum of the volatile part of the reaction mixture after THF removal due to the strong $\nu_{C=O}$ absorbance at 1724 cm^{-1}. The identity of this by-product is confirmed by comparison of the IR and ^{1}H NMR spectra to those of the independently synthesized authentic sample of 1,6-diol-diformate, [CH(O)-$(CH_2)_6$-CH(O)].[14]

The addition of a colorless aqueous solution of ferrothiocyanate $Fe(SCN)_2$[15] to a 2.1x10^{-4} **M** solution of **1** in THF, pressurized with 25 psig O_2 for 24 h, results in the immediate generation of the dark red color of ferrithiocyanate $Fe(SCN)_3$. Addition of the same peroxide test reagent to the pure THF solvent or to a 2.1x10^{-4} **M** THF solution of **2** under 1 atm of N_2 does not result in a positive test for peroxides.

IR Studies with $^{18}O_2$. Treatment of a 2.1x10^{-4} **M** THF solution of **1** with 1 atm of $^{18}O_2$ for 72 h results in the generation of γ-butyrolactone as monitored by ^{1}H NMR spectroscopy. The volatile part of the mixture, transferred to another vessel on the vacuum line without inclusion of the organometallic products, exhibits 36 cm^{-1} shift to a lower frequency in the 1600-1800 cm^{-1} region of the IR spectrum, as compared to the IR spectrum of the volatiles obtained after an analogous experiment employing a $^{16}O_2$ atmosphere. Both IR spectra are shown in Fig. 6-3. The volatile part of the reaction mixture (stripped of THF) contains mostly gBL (ν_{CO} at 1774 cm^{-1}, solid line) and a by-product of the reaction, 1,6-hexandiol-diformate (ν_{CO} at 1724 cm^{-1}, solid line).

Attempts to test the catalytic ability of the related complex Cp*Ru(NO)OTf_2 in THF under 25 psig of O_2 result in generation of 2-3 equiv of γ-butyrolactone (per one molecule of complex) and precipitation of the orange crystals of the known complex salt [Cp*Ru(NO)(μ-OH)]$_2$[OTf]$_2$ (OTf = OSO_2CF_3).[15]

Discussion

Synthesis and Spectroscopic Properties of Complex 2. The work of Yi and Hubbard shows that the treatment of Cp*Ru(NO)$(CH_3)_2$ with [H(OEt_2)][BAr_4'] in THF results in formation of complex

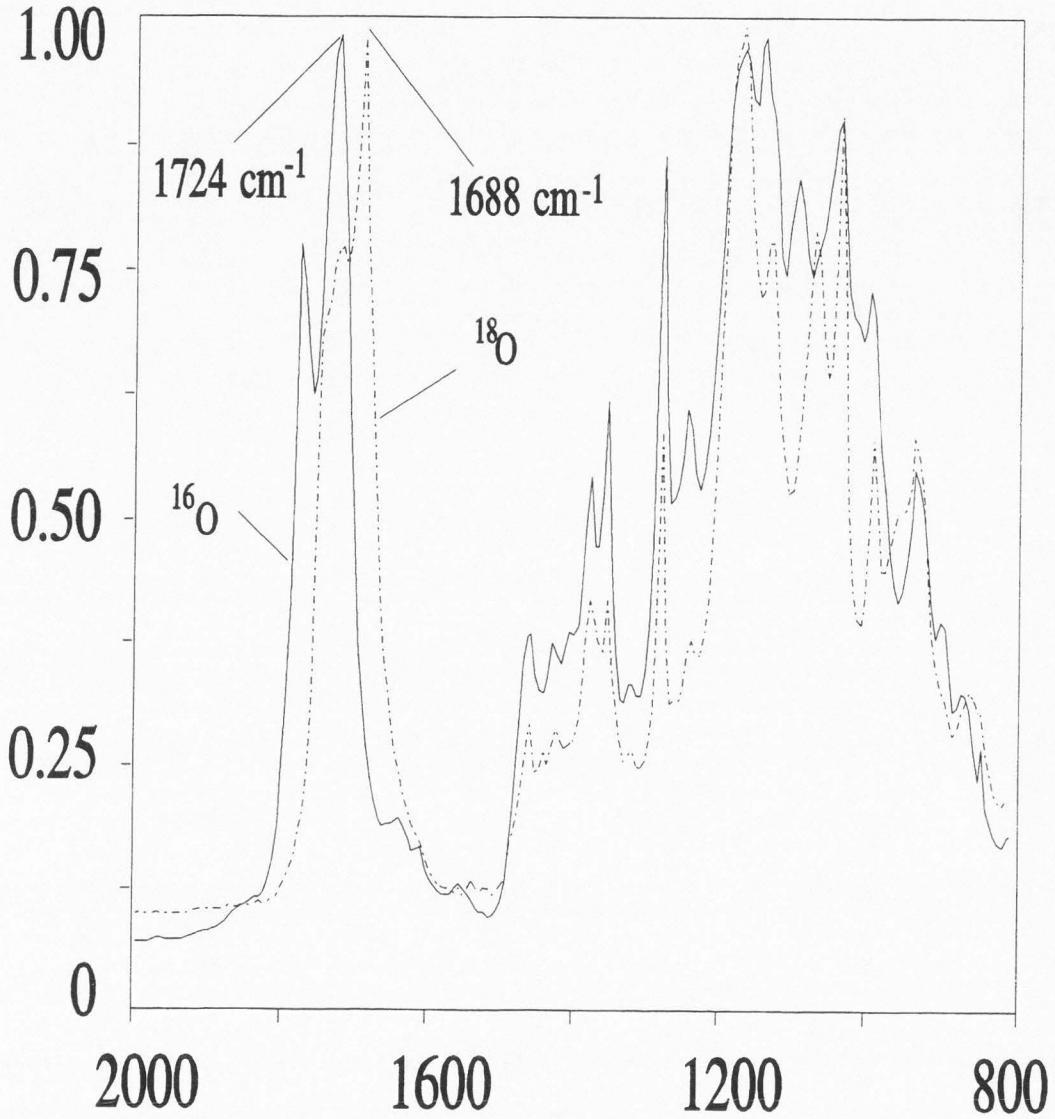

Figure 6-3. IR spectra of the volatiles from the THF-oxidation reaction.

salt [Cp*Ru(NO)(CH_3)(THF)][BAr_4'] (**1**) (Scheme 6-1).[13,16] The present work shows that **1** in the presence of O_2 leads to the catalytic oxidation of THF to gBL. Lower volatility of gBL leads to its accumulation in solution, while THF is removed under reduced pressure.[14] Then complex salt [Cp*Ru(NO)($CH_3$0(gBL)][BAr_4'] (**2**) is formed in quantitative yield.

The spectroscopic properties of complex **2** are consistent with it being an adduct of γ-butyrolactone to the [Cp*Ru(NO)(CH_3)]$^+$ cationic fragment. The ^{1}H and ^{13}C NMR spectra show the resonances of the bound γ-butyrolactone ligand downfield from those of the free molecule.[17] Additional splitting in the resonances of γ-butyrolactone ligand is due to the diastereotopism induced by the chiral metal center. In the ^{13}C NMR spectrum, the chemical shift of the carbon of the carbonyl group in the coordinated lactone is observed 12.5 ppm lower than for the carbonyl carbon of the uncoordinated lactone. The $\Delta\delta$ value of 7.5 ppm between the ^{13}C carbonyl signals of coordinated and uncoordinated of gBL is useful for the estimation of the strength of ligation of gBL to the [CpRe(NO)(PPh_3)]$^+$ fragment.[9] The ν_{CO} shift in the IR spectrum of complex **1** is 82 cm^{-1} lower than ν_{CO} for the free γ-butyrolactone, with corresponding value of 135 cm^{-1} for the rhenium system.[9] The shift of ν_{CO} to the lower energy is attributed to the possible interaction of a *d*-orbital of the ruthenium atom with the π^* orbital of the carbonyl group and the resulting enhancement of electron density in the π^* orbital, which leads to a lower strength of a C=O double bond in the coordinated lactone, compared with that in the free ligand. [9,18] Strong carbonyl absorption in the IR spectrum is more typical for σ-coordination than for π-coordination.[18] The lack of additional bands in the IR spectrum of complex **2** does not suggest the presence of the π-bound isomer. The ^{1}H NMR spectra of complex **2** do not undergo any measurable change in the range from 203 to 303 K. It has been shown, however, that observation of the minor isomers in the similar system by NMR method may require isotopic labeling and extremely low temperatures.[10] Gladysz has shown that in case of aliphatic aldehydes, binding to the [CpRe(NO)(PPh_3)]$^+$ fragment results in π-coordination, but in case of ketones the same reaction leads to the σ-coordinated complexes.[9,10] Methyl acetate complex of rhenium possesses σ-bound ester ligand.[9] Equilibrium studies for the σ/π-bound isomers for the

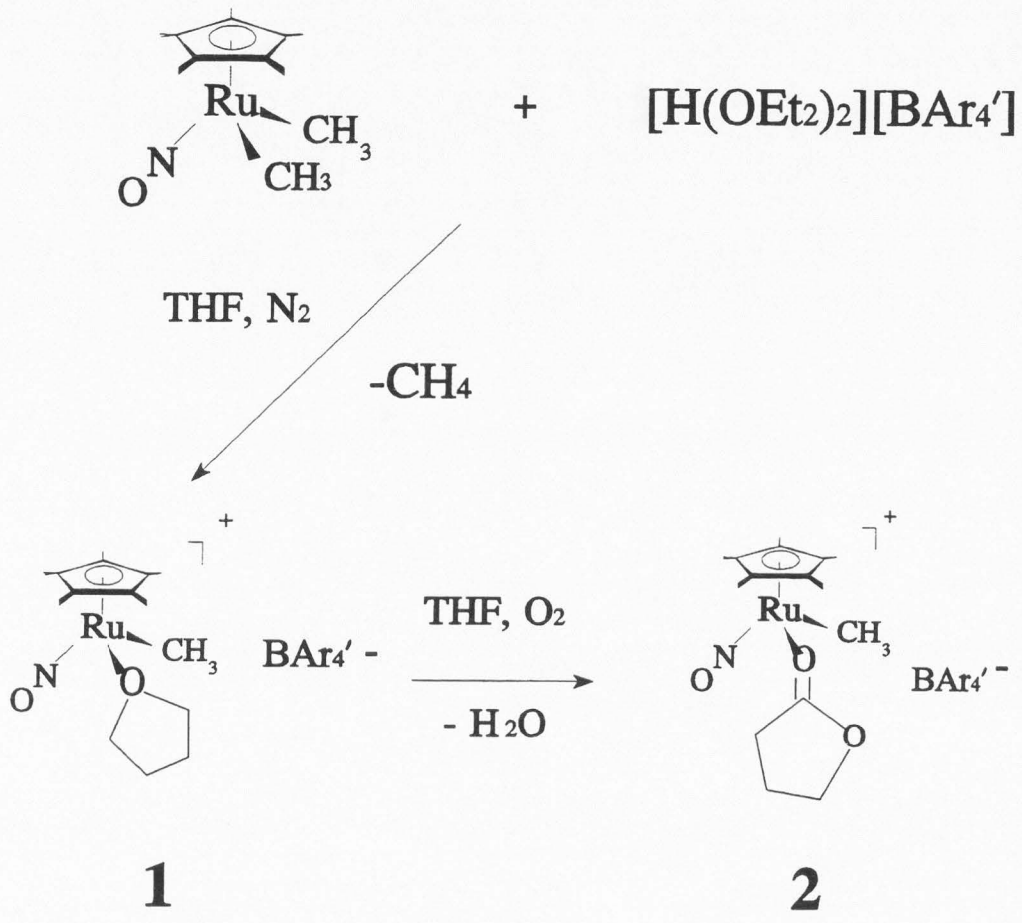
Ru
CH3
CH3
O
N
+
[H(OEt2)2][BAr4']
THF, N2
-CH4
+
Ru
CH3
O
N
O
BAr4' -
THF, O2
- H2O
Ru
CH3
O
N
O
O
BAr4' -

1 **2**

Scheme 6-1.

aldehydes are reported by means of variable temperature IR spectroscopy. The possibility of coordination of the lactone ligand via the ring oxygen seems unlikely in the presence of the available better carbonyl nucleophile. However, it is known that bound THF complexes exist where THF is bound in σ-fashion through the ring oxygen.[13]

X-ray Structure of Complex 1. The statistical 1:2 disorder in CH_3 and NO ligands does not obscure the overall three-legged piano-stool configuration of the cationic part of the complex (Fig. 6-1). The γ-butyrolactone ligand is clearly shown to be bound to the ruthenium center via the carbonyl oxygen in σ-fashion. The Ru-O(2) bond lies almost perfectly in the π-nodal plane approximated by the O2/C16/O3/C18 least-square plane, forming 5.6° angle with it, as expected of "in plane" σ complexes.[9,18,19] The C(16)-O(2) bond distance (1.224 (11) Å) is very similar to the 1.236 (6) Å carbonyl length found in [CpRe(NO(PPh$_3$)(γ-butyrolactone)][BF$_4$].[11] Experimental values for ∠ O(2)-Ru-N(1) and O(2)-Ru-C(6) deviate significantly from 90°, being 100.0(5)° and 84.4(6)° for ∠ O(2)-Ru-N(1) and O(2)-Ru-C(6), respectively, but are still typical for those reported for ketone and ester σ-complexes.[9-11,19] The [N(1)-Ru-O(2)-C(16)] torsion angle value of 35.1° indicates that overlap of the carbonyl π* orbital lobe with the HOMO of the ruthenium fragment is far from maximal (Fig. 6-4).[9] The Ru-O(2)-C(16) angle (130.8 (7)°) is also within range of values typical for σ-bound ester complexes. The Ru-N(1)-O(1) angle is less acute than that found in the structure of [Cp*Ru(NO)(CH$_3$)(THF)][BAr$_4$'] complex.[13]

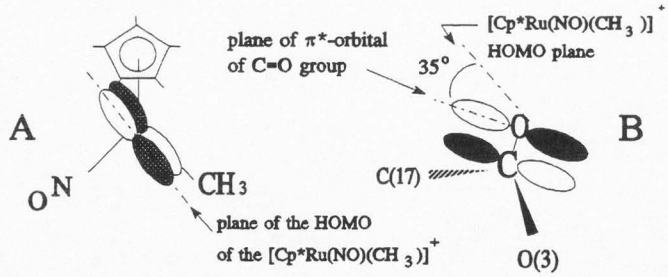

Figure 6-4. (A) HOMO of the [Cp*Ru(NO)(CH$_3$)]$^+$ fragment and (B) π*-orbital of the coordinated gBL carbonyl.

The possibility of disorder in O(3) and C(17) atoms in the lactone ring has been tested by the refinement of the structure based on the second model, where the positions of C(17) and O(3) are alternated, i.e., O(3) is placed in the *trans* position to ruthenium relatively to the C=O bond. Comparative analysis of the resulting structures allows elimination of the latter structure (shown in Fig. 6-3). Oversized thermal ellipsoid for the O(3) atom and small thermal ellipsoid for the C(17) atom of the lactone ring indicate that these two atoms are placed in their position incorrectly in this model. Interestingly, the corresponding rhenium complex $[CpRe(NO)(PPh_3)(gBL)][BF_4]$ possesses molecular structure where the ring oxygen is found in the *trans* conformation to the rhenium atom, while in the $[Cp^*Ru(NO)(CH_3)(gBL)]^+$ it is found in the *cis* configuration to the ruthenium atom. The smaller CH_3 ligand on ruthenium is expected to create a smaller steric hindrance for the CH_2 group of the lactone ring than is created by the bulkier PPh_3 ligand in the rhenium complex. Yet experimental results do not follow this trend, placing the CH_2 group of the ring closer to PPh_3 in the rhenium complex, but away from the CH_3 in the ruthenium complex.

Substitution Reactivity of Complex 1. Binding of γ-butyrolactone to the ruthenium center is reversible, since it can be substituted by THF when excess THF is added to solutions of **1**. The value of the K_{eq} for eq 1 is indicative of the fact that γ-butyrolactone is a stronger Lewis base than THF. This may be due to the fact that carbonyl oxygen in gBL is a stronger nucleophile, which is sterically more available than the ring oxygen in THF. However, Cl^- ligand easily displaces gBL. This reaction is driven by the strong electrostatic attraction, as well as entropic reasons (release of the neutral particles, while the number of ions in solution is being decreased).

Catalytic oxidation of THF. The results of the present study show that complex salts **1** and **2** are catalysts for the oxidation of THF with O_2 (eq 2). The rate of oxidation is dependent on the concentration of THF and pressure of O_2 in the system. The decrease in the production of gBL caused by addition of CH_2Cl_2 to the solution can be explained by the created hindrances in the access for the THF molecules to the reactive center on the ruthenium metal due to the second unreactive component in solution.

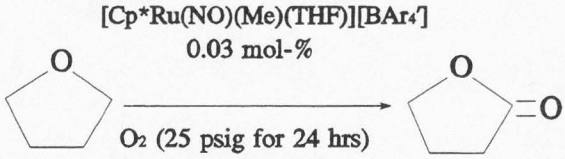

(eq 2)

The second product of the THF oxidation observed in the reaction mixture is 1,6-hexandiol-diformate CH(O)-$(CH)_6$-CH(O). Murai et al. in 1963 described generation of this by/product of the (radical) decomposition of THF hydroperoxide. The coupling of two radical fragments results in the formation of [CH(O)-$(CH)_6$-CH(O)] according to Scheme 6-2.[20] A positive reaction for the $Fe(SCN)_2$ test[15] also suggests that catalytic THF oxidation with O_2 in the presence of complex **2** probably proceeds via formation of hydroperoxy-THF.

IR spectroscopy studies with $^{18}O_2$ show complete incorporation of the ^{18}O label into the carbonyl group of gBL (Fig. 6-2). The carbonyl ν_{CO} region at 1600-1800 cm^{-1} is shifted about 30 cm^{-1} to lower energy. The experimental value for the $\nu_{CO\text{-}16}/\nu_{CO\text{-}18}$ ratio of 1.021 correlates very well with the value of 1.020 predicted from Hooks law (1688/1724 = 1.021, see Fig. 6-3).[19] No incorporation of ^{18}O is observed in the C-O stretch region at 1550-800 cm^{-1}. The treatment of THF solution of $Cp^*Ru(NO)OTf_2$ with 25 psig of O_2 results in the formation of gBL and $[Cp^*Ru(NO)(\mu\text{-}OH)]_2OTf_2$. The $[Cp^*Ru(NO)(\mu\text{-}OH)]_2OTf_2$ is formed upon dissolution of $Cp^*Ru(NO)OTf_2$ in H_2O.[15] Thus, H_2O appears to be a by-product of the oxidation reaction. Maitlis et al. reported that rhodium(III) tri-μ-hydroxy complex $[(Cp^*Rh)_2(\mu\text{-}OH)_3]Cl$ catalyses the oxygenation of THF to gBL.[8b] This reaction is enhanced by small amounts of water (presumably, in order to cleave the dimer), but is completely stopped by additions of larger amounts of water. Following the hypothesis outlined by Maitlis, the mechanism for the THF oxidation with ruthenium complex **1** is proposed (Scheme 6-3). This scheme also includes the reaction pathway, proposed by Murai for the metal assisted decomposition of hydroperoxy-THF.[20] The proposed mechanism is based on the idea that the role of the metal complex

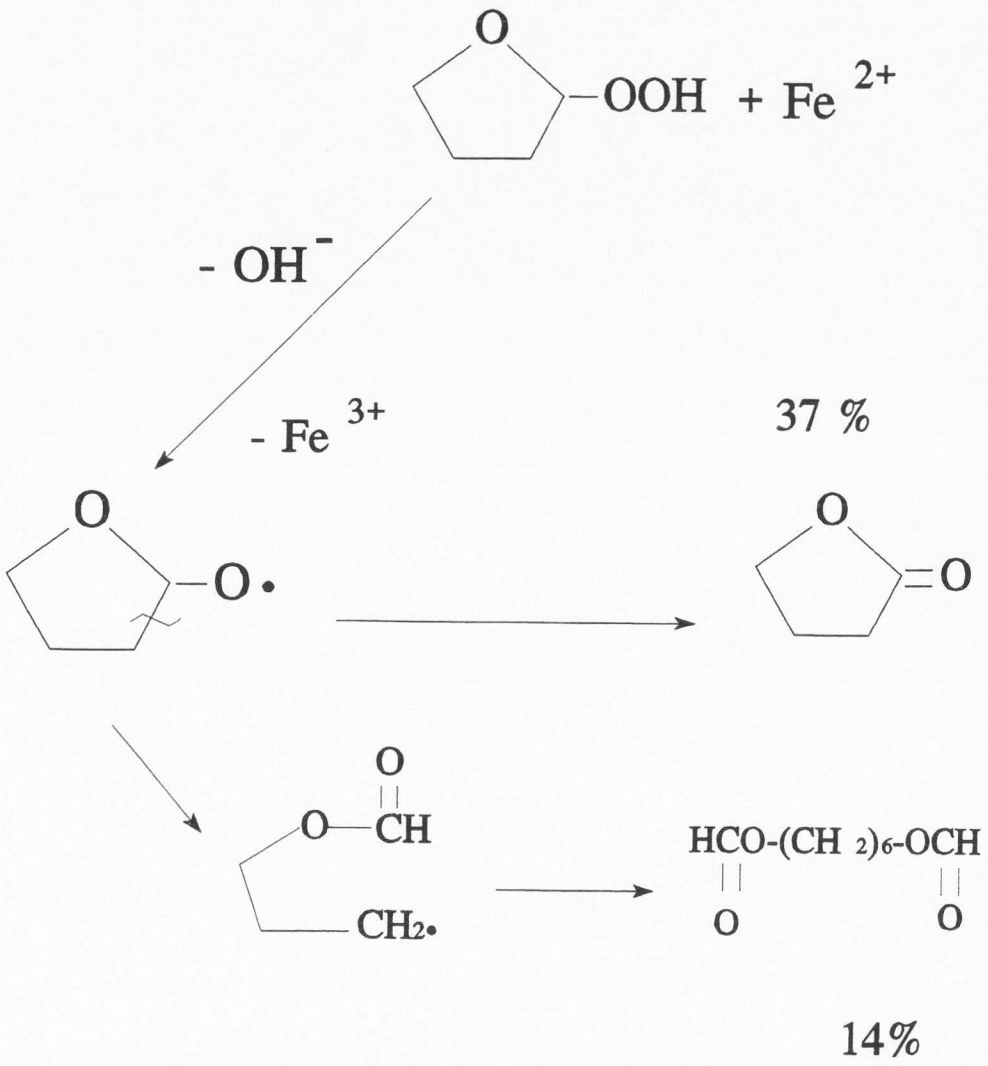

Scheme 6-2 (Adapted from ref. 21).

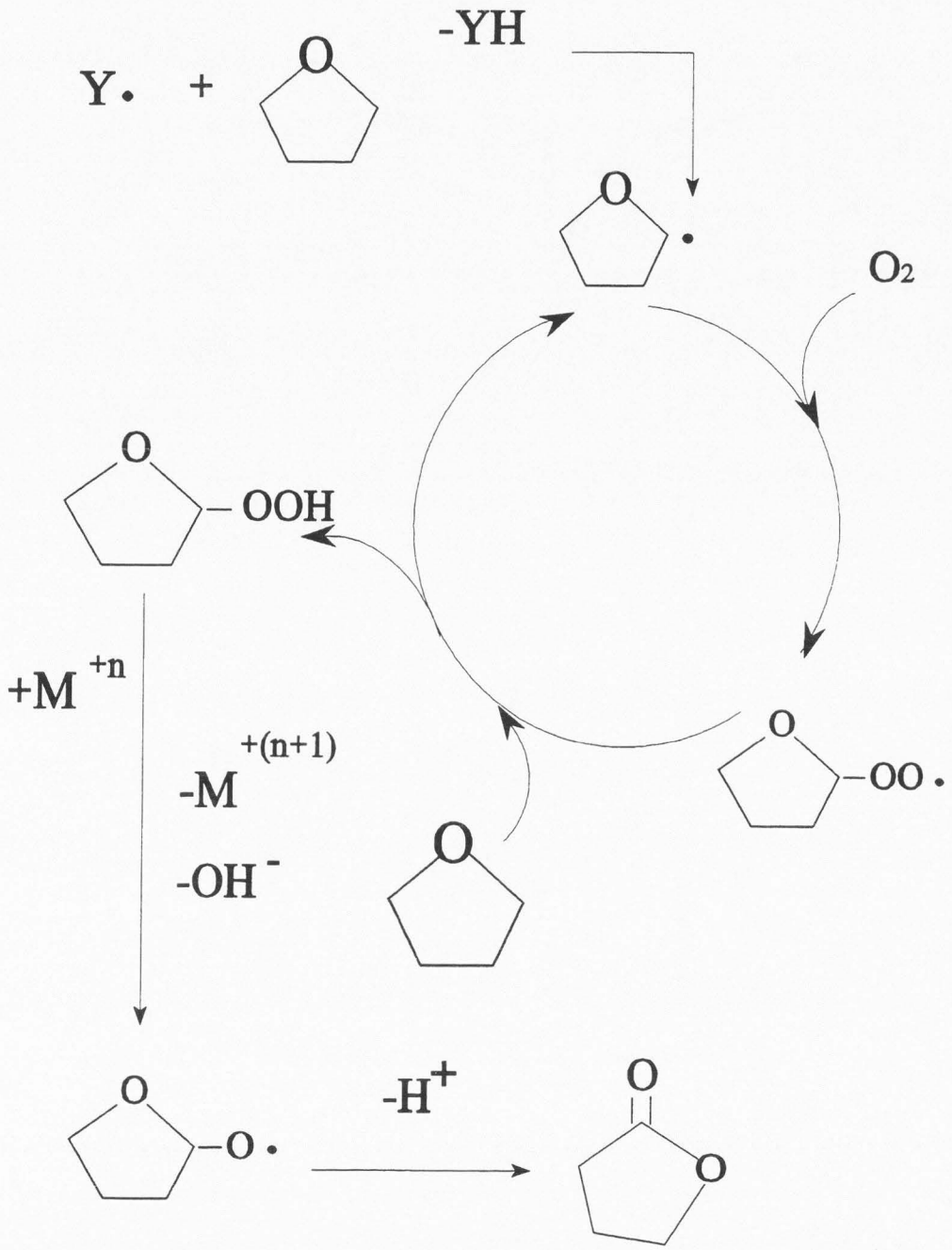

Scheme 6-3.

is chiefly to decompose the THF-hydroperoxyde, which is formed directly (Scheme 6-4).[8b]

An alternative mechanism may be proposed based on the recent report of O'Halloran et al., stating that the Mn(III) alkoxide-bridged dimer $Li_2[MnL]_2$ undergoes air-oxidation to yield a terminal-oxo complex $[Mn^{(V)}(O)L]^-$, which participates in stoichiometric oxo-transfer reactions with THF.[5] A terminal O_2-bound intermediate assists the Ru-O bond cleavage and THF->hydroperoxy-THF conversion within the coordination sphere of the ruthenium center (Scheme 6-4). The hypervalence of ruthenium center may be attained via Cp* slippage, as it was proposed for the case of the C-H bond activation in the Cp* ligand of the related complex [Cp*Ru(NO)(μ-OH)][2OTf].[15] Effective loss of H_2O in the next step results in formation of the γ-butyrolactone ligand, which can be displaced by another molecule of THF molecule from the solution, thus completing a catalytic cycle. Release of H_2O as a by-product may "poison" the catalyst, since H_2O can also be a strongly binding ligand to the ruthenium center.[15]

Experimental

General. Standard Schlenk techniques were employed in all syntheses. The nitrogen reaction atmosphere was purified by passing through scavengers for water (Aquasorb, Mallinckrodt) and oxygen (Catalyst R3-11, Chemical Dynamics, So. Plainfield, NJ). Organic solvents were distilled under nitrogen over appropriate drying agents prior to use. All chemical reagents were used as received from Aldrich unless stated otherwise. Infrared spectra were recorded on a Mattson Polaris-Icon FT-spectrometer.

The ^1H and ^{13}C NMR spectra were recorded on a Bruker ARX-400 NMR spectrometer operating at 400 MHz (^1H), 61.42 MHz (^2H), 100.62 Mhz (^{13}C), and 376.2 Mhz (^{19}F). The residual solvent peak of $CDCl_3$ was used as the internal NMR standard (^1H δ 7.24; ^{13}C δ 77.0 ppm), as well as the residual peak of HDO (^1H δ 4.70). Spectra were recorded at 298 K unless otherwise stated. NMR spectra in CH_2Cl_2 and THF were measured using solvent presaturation techniques and were shimmed and referenced to the signals from $CDCl_3$ sealed inside a 1.5-mm capillary located concentrically

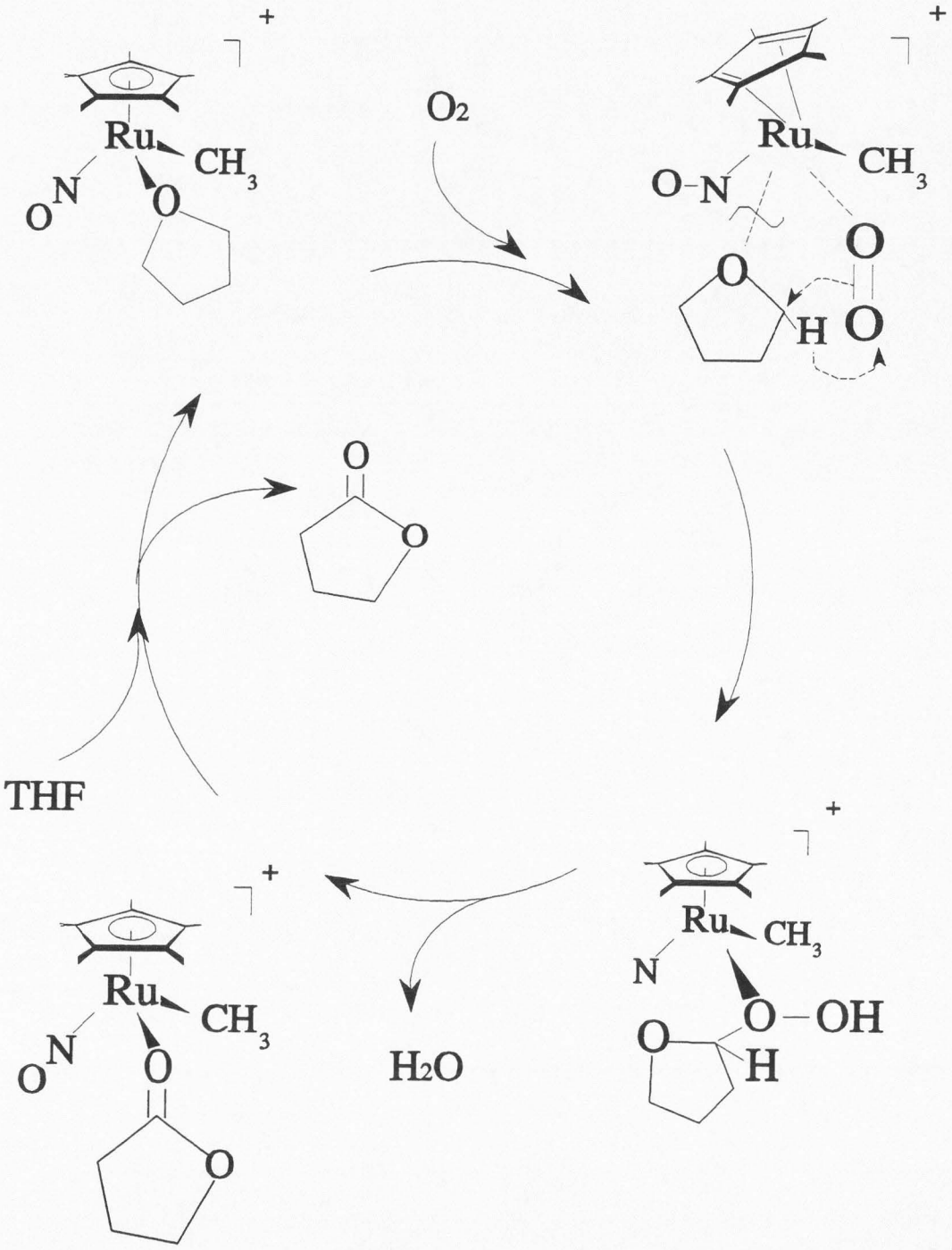

Scheme 6-4.

inside the 5-mm NMR tube. When necessary, 5-mm NMR tubes with resealable Teflon valves were used (Brunfeld Co., Bartlesville, OK). The chemical shifts reported for the complexes in CH_2Cl_2 are identical to those in the analogous deuterated solvents.

Melting points were measured with a Mel-Temp device (Laboratory Devices) in open capillaries and are uncorrected. Combustion analysis was performed by Atlantic Microlab, Inc., Norcross, GA.

Complex $Cp^*Ru(NO)(CH_3)_2$,[21] as well as $HBAr_4'$,[16] 1,6-hexandiol-diformate[14] and $Fe(SCN)_2$[22] were prepared according to published procedures.

Preparation of $[Cp^*Ru(NO)(CH_3)(\gamma\text{-butyrolactone})]^+[BAr_4']^-$ (1). (BAr_4' = (3,5-$(CF_3)_2C_6H_3)_4B$) (1). Solution of $HBAr_4'$ (2.41 g, 2.41 mmol) in CH_2Cl_2 (10 mL) was added dropwise to the stirred solution of $Cp^*Ru(NO)(CH_3)_2$ (0.680 g, 2.30 mmol) in THF (40 ml). After 1.5 h stirring, solvent was removed in vacuo, which resulted in obtaining 3.6 g of the dark red-brown solid (90-95 % yield (crude product)). After recrystallization from CH_2Cl_2:hexane (1:5) the red crystals were identified as (2), mp 108 °C. IR (CH_2Cl_2): ν(NO) 1790 cm^{-1}, $\nu_{C=O}$ 1688 cm^{-1}. ^1H NMR ($CDCl_3$): δ7.67 (Ar_F, 8H), δ7.51 (Ar_F, 4H), δ4.64(γ-butyrolactone, 2H, m), δ2.72(γ-butyrolactone, 2H, m), δ2.33(γ-butyrolactone, 2H, m), δ1.65($C_5(CH_3)_5$, 15H), δ1.17(CH_3,3H). $^{13}C\{^1H\}$ NMR ($CDCl_3$): δ190.02 (γ-butyrolactone, C_1), δ161.7 (q, $J_{C\text{-}B}$=50Hz, C_{ipso}), δ135.30(s, C_{ortho}), δ129.1 (q,$J_{C\text{-}F}$=32Hz, C_{meta}), δ124.50 (q, $J_{C\text{-}F}$=275Hz, CF_3), δ117.4 (s, C_{para}), δ108.1(s, $C_5(CH_3)_5$ skeletal C), δ74.65 (s, γ-butyrolactone, C_4), δ30.73(s, γ-butyrolactone, C_2), δ22.2 (s, γ-butyrolactone, C_3), δ9.00(s, $C(CH_3)_5$), δ6.03 (s, Ru-CH_3). Anal. Calcd. from $C_{48}H_{38}O_3NCl_2F_{24}BRu$ ((1)·CH_2Cl_2) : C, 43.82; H, 2.92; N, 1.06. Found: C, 43.95; H, 2.91; N, 1.03.

X-Ray Structural Analysis of 2. A suitable specimen was selected and centered vertically at 173 K on a Siemens P4 Autodiffractometer equipped with the LT-2a temperature controller preset at -100 °C The computer centering of 25 random reflections revealed the monoclinic lattice with a = 13.957 (4) Å, b = 21.740 (6) Å, c = 17.819 (4) Å; β = 97.85 (2)°, V = 5456 (2) Å^3. Data collection of $0 \leq h \leq 16$, $0 \leq k \leq 24$, $-20 \leq l \leq 20$ showed a *P*-lattice with a *c* glide plane

indicated by the systematic absences h0l, h00, and 00l when h ≠ 2n and l ≠ 2n. The presence of a 2_1 screw axes was indicated by 0k0 absences when k ≠ 2n. Structure solution was performed using direct methods. Subsequent refinement of the structure was carried out on an IBM-compatible 486 personal computer using the SHELXS-86[23] and SHELXL-93[24] programs from Sheldrick.[25] Difference maps led to the location of all the nonhydrogen atoms of four independent molecules in the asymmetric unit; all nonhydrogen atoms were positioned in a riding model with fixed C-H distances and isotropic thermal parameters. Convergence led to final R/wR2 values of 0.0806/0.1961 with 8320 data ($F^2 > 2\sigma F^2$) and 595 parameters. The N(1)-O(1) and C(6) peaks were successfully modeled isotropically as a 2:1 disorder of a NO ligand and an CH_3 ligand.

Reaction of (2) with [Ph_3PNPPh_3]Cl. Twenty-fold excess of [Ph_3PNPPh_3]Cl was added to the solution of 5 mg of **2** in 0.8 mL of $CDCl_3$ in the NMR tube. This led to the instantaneous clean substitution of γ-butyrolactone ligand by Cl^- and formation of $Cp^*Ru(NO)(CH_3)(Cl)$ (^1H NMR: δ1.76 (Cp^*, 15H,s), δ1.33 (CH_3, 3H, s). Volatile part of the solution was transferred in vacuo into another NMR tube (with liquid N_2 trap), and the proton NMR spectrum was recorded, compared, and found identical to that of $CDCl_3$ solution of an authentic sample of γ-butyrolactone.

Catalytic Oxidation of THF in the Presence of O_2 and 1. In the representative experiment, a Schlenck tube was charged with 10 mg (1) in 10 ml of THF. O_2 was bubbled through the solution for 5 min. Then a Schlenk tube was sealed and left stirring for 72 h at ambient temperature. Transformations in the reaction mixture have been monitored by ^1H NMR spectroscopy of the aliquots of the solution, collected via syringe. Amount of γ-butyrolactone formed in the course of reaction was estimated by the integral ratio versus internal standard (toluene), previously added to the solution. In 48 h no presence of **1** or **2** was detected. Molar ratio of γ-butyrolactone formed versus initial amount of **1** was found ca. 10:1. In the alternative experiment, a thick-walled flask with the identical solution of **1** in THF was pressurized with 25 psig of O_2 and left stirring for 24 h. Amount of the γ-butyrolactone produced was estimated as described above. In this case, molar ratio of γ-butyrolactone formed versus initial amount of **1** was found ca. 25:1. For analysis of the non-organometallic

products of the reaction, THF solvent was removed under reduced pressure. The rest of the non-organometallic products of the reaction was transferred to another vessel on the vacuum line, using 50 °C water bath and liquid N_2 trap under the collector flask. The collected viscous colorless liquid was then analyzed by IR and ^1H NMR spectroscopic methods (see text for the results of analysis).

References

(1) Collman, J. P.; Hegedus, L. S.; Norton, J. R.; Finke, R. G. *Principles of Organotransition Metal Chemistry*; University Science Books: Mill Valley, CA, 1987; pp. 199, 485 and references therein. (b) Neiderhoffer, E. C.; Timmons, J. H; Martell, A. E. *Chem. Rev.* **1984**, *84*, 137 and references therein.

(2) Fazlur-Rahman, A. K., Tsai, J. -C., Nicholas, K. M. *J. Chem. Soc, Chem.Com.* **1992**, *67,* 1335.

(3) Aresta, M., Fragale, C., Quaranta, E., Tommasi, I. *J. Chem. Soc., Chem. Comm.*. **1992**, *89,* 315.

(4) Hata, E.; Takai, T.; Mukaiyama, T. *Chem.Lett.* **1993**, *93,* 1513.

(5) O'Halloran, T. V.; Fackler, N.; Zhang, S.; MacDonnell, F. *Abstracts of 207th ACS National Meeting, Division of Inorganic Chemistry, San Diego, California,* **1994**, *57*, 37.

(6) Carlsen, H. J., Katsuki, T., Martin. V., Sharpless, B. *J. Org. Chem.* **1981**, *46*, 3936.

(7) Bressan, M., Morvillo, A., Romanello., G *Inorg. Chem.* **1990**, *29*, 2976.

(8) (a) Braunstein, P., Matt, D., Nobel, D. *J. Am. Chem. Soc.* **1988**, *110*, 3207. (b) Hirai, K.; Nutton, A.; Maitlis, P. M. *J. Mol. Cat.* **1981**, *10*, 203.

(9) Saura-Llamas, I.; Dalton, D. M.; Arif, A. M.; Gladysz, J. A. *Organometallics*, **1992**, *11*, 683.

(10) Dalton, D. M.; Fernandez, J. M.; Emerson, K.; Larsen, R. D.; Arif, A. M. Gladysz, J. A. *J. Am. Chem. Soc.*, **1990**, *112*, 9198.

(11) (a) Klein, D. P.; Dalton, D. M.; Mendez, N. Q.; Arif, A. M.; Gladysz, J. A. *J. Organomet.*

Chem. **1991**, *81*, C7. (b) Mendez, N. Q.; Arif, A. M.; Gladysz, J.A. *Angew. Chem., Int. Ed. Engl.*, **1994**, *29*, 1473.

(12) Bringmann, G.; Schupp, O.; Peters. K.; Walz, L.; von Schnering, H. G. *J. Organomet. Chem.* **1992**, *438*, 117.

(13) Yi, G.-B. Dissertation, Utah State University, 1995.

(14) Werner, W. *J. Chem. Research (M)* **1980**, *33*, 2769.

(15) Svetlanova-Larsen, A.; Hubbard, J. L. *Organometallics*, in press.

(16) Brookhart, M.; Grant, B.; Volpe, A. F. Jr. *Organometallics*, **1992**, *11*, 3920.

(17) Pouchert, C. J. *The Aldrich Library of Infrared Spectra;* Aldrich Chemical Co.: Milwaukee, WI, 1981.

(18) (a) Corcoran, R. C.; Ma, J. *J. Am. Chem. Soc.*, **1992**, *114*, 4536. (b) Daniels, F.; Alberty, R. A. *Physical Chemistry;* John Wiley & Sons, Inc.: New York-London-Sydney-Toronto, 1975; Ch. 15.

(19) (a) Mendez, N. Q.; Arif, A. M.; Gladysz, J. A. *Angew. Chemie Int. Ed. Engl.* **1990**, *12*, 1473. (b) Garner, C. M.; Mendez, N. Q.; Kowalczyk, J. J.; Fernandez. J. M.; Emerson, K.; Larsen, R. D.; Gladysz, J. A. *J. Am. Chem. Soc.*, **1990**, *112*, 5146.

(20) Murai, D., Sonoda, N., Tsutsumi, S. *Bull. Chem. Soc. Jpn.* **1963**, *36*, 527.

(21) Seidler, M. D.; Bergman, R. G. *J. Am. Chem. Soc.*, **1984**, *106*, 6110.

(22) Gordon, J. A.; Ford, R. A. *The Chemist's Companion;* John Wiley & Sons: New York-London-Sydney-Toronto, 1972; 437.

(23) Sheldrick, G. M. *Acta Cryst.* **1990,** *A46*, 467-473.

(24) Sheldrick, G. M. *J. Appl. Crystallogr.*, in press. SHELXL-93 scattering factors from: *International Tables for X-ray Crystallography* Vol. C; Ed. A. J. C. Wilson, Kluwer Academic Publishers: Dordrect, 1992; Tables 6.1.1.4 (pp. 500-502, neutral atom scattering factors), 4.2.6.8 (pp. 219-222, f′,f′′), and 4.2.4.2 (pp. 193-199, absorption coefficients)

(25) SHELXL-93 is available from: Siemens Analytical X-ray Instruments, 6300 Enterprise Lane,

Madison, WI 53719 or directly from G. Sheldrick, Institüt für Anorganische Chemie,der Universität, Tammannstrasse 4, D-37077 Göttingen, Germany: gsheldr@shelx.uni-ac.gwdg.de

CHAPTER 7

CONCLUSIONS

The major part of the present study addresses thermodynamic and kinetic aspects of small molecules binding and activation by a $[Cp^*Ru(NO)]^{+2}$ fragment. The $[Cp'Ru(NO)]^{+2}$ core is a robust electrophilic moiety that is stable under wide range of conditions and capable of diverse forms of reactivity. This is especially the case when counterions like OTf^- and $BAr_4'^-$ are used ($OTf = OSO_2CF_3$, $[BAr_4'] = [(3,5\text{-}(CF_3)_2C_6H_3)_4B]$). Nitrosyl ligands are valuable ancillary ligands for stabilizing the metal centers. By changing from linear to a bent geometry, nitrosyl ligands can adjust from formal 3-electron donation to 1-electron donation. Thus, NO serves as an "indicator" of the donor-acceptor competition around the metal center as assessed by IR spectroscopy and X-ray crystallography methods. The isolation and reactivity of $Cp'Ru(NO)L_2$ complexes permit the application of the various techniques like heteronuclear dynamic NMR, IR, UV spectroscopy, and X-ray crystallogpraphy. The van't Hoff treatment of the equilibrium data in solution is based on the VT-NMR spectroscopy data and permits the determination of important thermodynamic values for the binding and exchange of various ionic and neutral species around the electrophilic metal center. Kinetic studies of the homogenous reactions facilitate a better mechanistic understanding for these processes.

The study described in Chapter 2 clarifies the picture of OTf^- binding to an electrophilic metal center. It is shown that OTf^- binds quite strongly with apparent ionic and covalent interactions with the metal. In wet CH_2Cl_2, OTf^- dissociation to give aqua complexes is unfavorable due to entropy costs associated with the formation of solvated ion pairs. In neat coordinating solvents like THF, the formation of solvento complexes is much more favorable. In protic coordinating solvents like H_2O, complete OTf^- dissociation occurs due to the ease of H^+ ionization from the bound-H_2O ligand facilitated by the extremely electrophilic $[Cp'Ru(NO)]^{+2}$ moiety. The response of the NO ligand to H_2O coordination shows the H_2O ligand to be a significant π- and σ-donor. Such π-donation

may possibly be a factor in the observed H/D exchange on the Cp'-ligand methyl positions and may have implications about the role of H_2O in other catalytic processes.

Chapter 3 describes the study of rhodium triflate complexes in solution and in solid state and should be regarded in conjunction with Chapter 2. The study shows that solid *trans*-$[Rh(CO)(PPh_3)_2(OH_2)][OTf]$ precipitates preferentially from wet CH_2Cl_2 or benzene solutions rather than anhydrous *trans*-$[Rh(CO)(PPh_3)_2(OTf)]$. In CH_2Cl_2 solution, however, the OTf^- ligand is a substantially better ligand than water, leading to *trans*-$[Rh(CO)(PPh_3)_2(OTf)]$ as the only detectable species. Triflate displacement from Rh by H_2O does not occur to a significant extent in CH_2Cl_2 or benzene. Thus, the OTf^- ion in these solvents cannot be classified as a weak ligand in the same category as BF_4^-.

The study described in Chapter 4 provides a clearer picture of the process of OTf^- substitution by alcohols and the thermodynamic characterization of the triflate/alcohol exchange equilibria in CH_2Cl_2. Similar to the process of displacement of OTf^- by H_2O ligands in CH_2Cl_2, the binding of ROH is not favorable for entropic reasons, requiring solvent reorganization due to the formation of ion pairs. The lability of the $[Cp^*Ru(NO)(ROH)_2]^{+2}$ complexes and difficulties in their isolation are overcome by utilization of the chelate stabilization effect in the diol-coordinated complex salt $[Cp^*Ru(NO)(HO\text{-}CH_2CH_2\text{-}OH)][OTf_2]$. X-ray structure of the complex salt $[Cp^*Ru(NO)(HO\text{-}CH_2CH_2\text{-}OH)][OTf_2]$ reveals significant hydrogen-bonding interactions between triflate counterions and the hydroxyl protons of the diol fragment. In the part of this work concerning oxidative reactivity of $Cp^*Ru(NO)(OTf)_2$ with alcohols, the quantitative stoichiometry of the Ru(II)->Ru(0) conversion and the identity of the major organometallic product, $[Cp^*Ru(\mu\text{-}NO)]_2$, are determined unambiguously for the first time. The kinetic study reported here is one of the very few mechanistic studies performed on reactions of this kind. The determination of the first-order reactivity in complex 1 and *i*-PrOH supports the proposed β-hydrogen elimination scheme of the alcohol oxidation process.

The study of alkyl halide binding to the $[Cp^*Ru(NO)(CH_3)]^+$ fragment was described in Chapter 5. It is shown that alkyl iodide complexes can be generated in situ by substitution reaction

with weakly coordinated THF complex $[Cp^*Ru(NO)(CH_3)(THF)]^+$. They are sensitive to further reactions in solution, driven by the loss of methyl ligand on ruthenium center. This transformation leads to the formation of the dinuclear complex $[Cp^*Ru(NO)(\mu\text{-}I)]_2^{+2}$, which crystallizes in a *trans*-configuration. Molecular structure and spectroscopic properties of heteronuclear Ru-Cr complex $[Cp^*Ru(NO)(\mu\text{-}I)(Cp)Cr(NO)_2]^+$, containing direct M-I-M' link, allow for evaluation of the comparative strength of $[CpCr(NO)_2]^+$ and $[Cp^*Ru(NO)(CH_3)]^+$ as Lewis acids competing for the bridging iodine atom. Another synthetic approach leads to the generation of the weakly coordinated CH_2Cl_2 species $[Cp^*Ru(NO)(CH_3)(ClCH_2Cl)]^+$ via protonation of $Cp^*Ru(NO)(CH_3)_2$ in CH_2Cl_2 at low temperature. Extreme lability of CH_2Cl_2 ligand could potentially make the species $[Cp^*Ru(NO)(CH_3)(ClCH_2Cl)]^+$ an important synthon for various organometallic transformations. This is also illustrated by reports of the rich reactivity of the related alkyl-halide complexes.

The study in Chapter 6 has established the synthetic route to the ruthenium γ-butyrolactone complex $[Cp^*Ru(NO)(CH_3)(\eta^1\text{-}gBL)]^+$ via aerobic oxidation of THF subsequent to the protonation of $Cp^*Ru(NO)(CH_3)_2$ with $[H(OEt_2)_2][BAr_4']$. The gBL ligand is shown to coordinate reversibly to the ruthenium center in mostly σ-fashion, as follows from analysis of the spectroscopic and structural properties of $[Cp^*Ru(NO)(CH_3)(\eta^1\text{-}gBL)][BAr_4']$ in solution and in solid state. Aerobic oxygenation of THF to give γ-butyrolactone is catalyzed by $[Cp^*Ru(NO)(CH_3)(\eta^1\text{-}gBL)][BAr_4']$ and $[Cp^*Ru(NO)(CH_3)(THF)][BAr_4']$. The evidence presented suggests that the reaction proceeds via formation of an intermediate hydroxy-THF species.

APPENDIX

American Chemical Society

PUBLICATIONS DIVISION
COPYRIGHT OFFICE

1155 SIXTEENTH STREET, N.W.
WASHINGTON, D.C. 20036
Phone (202) 872-4367 or -4368
Fax (202) 872-6060

FAX NUMBER: _____

DATE: May 10, 1996

646-07-6881

MEMORANDUM

TO: Anna Svetlanova-Larsen

Utah State University, Dept. of Chemistry & Biochemistry

Logan, Utah 84322-0300

FROM: C. Arleen Courtney
Copyright Assistant

RE: Your letter dated May 1, 1996

Thank you for your recent letter, regarding your request for permission to include your paper(s) or portions of your paper(s), per your attached letter, in your thesis. Please note the following:

* If your paper has already been published by ACS, I would be happy to grant you this permission royalty free provided that you print the required ACS copyright credit line on the first page of your article: "Reprinted (or 'Reprinted in part') with permission from FULL REFERENCE CITATION. Copyright YEAR American Chemical Society."

  Note: If you plan to submit your thesis to UMI, please inform them that permission to include your already published ACS article as part of your thesis is granted for paper and microform copies only; the ACS copyright notice (see above) must appear on the first page of the ACS article.

* If your paper has not already been published by ACS, you may include it in your thesis provided that you print the following ACS copyright credit line on the first page of your article: "Reprinted (or 'Reprinted in part') with permission from JOURNAL NAME, in press (or 'submitted for publication'). Unpublished work copyright CURRENT YEAR American Chemical Society."

  Note: If you plan to submit your thesis to UMI, you may NOT include the ACS paper in the version that you submit to UMI until ACS has published your paper.

* Other: _____

Thank you for writing. If you have any questions, please call me at 202/872-4368.

4/25/95

May 1st, 1996

Ms. C. Arleen Courtney
ACS Copyright Office
Publication Division
1155 Sixteenth Street, NW
Wasgington, DC 20036
FAX: (202)872-6060

Dear Ms. Courtney:

I am in the process of preparing my Ph. D. dissertation in the Department of Chemistry and Biochemistry at Utah State University. I hope to complete in the Spring quarter of 1996. I need to include, as part of my dissertation, some of my experimental results published in ACS journals. The authors of the papers and the journal particulars are:

Anna Svetlanova-Larsen, Christopher R. Zoch and John L. Hubbard. *Organometallics*, 1996, accepted for publication April 2, 1996.

Anna Svetlanova-Larsen and John L. Hubbard. *Inorg. Chem.*, in press.

An appropriate bibliography citation will be made for each material used. I need copyright permission from you to be able to include, as part of my dissertation, the experimental results published in the above mentioned articles.

Thank you for your time and assistance.

Sincerely,

Anna Svetlanova-Larsen
FAX:(801)797-3390
Department of Chemistry and
Biochemistry
Utah State University
Logan UT 84322-0300